Title
Chemistry of the protein radical generated from the reaction of horse myoglobin with hydrogen peroxide

Author
Choe, Yearn Seong

Publication Date
1991

Peer reviewed|Thesis/dissertation

CHEMISTRY OF THE PROTEIN RADICAL GENERATED FROM THE REACTION OF HORSE MYOGLOBIN WITH HYDROGEN PEROXIDE

by

YEARN SEONG CHOE

DISSERTATION

Submitted in partial satisfaction of the requirements for the degree of

DOCTOR OF PHILOSOPHY

in

PHARMACEUTICAL CHEMISTRY

in the

GRADUATE DIVISION

of the

UNIVERSITY OF CALIFORNIA

San Francisco

To my parents, Yoon Sik and Wol Hang Choe

who have supported me through all my years with love and patience

ACKNOWLEDGEMENTS

I would like to express my special thanks to my advisor, Dr. Paul Ortiz de Montellano for his advice, encouragement and guidance which not only helped all aspects of my research but also developed my way of scientific thinking. I am also grateful to Drs. George Kenyon and Brad Gibson for their helpful discussions and suggestions in writing this thesis.

Through my years at UCSF, my research has benefited from the stimulating environment my colleagues in POM lab have provided. Their sense of humor and friendship made my long hours in the lab bearable and often enjoyable. Appreciation extends to Bob, Barbara and Christa for their editorial help and Angela for providing me with the recombinant sperm whale myoglobin and the mutants. A part of my research grew out of the work that Dr. Carlos Catalano initially conducted. He kindly helped me to become familiarized with the lab when I started my research in POM lab.

I would like to thank Dr. Dave Maltby for his help in obtaining the mass spectra of modified hemes and heme-peptides and Dr. Vladimir Basus for his helpful discussions on NMR.

CHEMISTRY OF THE PROTEIN RADICAL GENERATED FROM THE REACTION OF HORSE MYOGLOBIN WITH HYDROGEN PEROXIDE

YEARN SEONG CHOE

ABSTRACT

Chloroperoxidase, unlike other peroxidases, has a cysteine heme ligand like cytochrome P-450 and catalyzes the oxidation of styrene to styrene oxide and phenylacetaldehyde by a mechanism that is indistinguishable from that of cytochrome P-450. The reaction involves quantitative incorporation of oxygen from the peroxide and complete retention of the olefin stereochemistry. 11-Microperoxidase and the globins, which have a histidine fifth heme ligand, also catalyze the epoxidation of styrene, suggesting that the cysteine thiolate heme ligand is not required for catalysis of epoxidation reactions.

Horse metmyoglobin is oxidized by H_2O_2 to a ferryl oxygen species and a protein (Tyr 103) radical. The epoxidation of styrene by this active species involves incorporation of oxygen from both the peroxide and molecular oxygen. The participation of the protein radical in the epoxidation reaction was confirmed by the demonstrations that the reaction of an [Fe(IV)=O] species with styrene does not yield the epoxide and the rate of decrease in the product yield parallels the decay of the protein radical. In addition, the epoxidation results in modification of the protein, presumably at Tyr 103.

The heme is covalently bound to Tyr 103 of the protein when horse myoglobin is treated with H_2O_2. The experiments with reconstituted mesomyoglobin show that the heme vinyl groups are not the primary site of attachment of the heme to the protein. Protein-protein crosslinking occurs between Tyr 103 of one subunit and Tyr 151 of the other when sperm whale myoglobin is treated with H_2O_2. The involvement of Tyr 151 in

the dimerization was confirmed by the observation of dimerization in the reactions of H_2O_2 with recombinant sperm whale myoglobin and the Tyr146Phe mutant but not the Tyr151Phe mutant.

The H_2O_2-dependent reactions of alkylhydrazines with myoglobin show that the alkyl radicals formed from the alkylhydrazines add to the γ-*meso* carbon, a site different from that of the reaction of phenylhydrazine with myoglobin and a position never before modified in a hemoprotein reaction.

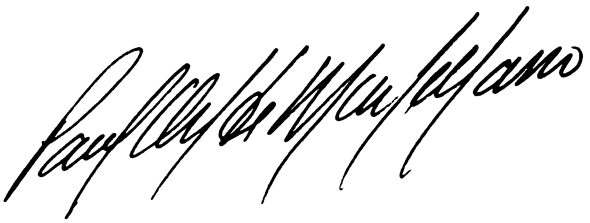

TABLE OF CONTENTS

LIST OF FIGURES

LIST OF SCHEMES

LIST OF TABLES

ABBREVIATIONS

DETAPAC	Diethylenetriaminepentaacetic acid
EDTA	Ethylenediaminetetraacetic acid
EPR	Electron paramagnetic resonance
FAD	Flavin adenine dinucleotide
FMN	Flavin mononucleotide
FPLC	Fast protein liquid chromatography
GLC	Gas-liquid chromatography
Heme	Iron protoporphyrin IX regardless of the iron oxidation state and ligands
HPLC	High pressure liquid chromatography
IEF	Isoelectric focusing
LSIMS	Liquid secondary ion mass spectrometry
NADPH	Nicotinamide adenine dinucleotide phosphate (reduced)
NMR	Nuclear magnetic resonance
NOE	Nuclear Overhauser effect
NOESY	Two-dimensional nuclear Overhauser enhancement spectroscopy
P-450	Cytochrome P-450
POBN	α-(4-Pyridyl-1-oxide)-N-*tert*-butylnitrone
PPIX	Protoporphyrin IX
SDS-PAGE	Sodium dodecyl sulfate polyacrylamide gel electrophoresis
TFA	Trifluoroacetic acid

CHAPTER 1

Introduction

1.0 Hemoproteins

The hemoproteins contain iron protoporphyrin IX as the prosthetic group (Fig. 1.1). Despite the fact that hemoproteins share a common prosthetic group, they exhibit diverse biological functions, including electron transport (cytochromes b, c and a), oxygen transport (hemoglobin and myoglobin), oxygen transfer (cytochrome P-450s), and one

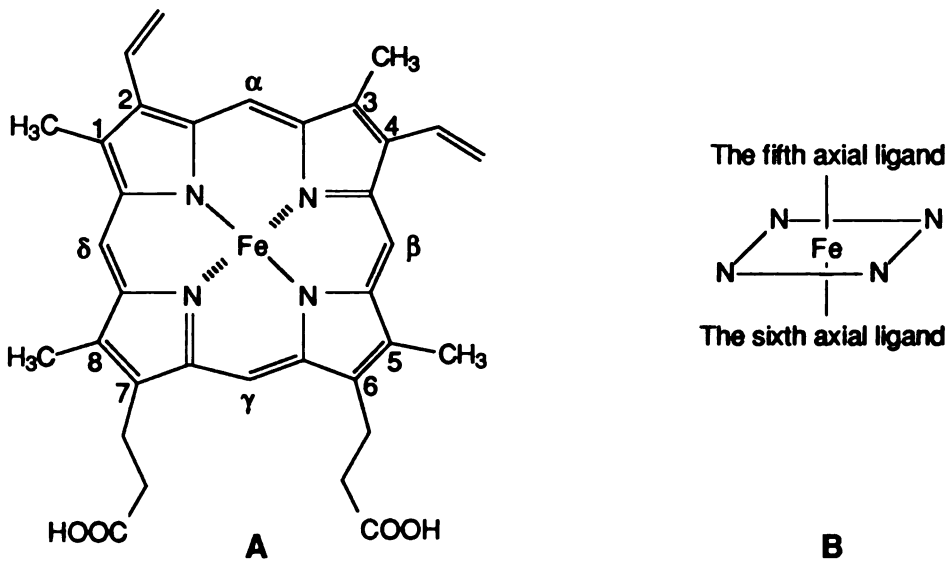

Fig. 1.1 The structure of iron protoporphyrin IX. Structure A is simplified by an iron in a square of four nitrogens in B, where the axial heme ligands are also shown.

electron oxidation (peroxidases). Likewise, the active species generated from the oxidation of hemoproteins by a two electron oxidant such as H_2O_2 is not identical in all hemoproteins. The active species of hemoproteins is thought to be complex (formally [Fe^{V}] or [FeO^{III}]), two oxidation equivalents above the ferric state. One of the oxidation equivalents is used for the oxidation of [Fe^{III}] to [Fe^{IV}] and the other for the oxidation in

most peroxidases of the porphyrin, in the globins and cytochrome c peroxidase of the protein, and in cytochrome P-450 of an undetermined site. The reactivity of the heme prosthetic group is therefore controlled by the protein.

The major factor regulating the reactivity of the heme prosthetic group is a difference in the heme iron environment. The fifth heme ligand, which connects the prosthetic group to the protein (Fig. 1.1), may play a role in differentiating the reactivity of the hemoproteins. The iron atom is coordinated to the nitrogen of a histidine residue in respiratory cytochromes, the globins and peroxidases (Salemme, 1977; Dickerson & Geis, 1983; Saunders et al., 1964; Dunford & Stillman, 1976), a cysteine thiolate in cytochrome P-450s, chloroperoxidase (Dawson et al., 1976) and prostacyclin synthase, and the phenoxyl oxygen of a tyrosine residue in catalase (Murthy et al., 1981). When the high valent iron-oxo species are formed, the electron-rich cysteine thiolate ligand acts as an electron donor to facilitate cleavage of the O-O bond, whereas the histidine imidazole ligand of horseradish peroxidase depends on charged residues on the distal side to help cleave the peroxide bond (Poulos, 1988; Dawson et al., 1976; Sono et al., 1982). The tyrosine phenolate ligand is strong enough to promote cleavage of the peroxide bond without the assistance of charged residues (Dawson, 1988).

Accessibility of the substrate to the heme iron may help to determine the reactivity of the prosthetic group. The heme is buried but the iron atom is accessible to substrates in cytochrome P-450 (Fig. 2.1), whereas only the δ-*meso* heme edge is available to the substrate in horseradish peroxidase (Fig. 2.1). This difference in accessibility of substrates to the prosthetic iron atom generally determines whether a hemoprotein is a monooxygenase or peroxidase (Ortiz de Montellano, 1987; Ator & Ortiz de Montellano, 1987). Since chloroperoxidase functions as both a peroxygenase and peroxidase, both iron atom and *meso* heme edge may be accessible to the substrate (Dawson, 1988).

It is apparent that the heme iron environment controls the reactivity of the heme prosthetic group. The proximal heme ligand is, however, less important than other factors

because cytochrome P-450 and chloroperoxidase have a cysteine fifth heme ligand but, the former is a monooxygenase and the latter halogenates substrates.

1.1 The globins

1.1.1 Structure and properties

Myoglobin is a water-soluble hemoprotein with M_r 17,000-18,000. It consists of one prosthetic heme group and a polypeptide chain of 153 amino acids (Dickerson & Geis, 1983). Strong similarities are observed in the sequences of myoglobins of different species such that 82 out of 153 amino acid residues are invariant among the myoglobins of 24 species (Takano, 1977a; Dickerson & Geis, 1983). The crystal structure of sperm whale myoglobin shows that myoglobin contains eight right-handed α helices, A through H, with 131 amino acids involved in the helices and the rest in making turns between helices (Kendrew et al., 1960; Kendrew, 1961; Takano, 1977a). The heme group is buried in a heme binding pocket with the propionic acid side chains exposed to the solvent. The protein surface is covered with hydrophilic amino acids which are hydrogen bonded to water molecules whereas the inside of the protein is composed of hydrophobic amino acids. The structure of horse myoglobin is similar to that of sperm whale myoglobin based on their X-ray structures (Takano, 1977a; Evans & Brayer, 1988) (Fig. 1.2, A and B).

The fifth heme ligand in both sperm whale and horse myoglobins is His 93 and the sixth coordination site is available for the binding of oxygen or other ligands. The sixth heme coordination site is vacant in deoxymyoglobin, in which the iron atom is 0.55 Å above the heme plane toward the proximal ligand (Takano, 1977b), but it is filled by a water molecule in metmyoglobin, in which the iron atom is 0.4 Å above the heme plane. When the sixth heme ligand is oxygen or carbon monoxide, the iron atom is only 0.26 or 0.24 Å above the heme plane, respectively (Dickerson & Geis, 1983). Carbon monoxide binds to the iron in a linear fashion and much more strongly than does oxygen. The

discrimination between CO and O_2 binding is much reduced when they bind to the globins rather than free heme, because the distal His 64 prevents the linear binding of CO but stabilizes bound oxygen through hydrogen bonding (Stryer, 1981; Springer et al., 1989). The fact that CO binds much more strongly to free heme than to the globins implies regulation of the reactivity of the prosthetic group by the protein. The presence of the distal histidine residue is also important because the rate of autooxidation of the mutants is much faster than that of the native globins when it is replaced by other amino acids (Gerald & Effron, 1961; Springer et al., 1989).

Tyrosine residues have been the focus of attention because Tyr 103 is the site of the protein radical and Tyr 151 is responsible for the dimerization of myoglobin. Sperm whale myoglobin has three tyrosine residues (Y103, Y146 and Y151), horse myoglobin has two (Y103 and Y146) and kangaroo myoglobin has only Y146. Tyr 146 has a pK_a of 12.7-12.9 due to its hydrophobic environment but Tyr 103 has a somewhat lower pK_a (Uyeda & Peisach, 1981). Tyr 151 has a pK_a of about 10.3, a value very similar to that of a tyrosine residue in aqueous solution. NMR spectroscopy of cyanoferrimyoglobin suggests that Tyr 146 is buried in the protein, Tyr 151 is relatively exposed to the solvent, and Tyr 103 has intermediate properties (Wilbur & Allerhand, 1976). The properties of tyrosine residues obtained by pK_a and NMR studies are consistent with those inferred from the crystal structures (Fig. 1.2). Tyr 146, which is present in all myoglobins, is buried in the protein and Tyr 103 is in contact with both the heme and the solvent. Tyr 151 in sperm whale myoglobin protrudes into the solvent and is coordinated to two water molecules whereas Phe 151 in horse myoglobin is positioned toward the protein (Takano, 1977a; Evans & Brayer, 1988).

Hemoglobin, which is a tetrameric hemoprotein, consists of four heme groups and four polypeptide chains containing two identical α chains of 141 amino acids and two identical β chains of 146 amino acids (Dickerson & Geis, 1983). Each chain of hemoglobin is folded in a manner very similar to that of myoglobin, so that four heme

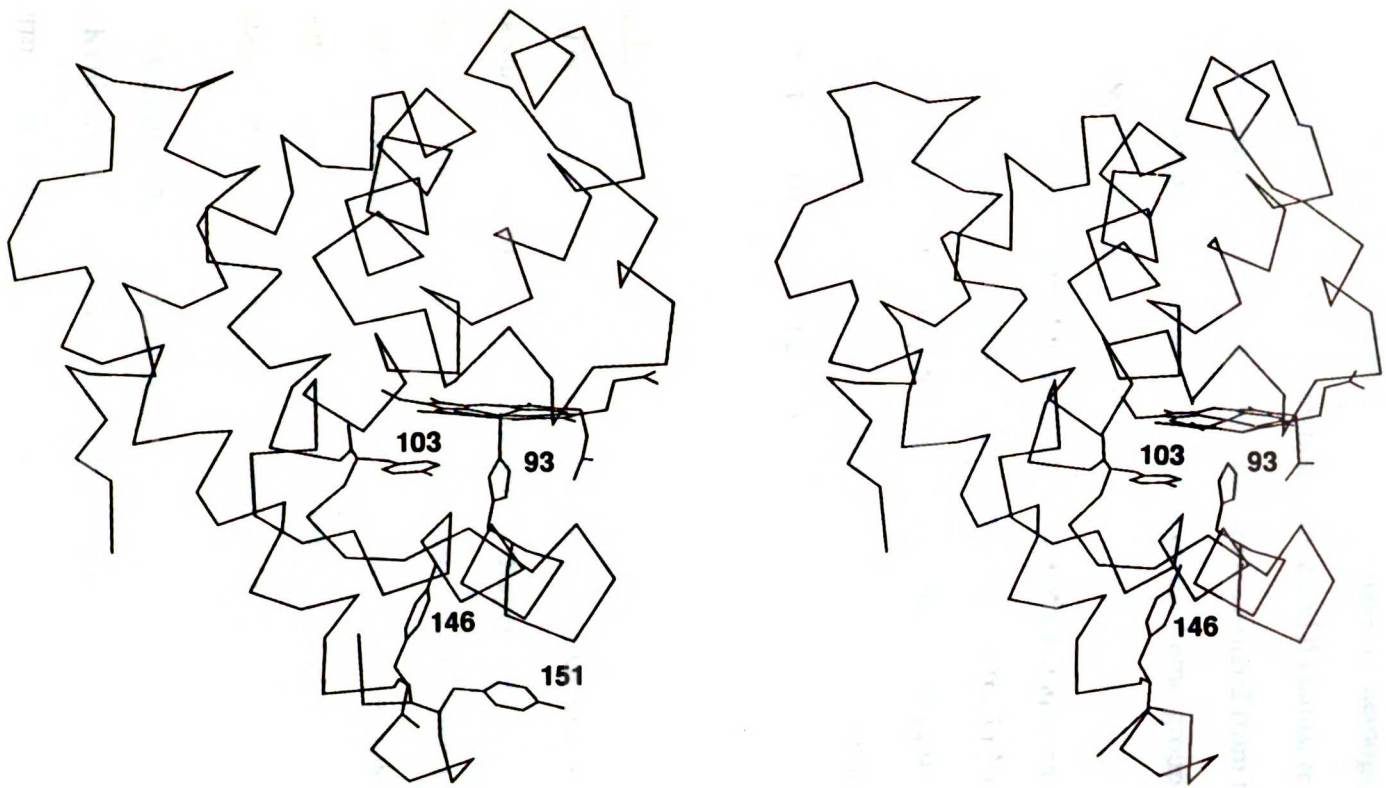

Fig. 1.2 Crystal structures of sperm whale myoglobin (A) and horse heart myoglobin (B). The proximal heme ligand, His 93 is shown. Tyr 103 is located close to the heme group and Tyr 146 is buried in the protein. Tyr 151 in (A) protrudes into the solvent.

pockets are exposed at the surface of the tetrameric molecule. Five amino acids, including the proximal histidine residue, are invariant among myoglobin and the α and β chains of hemoglobin (Dickerson & Geis, 1983). The heme is coordinated to the imidazole nitrogen of His 87 in the α chains and His 92 in the β chains of hemoglobin. The distal histidine residues are His 58 and 63 of the hemoglobin α and β chains, respectively. When oxygen binds to hemoglobin, the quaternary structure is changed from the T to the R form due to structural changes that include movement of the heme group and the proximal ligand (Stryer, 1981).

The cysteine residue of hemoglobin is one of the major sites of adduct formation with xenobiotics. There are six cysteine residues (104α, 112β and 93β) in the human hemoglobin tetramer but only the sulfhydryl group of Cys 93 is available for reaction. Although Cys 93 is buried in the protein, xenobiotics may induce conformational changes in the protein that allows them to approach the sulfhydryl group (Ringe et al., 1988; Haugen, 1989).

1.1.2 Function

The globins bind molecular oxygen reversibly like other respiratory proteins such as hemocyanin, chlorocruorin, and hemerythrin (Kagen, 1973). The globins bind molecular oxygen only when they are in the ferrous state. Myoglobin is found in muscles and is particularly abundant in aquatic diving mammals due to its role in the storage of oxygen. Hemoglobin, which is located in the red blood cells, binds oxygen in the lungs and delivers it to the tissues, and also brings the by-product CO_2 back to the lungs (Stryer, 1981).

1.1.3 Reaction with hydrogen peroxide

Keilin and Hartree demonstrated that 1 mole of H_2O_2 was required per metmyoglobin to form a red complex which reverted to metmyoglobin upon treatment with reducing agents (Keilin & Hartree, 1935). Later, George and Irvine considered that metmyoglobin was one-electron oxidized in the red complex because 1 equivalent of ferrocyanide reduced

the complex completely to metmyoglobin. This result was supported by magnetic susceptibility studies indicating that the red complex had four unpaired electrons on the iron atom (George & Irvine, 1952). The pH optimum for formation of the complex ranged between pH 8 and 9 because oxidative attack on the porphyrin ring occurred outside that pH range (George & Irvine, 1952). Other oxidizing agents, such as $NaClO_2$, KIO_4, $K_3Mo(CN)_8$ and K_2IrCl_6, gave a complex one oxidation equivalent above the ferric state which had the same spectroscopic properties as the peroxide complex (George & Irvine, 1954). However, when the ferrocyanide was added to metmyoglobin before H_2O_2, the two oxidation equivalents of the peroxide could be accounted for. Based on this, George and Irvine proposed that metmyoglobin may be oxidized by H_2O_2 to ferryl myoglobin, containing quadrivalent iron, and a hydroxyl radical, the latter being a transient species (Equation 1) (George & Irvine, 1952).

$$[Fe^{III}] + H_2O_2 \longrightarrow [Fe^{IV}] + {}^{-}OH + {}^{\bullet}OH \qquad (1)$$

Formulation of the ferryl oxygen species as containing quadrivalent iron was done by King and Winfield, who observed an [Fe(IV)=O] species with an absorption peak at 545 nm in the reaction of metmyoglobin and methemoglobin with H_2O_2 at neutral pH. At pH lower than 5, the major product absorbed at 525 nm and was proposed to be the protonated ferryl species, [Fe(IV)-OH]. The formation of the two species was reversible, depending on the pH, although the protonated form was irreversibly oxidized by H_2O_2 to a product having an absorption peak at 586 nm (King & Winfield, 1966). Resonance Raman, X-ray edge absorption, and Mossbauer studies have confirmed the [Fe(IV)=O] formulation (Sitter et al., 1985; Chance et al., 1986; Maeda et al., 1973).

George and Irvine proposed two reaction mechanisms for formation of ferrylmyoglobin from the reaction of metmyoglobin with H_2O_2 (George & Irvine, 1956). One mechanism, as already noted, involves formation of ferrylmyoglobin and the hydroxyl radical, a reaction analogous to the Fenton reaction except that the redox state of the iron

atom is one equivalent higher in the myoglobin reaction (Equation 1). The other mechanism involves transient formation of the [Fe(V)=O] species as in Equation 2 (George & Irvine, 1956). They found that the first mechanism does not satisfy the energetics and

$$[Fe^{III}] + H_2O_2 \longrightarrow [Fe^{V}] \longrightarrow [Fe^{IV}] + ? \qquad (2)$$

experimental results. Further demonstration that formate is not oxidized to carbon dioxide by myoglobin and H_2O_2 also argues against the formation of the hydroxyl radical (Kanner & Harel, 1985b; Bielski & Richter, 1977). The initial formation of the [Fe(V)=O] species in the reaction of metmyoglobin with H_2O_2 is supported by the kinetic studies by Kremer (Kremer, 1981). The reaction includes two-electron oxidation as is confirmed by titration of the complex with ferrocyanide. He proposed that the [Fe(V)=O] species may be formed before the ferryl oxygen complex formation because EPR studies show that a transient species exists before the formation of the ferryl oxygen complex (King & Winfield, 1963; Yonetani & Schleyer, 1967).

The identity of the second oxidizing species has been extensively studied since Gibson et al. observed a free radical from the reaction of methemoglobin and sperm whale myoglobin with H_2O_2 at pH 8 (Gibson & Ingram, 1956; Gibson et al., 1958). King and Winfield suggested that the free radical is lost by reaction with another free radical and H_2O_2, and the ferryl species reverts to the ferric state with concomitant two-electron oxidation of an amino acid. The hemoprotein can cycle in this manner eight times before it can no longer react with H_2O_2 (King & Winfield, 1963). It was proposed from EPR studies that the free radical resides close to the iron atom and is initially on a distal side phenylalanine or histidine residue but rapidly transfers to a tyrosine residue (Equation 3) (King et al., 1964). The formation of a tyrosine radical is supported by the finding that

$$[Fe^{III}] + H_2O_2 + PH \longrightarrow [Fe^{IV}] + \cdot P \qquad (3)$$

* PH stands for the protein.

model phenoxyl radicals have the same specific saturation coefficient (Tyr = 2.3) and line width (12 G) as the EPR signal of the globins (King et al., 1967). Crystal structures of the myoglobins suggest Tyr 103 as the site of the protein radical because Tyr 103 is 3-4 Å away from the edge of the prosthetic heme group (Takano, 1977a; Evans & Brayer, 1988). King and Winfield measured the concentration of the protein radical in the reaction of horse myoglobin with H_2O_2 and showed that it comprised 16% of the total protein 0.6 min after initiation of the reaction at 0°C. This concentration corresponds, by extrapolation, to approximately 50% of the total protein at the beginning of the reaction (King & Winfield, 1963). Recent stopped flow EPR studies showed that the protein radical decays with a half life of 30 seconds when horse myoglobin (1 mM) is rapidly mixed with an equivalent of H_2O_2 (Davies, 1991). The EPR signals of the protein radicals formed from the reactions of the globins with H_2O_2 were compared. The protein radical generated from horse myoglobin exhibits signals at g = 2.004 and g = 2.027, the latter being smaller than the former (Fig. 2.11). When horse myoglobin is replaced with sperm whale myoglobin, less protein radical is detected and the low field signal at g = 2.027 is not seen. The protein radical obtained from horse hemoglobin decays faster than that of horse myoglobin (King et al., 1967).

Shiga and Imaizumi proposed that the species generated from the reaction of methemoglobin with H_2O_2 has chemical reactivity similar to that of horseradish peroxidase Compound I (Shiga & Imaizumi, 1975). The reaction of metmyoglobin with H_2O_2 may form a porphyrin cation radical that later oxidizes the protein (Equations 4 and 5).

$$[Fe^{III}] + H_2O_2 \longrightarrow [Fe^{IV+\bullet}] \qquad (4)$$

$$[Fe^{IV+\bullet}] + PH \longrightarrow [Fe^{IV}] + \bullet P \qquad (5)$$

However, the demonstration that the absorption spectra of the [Fe(IV)=O] species and the [Fe(IV)=O/protein radical] are identical suggests that the free radical can only be transiently derived from the porphyrin or an amino acid directly linked to the iron atom (King &

Winfield, 1963).

Although the outcome of the reaction of the globins with H_2O_2 is not clearly defined, Equation 3 is generally accepted.

The protein radical generated from the reaction of metmyoglobin with H_2O_2 is involved in heme-protein and protein-protein crosslinking reactions. Fox and coworkers observed that some heme is retained by the protein after reaction of myoglobin with H_2O_2 at pH 4.5 (Fox et al., 1974). They suggested that the heme that remains after heme extraction is bound to the distal histidine residue which is oxidized under acidic conditions. Later, Catalano et al. showed that the heme is covalently bound to Tyr 103 when horse metmyoglobin is treated with H_2O_2 at pH 7.4 (Catalano et al., 1989). Sperm whale myoglobin, which has an additional tyrosine residue (Tyr 151), undergoes dimerization upon treatment with H_2O_2 (Rice et al., 1983). Rice and coworkers have shown that the reaction of sperm whale myoglobin with H_2O_2 results in a decrease in the tyrosine content (1.4 of 3) from the treated monomers and (1.8 of 3) from the dimers (Rice et al., 1983). Tew and Ortiz de Montellano demonstrated that the dimerization occurs only in the reaction of H_2O_2 with ferric sperm whale myoglobin, and neither zinc sperm whale myoglobin nor a mixture of zinc whale and ferric horse myoglobins dimerizes, indicating that the dimerization reaction requires Tyr 151 and that the formation of the Tyr 151 radical occurs by intramolecular electron transfer. Further characterization of chymotryptic digests of the myoglobin dimers indicates that Tyr 103 of one myoglobin is covalently bound to Tyr 151 of the other. They proposed that an electron is transferred intramolecularly from Tyr 151 to Tyr 103, possibly via Tyr 146 (Tew & Ortiz de Montellano, 1988).

1.1.4 Epoxidation reactions

The major redox reaction studied with the globins is the epoxidation of olefins, notably styrene, *cis*-stilbene and 7,8-dihydroxy-7,8-dihydrobenzo[*a*]pyrene (Ortiz de Montellano & Catalano, 1985; Catalano & Ortiz de Montellano, 1987). Part of the

epoxidation reaction proceeds via the mechanism proposed for the reaction catalyzed by cytochrome P-450. A second epoxidation mechanism distinct from that of the P-450-catalyzed epoxidation is a protein-mediated cooxidation. In this pathway, molecular oxygen is thought to bind to the tyrosine radical to generate a peroxyl radical that epoxidizes the olefin. This pathway allows carbon-carbon bond rotation before epoxide ring closure and thus results in loss of the olefin stereochemistry. Scheme 1.1 shows the mechanisms proposed based primarily on ^{18}O and stereochemical studies. If the enzyme catalyzes a ferryl oxygen transfer like P-450, the epoxide oxygen will derive from the peroxide and the stereochemistry will be retained (pathway A, Scheme 1.1). If molecular oxygen is incorporated into the epoxide, the reaction presumably proceeds by a protein-mediated mechanism (pathway B). In the case that the epoxide oxygen comes from the aqueous medium, the oxidation of the olefin to a radical cation produces the epoxide by addition of water, loss of an electron and epoxide ring closure (pathway C). The stereochemistry is not retained in pathways B and C unless free rotation of the carbon-carbon bond is restricted. The epoxidation catalyzed by the globins proceeds via different pathways depending on the olefin and the globin. For instance, the epoxide oxygen derives from the peroxide and molecular oxygen when styrene is epoxidized by myoglobin (Ortiz de Montellano & Catalano, 1985). In accord with this mechanistic heterogeneity, the overall stereochemistry is partially scrambled. In the hemoglobin-catalyzed epoxidation of *cis*- and *trans*-stilbenes to the *cis*- and *trans*-epoxides, respectively, the epoxide oxygen also comes from the peroxide and molecular oxygen (Catalano & Ortiz de Montellano, 1987). However, in the epoxidation of *cis*-stilbene to *trans*-stilbene oxide, the epoxide oxygen derives from molecular oxygen and the aqueous medium. When *trans*-7,8-dihydroxy-7,8-dihydrobenzo[*a*]pyrene is epoxidized by hemoglobin and then hydrolyzed to the tetrol, the epoxide oxygen originates from the peroxide and water (Catalano & Ortiz de Montellano, 1987). The fact that only styrene and *cis*-stilbene are epoxidized by the

cooxidative mechanism may be partially explained by steric or lipophilic properties of the substrates that restrict their access to the protein peroxyl radical.

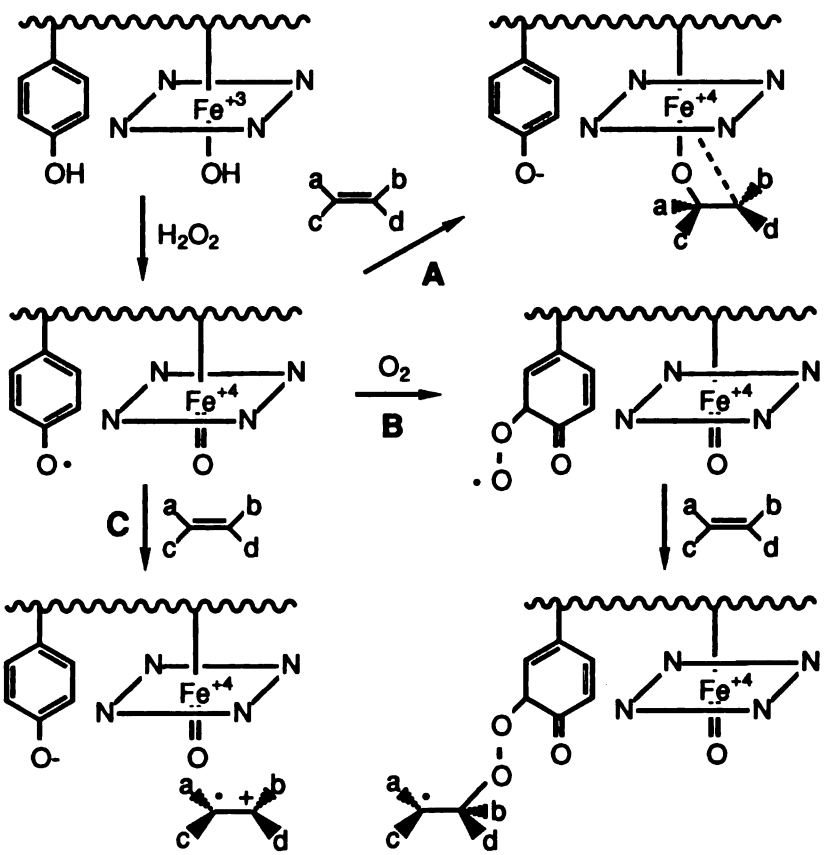

Scheme 1.1 Proposed mechanisms for the globin-catalyzed epoxidation of olefins. The four nitrogens indicate the porphyrin and the wavy line indicates the protein surface. A tyrosine is shown as the amino acid. The oxygen transfer, protein-mediated cooxidation and radical cation mechanisms are shown.

1.1.5 Other reactions

The activated globins catalyze the oxidation of phenols, uric acid, β-carotene, ascorbic acid and the cooxidation of salicylate (Shiga & Imaizumi, 1975; Ames et al., 1981; Kanner & Harel, 1985b; Galaris et al., 1988). It has been shown that hemoglobin has a monooxygenase-like activity *in vitro* in the presence of oxygen, NADPH and cytochrome P-450 reductase. "Reconstituted" hemoglobin catalyzes the aromatic hydroxylation of

aniline (Mieyal et al., 1976), O-demethylation of aromatic ethers (Starke et al., 1984), N-hydroxylation of *para*-chloroaniline (Golly & Hlavica, 1983) and aliphatic hydroxylation of cyclohexane (Starke & Mieyal, 1989).

Lipid peroxidation seems to be initiated by the active species generated from the reaction of the ferric myoglobin and hemoglobin with peroxide (Kanner & Harel, 1985b; Galaris et al., 1990). It is likely that the active species of the globins oxidizes lipid to lipid radical that binds molecular oxygen. The resulting lipid peroxyl radical then abstracts a hydrogen from another lipid. The lipid peroxide can be oxidized by the ferryl species, which returns to the resting state, and the resulting lipid peroxyl radical can undergo a radical chain reaction until the reaction is terminated (Kanner & Harel, 1985a; Harel & Kanner, 1985). Free iron released from the globins by prolonged incubation with peroxide may also promote lipid peroxidation (Gutteridge, 1986). Since the redox potential of the activated myoglobin is +1.4 V, it is high enough to oxidize polyunsaturated fatty acids (Shiga & Imaizumi, 1975). The initiation of lipid peroxidation by hemoglobin is also supported by the fact that the ferrihemoglobin catalyzes 80% homolytic and 20% heterolytic cleavage of the peroxide bond of 10-hydroperoxy-8,12-octadecadienoic acid (Labeque & Marnett, 1987).

1.2 Chloroperoxidase

1.2.1 Properties

Chloroperoxidase is a monomeric hemoprotein of M_r 42,000 secreted by the marine fungus, *Caldariomyces fumago* (Shaw & Hager, 1959). It has two major isoenzymes, A and B, which have the same amino acid composition and specific activity but different carbohydrate content (Kenigsberg et al., 1987). It has been crystallized but its crystal structure is not available presumably due to the heterogeneity caused by the heavy content (25%) of carbohydrate. Forty five percent of the total amino acid content is composed of

Asp, Glu, Ser, and Pro and the enzyme therefore has a low pI of 4, which is similar to that (4.55) of P-450$_{cam}$ (Morris & Hager, 1966; Dus et al., 1970). The redox potential of chloroperoxidase is around -140 mV at pH 6.9, close to that (-170 mV) of substrate-bound P-450$_{cam}$ (Makino et al., 1976). The heme group can be split from the apoprotein but reconstitution has not been successful. Pure enzyme has an R_z value (optical density of 403/280 nm) ranging between 1 and 1.44 (Hollenberg & Hager, 1978).

1.2.2 Structure

A cDNA for chloroperoxidase has been cloned, isolated and sequenced (Fang et al., 1986). The fifth heme ligand has been assigned as a cysteine thiolate by absorption, magnetic circular dichroism (Dawson et al., 1976), NMR (Krejcarek et al., 1976), EPR (Rutter & Hager, 1982), and Mossbauer (Champion et al., 1975) spectroscopies. EXAFS studies further suggest that the ferric and oxy-ferrous enzymes have an Fe-S bond in which the bond length is consistent with those of P-450 and model iron-porphyrin complexes (Cramer et al., 1978; Dawson et al., 1986). Resonance Raman spectroscopy also supports the presence of a cysteine thiolate as the fifth heme ligand by showing the same iron-sulfur bonding geometry between chloroperoxidase and P-450$_{cam}$ (Bangcharoenpaurpong et al., 1986). Strong evidence for the cysteine thiolate ligand is provided by the demonstration that the ferrous CO complex of chloroperoxidase has a Soret band at 446 nm, a position very similar to the 450 nm maximum of the cytochrome P-450$_{cam}$ complex (Dawson & Sono, 1987).

Since there are three cysteines (29, 79 and 87), and two of them are linked by a disulfide bond, the third cysteine must provide the heme ligand. Cys 87 was predicted as the fifth axial heme ligand due to some sequence identity shared between this region and the axial ligand region of P-450$_{cam}$ (Kenigsberg et al., 1987). Later, Cys 29 was identified as the axial heme ligand by incubation of apochloroperoxidase with Ellman's reagent under reducing and denaturing conditions (Blanke & Hager, 1988). There is no sequence identity

between the proximal cysteine region of chloroperoxidase and that of P-450$_{cam}$. Cys 29 is located between two proline residues but a β-turn is expected in this region based on secondary structure predictions (Chou & Fasman, 1978).

Chloroperoxidase	T G S D - C (87)	- G D S L V N L T
Cytochrome P-450$_{cam}$	H G S H L C (357)	L G Q H L A R R Q
Chloroperoxidase	D S R A P C (29)	P A L N A L A N H (38)
Cytochrome c peroxidase	N Y I G Y G	P V L V R L A W H (53)

There is no sixth heme ligand in the pH range 2.2 to 7.0, as determined by resonance Raman spectroscopy (Blanke et al., 1989). Blanke and Hager proposed the presence of a distal histidine residue by experiments with diethyl pyrocarbonate, which specifically derivatizes histidine residues (Blanke & Hager, 1990). The radiolabeled agent stoichiometrically derivatizes a histidine residue and inactivates the enzyme. It is highly likely that the distal histidine residue is His 38 based on the sequence identity between this region of chloroperoxidase and the distal histidine (His 53) region of yeast cytochrome c peroxidase, for which a crystal structure is available (Blanke & Hager, 1990). They also proposed that two asparagine residues near His 38 may serve as charged residues that polarize the peroxide bond and facilitate its cleavage. These residues, including His 38, may be located on the distal side based on secondary structure predictions.

The active site is believed to contain polar amino acid residues because ligand binding studies show that there are charged amino acids which affect ligand binding (Sono et al., 1986). This is further supported by the fact that the oxidation of styrene by chloroperoxidase yields a low molar ratio of styrene oxide to phenylacetaldehyde (1.2:1) compared to that of P-450 (33:1), suggestive of a polar active site (Ortiz de Montellano et al., 1987).

1.2.3 Function

The halogens in seawater appear to be involved in the biosynthesis of bromine-containing terpenes, acetogenins, and phenolic compounds. It is likely that marine metabolites function in the defensive adaptation to the marine environment (Fenical, 1982). Caldariomycin, a metabolite of *C. fumago*, was first synthesized by Clutterbuck and coworkers (Clutterbuck et al., 1940; Shaw et al., 1959). β-Ketoadipic acid could be a precursor of caldariomycin because it is converted to caldariomycin by chloroperoxidase. Even though chloroperoxidase catalyzes the peroxidative chlorination of β-ketoadipic acid to δ-chlorolevulinic acid and carbon dioxide, the possibility that δ-chlorolevulinic acid is an intermediate is ruled out, however, because the C^{14}-labeled acid is not converted to caldariomycin by the growing mold (Beckwith et al., 1963).

1.2.4 Reactions

Chloroperoxidase has diverse catalytic abilities because it catalyzes peroxidative, catalatic, halogenative, and P-450-like reactions. Therefore, the active site of chloroperoxidase may share some common structure with those of peroxidase, catalase and P-450.

Peroxidative reaction

Peroxidase catalyzes the one electron oxidation of substrates at the expense of peroxide. Classical peroxidase substrates include guaiacol, pyrogallol and leucomalachite. The rate of oxidation of guaiacol by chloroperoxidase is about 10% of that of horseradish peroxidase under similar conditions. Peroxidase is oxidized by peroxide to Compound I, a species two oxidation equivalents above the ferric state (Equation 6). The green Compound I oxidizes the substrate and is concomitantly converted to red Compound II, which returns to the resting ferric protein when it is reduced by a second molecule of the substrate (Equations 7 and 8). However, chloroperoxidase Compound I with a Soret maximum at 367 nm is very unstable and its Compound II has not been isolated.

$[Fe^{III}] + ROOH \longrightarrow$ Compound I + ROH (6)

Compound I + AH $\longrightarrow$ Compound II + $\cdot$A (7)

Compound II + AH $\longrightarrow$ $[Fe^{III}]$ + $\cdot$A (8)

* AH stands for a reducing substrate.

Chloroperoxidase Compound I possesses a π-cation radical because it exhibits spectroscopic properties similar to those shown by horseradish peroxidase Compound I. Mossbauer spectra of horseradish peroxidase Compounds I and II are very similar and have been interpreted to indicate that both hemoproteins are in an Fe^{IV} state (Moss et al., 1969; Schulz et al., 1979). EXAFS spectroscopy showed that horseradish peroxidase Compounds I and II, as well as synthetic analogs, have a short Fe-O bond distance of 1.64 Å, indicative of the presence of an Fe^{IV}=O (Penner-Hahn et al., 1986). The assignment of a porphyrin cation radical is further supported by electron nuclear double resonance, showing that an electron is removed from a porphyrin π molecular (A_{2u}) orbital in horseradish peroxidase Compound I (Roberts et al., 1981) whereas an electron is removed from an A_{1u} orbital in chloroperoxidase Compound I (Rutter & Hager, 1982). The EPR signal of Compound I is observed in the g = 2 region with very broad wings, again suggestive of a porphyrin cation radical species (Schulz et al., 1984).

The formation of an analogous Compound I is not observed in all peroxidases. Cytochrome c peroxidase forms the ferryl oxygen species and a protein radical rather than a porphyrin cation radical, like the globins, but the site of the protein radical is not well defined (Yonetani, 1976). Lactoperoxidase first forms the porphyrin cation radical intermediate which rapidly oxidizes the protein (Courtin et al., 1982; Courtin et al., 1984).

Catalatic reaction

Catalase catalyzes the dismutation of hydrogen peroxide to form water and molecular oxygen (Equations 9 and 10). This reaction is also catalyzed by horseradish peroxidase

and chloroperoxidase, but the reactivity of the former is less than 0.01% whereas that of the latter is 0.2% compared to catalase (Thomas et al., 1970). Catalase can oxidize ethanol

$$[Fe^{III}] + H_2O_2 \longrightarrow \text{Compound I} + H_2O_2 \quad (9)$$

$$\text{Compound I} + H_2O_2 \longrightarrow [Fe^{III}] + O_2 + H_2O \quad (10)$$

to acetaldehyde whereas most peroxidases cannot. Chloroperoxidase, however, catalyzes not only this reaction (yield: 4%) but also the oxidation of allylic (yield: 29%), propargylic (yield: 36%) and benzylic alcohols (yield: 43%) to the corresponding aldehydes (Thomas et al., 1970; Geigert et al., 1983a). This chloroperoxidase-catalyzed reaction is pH-dependent, with a pH optimum of 5, whereas that of catalase is pH-independent (Thomas et al., 1970).

Halogenative reaction

Peroxidase catalyzes the bromination and iodination of organic substrates in the presence of halide anion and H_2O_2. Chloroperoxidase chlorinates substrates by using chloride or chlorite, although the latter agent does not require H_2O_2. Horseradish peroxidase can chlorinate substrates by using chlorite but not chloride and H_2O_2, and myeloperoxidase can use chloride but is inactivated by chlorite (Hollenberg et al., 1974; Harrison & Schultz, 1976). In the chlorination reaction, various chlorinating intermediates including free HOCl and the enzyme·hypochlorite complex (Equations 11, 12 and 13) have been proposed (Hollenberg et al., 1974; Libby et al., 1982). The binding and reaction of

$$[Fe^{III}] + H_2O_2 \longrightarrow \text{Compound I} + H_2O \quad (11)$$

$$\text{Compound I} + X^- \longrightarrow \text{Compound X } ([Fe^{III}\text{-OX}]) \quad (12)$$

$$\text{Compound X} + AH \longrightarrow [Fe^{III}] + AX + H_2O \quad (13)$$

* X is Cl^-, Br^- or I^-.

chloride ion appear to be the most difficult steps in chlorination reactions but Compound I formation and bromide oxidation are the rate limiting steps in bromination reactions (Libby

& Rotberg, 1990). Typical substrates are halogen acceptors such as β-diketones and the pH optimum for the halogenation reaction is 2.75. Chloroperoxidase seems to be inactivated in the presence of chloride ion and H_2O_2 if it is not protected by reducing substrates (Shaw & Hager, 1961; Nieder & Hager, 1984).

Cytochrome P-450-like reaction

Since chloroperoxidase and cytochrome P-450 share some physical properties, including a thiolate axial heme ligand, it is not surprising that they catalyze similar reactions by similar mechanisms. The oxidations of styrene and 1,3-butadiene are catalyzed by both chloroperoxidase and P-450 by a similar mechanism (Ortiz de Montellano et al., 1987; Elfarra et al., 1991). The oxidation of 1,3-butadiene by P-450 and chloroperoxidase produces butadiene monoxide and crotonaldehyde by a ferryl oxygen transfer mechanism. The formation of crotonaldehyde but not methyl vinyl ketone indicates that the transition state leading to the former is more stable than that to the latter, so the oxygen is regioselectively transferred to the terminal carbon of the olefin which favors the formation of crotonaldehyde. The butadiene monoxide to crotonaldehyde ratio is much lower when the reaction is catalyzed by chloroperoxidase rather than P-450, which is consistent with the result obtained in the oxidation of styrene to styrene oxide and phenylacetaldehyde. Cyclohexene is another substrate for the epoxidation reaction catalyzed by P-450 with either NADPH/O_2 or cumene hydroperoxide or by chloroperoxidase with H_2O_2 (McCarthy & White, 1983).

The oxidation of thioanisoles to sulfoxides by chloroperoxidase is catalyzed by a direct P-450-like oxygen transfer mechanism (Kobayashi et al., 1987). ^{18}O studies showed that the peroxide is incorporated into the sulfoxide in the reactions catalyzed by both chloroperoxidase and P-450 whereas other oxygen sources (e.g., water) are also involved in the formation of sulfoxide in the oxidation catalyzed by horseradish peroxidase (Kobayashi et al., 1986).

Other reactions

Chloroperoxidase catalyzes the formation of nitroso compound from amino group, the N-demethylation of N,N-dimethylaniline, the dismutation of chlorine dioxide, and the oxidation of iodine to iodate and dimethylsulfoxide to sulfone (Corbett et al., 1979; Shahangian & Hager, 1981; Kedderis et al., 1980; Kedderis et al., 1986; Thomas & Hager, 1968; Geigert et al., 1983b).

1.3 11-Microperoxidase

1.3.1 Structure

11-Microperoxidase is prepared from horse heart cytochrome c by peptic digestion (Fig. 1.3). Further digestion of 11-microperoxidse with trypsin yields 8-microperoxidase.

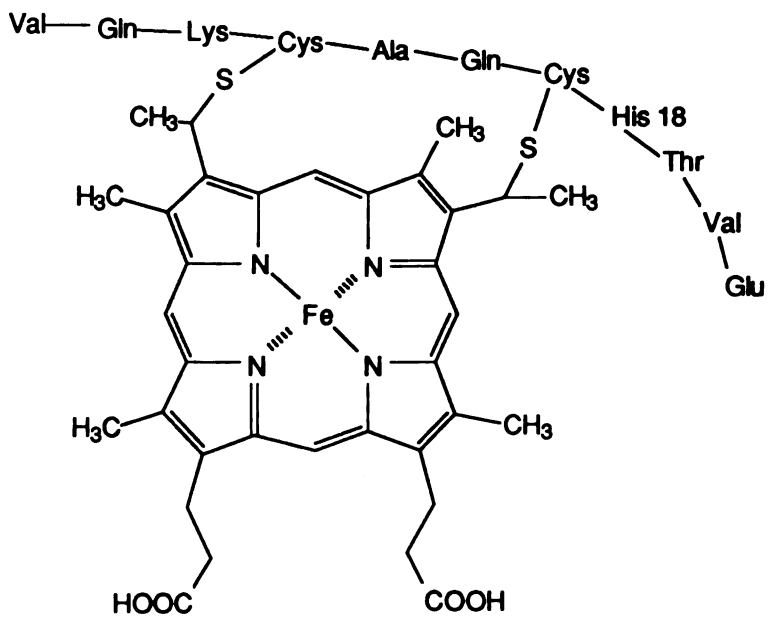

Fig. 1.3 Structure of 11-microperoxidase.

These peptides have the proximal His 18 and the two thioether linkages between the heme group and the cysteine residues. The sixth heme ligand is water or a nitrogen group from

another molecule (Harbury & Loach, 1959). The heme peptides do not have a substrate binding site and therefore are frequently used as models for the peroxidases.

1.3.2 Reactions

The enzyme reacts rapidly with H_2O_2 to form Compound I, like other peroxidases, and its peroxidatic activity is 20 times higher than that of cytochrome c when pyrogallol is used as a substrate (Paleus et al., 1955). When *ortho*-dianisidine is used as a hydrogen donor, 11-microperoxidase exhibits 0.01% of the peroxidatic activity shown by horseradish peroxidase but 200% of the activity shown by cytochrome c (Tu et al., 1968). 11-Microperoxidase is not denatured by heat whereas horseradish peroxidase loses its activity when it is heated. The pH optimum for peroxidative activity is 9 for 11-microperoxidase whereas those of horseradish peroxidase and cytochrome c are 4.5 and 6, respectively (Tu et al., 1968).

Microperoxidase catalyzes the oxidation of sulfide, styrene and *cis*-stilbene, and the demethylation of alkylamines whereas hemin-Cl does not catalyze such reactions, except perhaps to only a slight degree (Mashino et al., 1990). The oxidation of styrene by 11-microperoxidase and H_2O_2 produces styrene oxide and phenylacetaldehyde. The molar ratio of the epoxide to aldehyde is 1:2.5 and the aldehyde does not derive from the epoxide. *cis*-Stilbene is oxidized by 11-microperoxidase predominantly to *cis*-stilbene oxide and diphenylacetaldehyde (Mashino et al., 1990).

1.4 Cytochrome P-450

1.4.1 Properties, function and structure

Cytochrome P-450s are monomeric hemoproteins with M_r of 46,000-57,000 that are found in vertebrates, plants, yeast and bacteria. Mammalian cytochrome P-450s, of which there are many isozymes, are membrane-bound, whereas most bacterial enzymes are soluble. Mammalian cytochrome P-450s are involved in the metabolism of xenobiotics and

the biosynthesis of steroid hormones. The former is primarily performed by cytochrome P-450s located in the endoplasmic reticulum of the liver, lung, kidney and skin. The isozymes are induced by specific chemicals such as phenobarbital or polycyclic aromatic compounds. On the other hand, the latter is primarily carried out by P-450 in the mitochondria of steroidogenic tissues such as the adrenal cortex.

The only P-450 whose crystal structure is known is $P\text{-}450_{cam}$ (P-450CIA1) isolated from *Pseudomonas putida*. The crystal structure of substrate-bound $P\text{-}450_{cam}$ shows that camphor, which is surrounded by hydrophobic residues, is positioned next to the oxygen binding site above the heme pyrrole ring A with its carbonyl group forming a hydrogen bond with Tyr 96 (Poulos et al., 1987). The active site is filled with water molecules in the crystal structure of the substrate-free enzyme (Poulos et al., 1986). $P\text{-}450_{cam}$ is composed of twelve helices which are stacked in three layers with the heme group placed between two of them. Cys 357 serves as the fifth axial ligand and the proximal heme ligand region is highly conserved in all P-450s.

The three dimensional structure of $P\text{-}450_{cam}$ is approximately triangular with the heme group parallel to the plane of the triangle (Poulos et al., 1986). EPR spectroscopy of membrane-bound P-450 suggests that the heme group also lies parallel to the membrane (Case & Leigh, 1976). Since lipophilic substrates approach the active site from the membrane (Taniguchi et al., 1984), the substrate-binding site may face the membrane and the fifth axial ligand may be positioned away from the membrane.

Mammalian cytochrome P-450s are predicted to bind to the endoplasmic reticulum by one or two transmembrane segments. Tryptic digestion of phenobarbital-induced microsomes suggests that most polypeptide chains reside on the cytoplasmic side and either the free N-terminal end transverses the membrane so that it is on the lumen side or the N-terminal end is on the cytoplasmic side with a hairpin loop embedded in the membrane (Brown & Black, 1989). If the latter is the case, the cytoplasmic part of P-450 is very similar in size to the bacterial P-450 (Nelson & Strobel, 1988).

Cytochrome P-450 reductase is purified as a detergent-solubilized form. The acetylated N-terminal residue of the reductase and a region between Val 16 and Phe 32 are hydrophobic, and the latter region is likely to be involved in the binding of P-450 and phospholipid (Black & Coon, 1982). Like P-450, most of the polypeptide chain is on the cytoplasmic side of the membrane. Black and Coon proposed two conformations for microsomal P-450 reductase in that either both N- and C-termini are on the opposite side of the membrane or both termini are on the cytoplasmic side with a nonpolar region embedded in the membrane (Black & Coon, 1982).

1.4.2 Catalytic cycle

All cytochrome P-450s appear to have a common catalytic cycle (Ortiz de Montellano, 1986) (Fig. 1.4). The iron in the resting state is in the low spin hexacoordinate state.

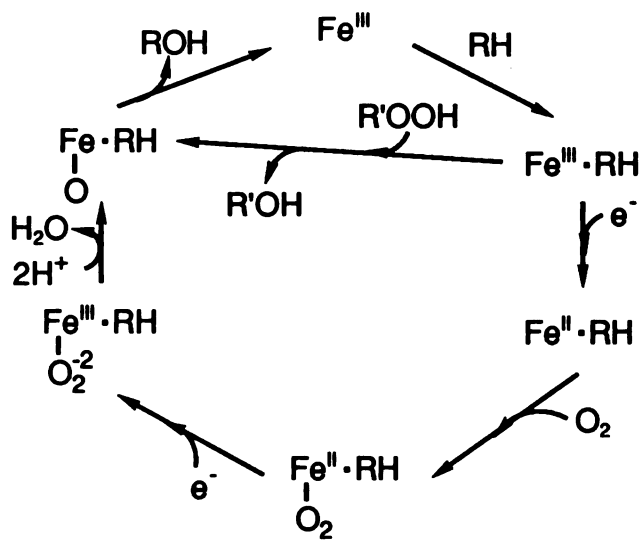

Fig. 1.4 Catalytic cycle of cytochrome P-450.

Upon binding to the substrate, it changes to the high spin pentacoordinate state which facilitates reduction of the iron by changing the reduction potential. The microsomal enzyme-substrate complex is reduced by the electron transport chain in which the reductase

(FAD) accepts two electrons from NADPH and the reduced reductase (FMN) transfers one electron at a time to the enzyme. The reduced enzyme can form a complex with CO, which exhibits a unique absorption maximum at 450 nm. In the presence of oxygen, the reduced enzyme binds oxygen to give a relatively stable oxy enzyme complex. The second electron from P-450 reductase or cytochrome b_5 is then transferred to the oxy complex. The normal O-O bond cleavage, which is facilitated by the fifth cysteine thiolate ligand, leads to the formation of water and an undetermined intermediate that oxygenates the substrate. The ferric enzyme-substrate complex can also directly form the final ferryl complex by reaction with alkyl hydroperoxides, PhIO or $NaIO_4$ in the absence of NADPH, P-450 reductase or oxygen. Mitochondrial P-450 is reduced by a system containing adrenodoxin reductase, adrenodoxin (an iron-sulfur protein) and NADPH. Bacterial $P\text{-}450_{cam}$ is reduced by a system containing putidaredoxin reductase, putidaredoxin (an iron-sulfur protein) and NADH analogous to that of the mitochondrial system.

1.4.3 Oxidation of substrates

Typical reactions catalyzed by cytochrome P-450 are hydrocarbon hydroxylation, heteroatom oxidation and olefin epoxidation.

Hydrocarbon hydroxylation

The insertion of oxygen into the C-H bond is likely to proceed by a nonconcerted mechanism (Ortiz de Montellano, 1986) (Scheme 1.2). The evidence is provided by stereochemical scrambling, allylic rearrangement and large intrinsic isotope effects (10-12).

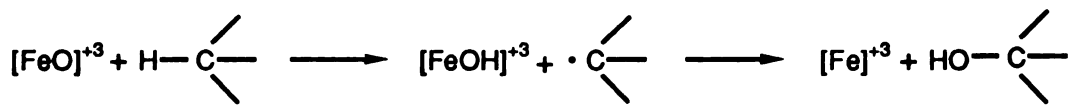

Scheme 1.2 A nonconcerted mechanism of hydrocarbon hydroxylation catalyzed by cytochrome P-450.

The stereochemical scrambling is shown in the hydroxylation of *exo*-tetradeuterated norbornane by purified P-450 (Groves et al., 1978). The enzyme abstracts the *exo*-deuterium or *endo*-hydrogen and the resulting radical intermediate is responsible for the loss of stereochemistry. The hydroxylation of the *endo* or *exo* position produces four products (Scheme 1.3). Hydroxylation of 5-*exo*- and 5-*endo*-deuterocamphor to 5-*exo*-hydroxycamphor by $P\text{-}450_{cam}$ proceeds by a similar mechanism to that of deuterated norbornane (Gelb et al., 1982). Allylic rearrangement is observed in the hydroxylation of 3,3,6,6-tetradeuterated cyclohexene by P-450 (Groves & Subramanian, 1984).

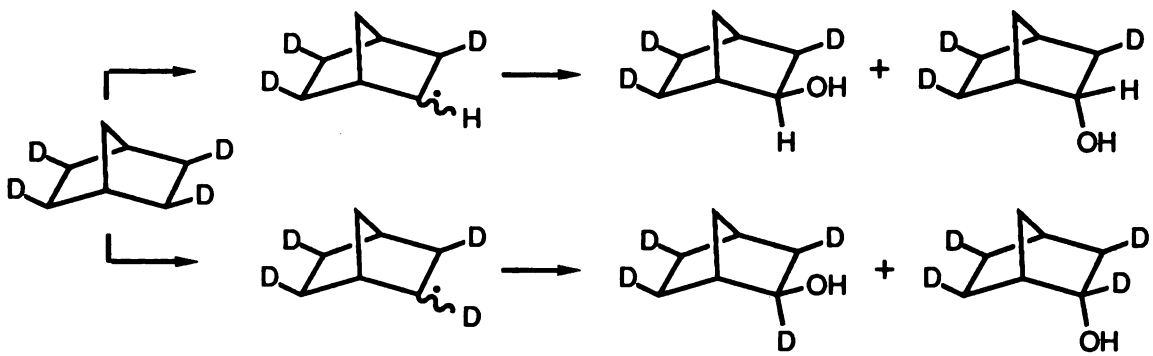

Scheme 1.3 Hydroxylation of *exo*-tetradeuterated norbornane by cytochrome P-450.

Heteroatom oxidation

Cytochrome P-450 catalyzes the oxidation of nitrogen and sulfur to the corresponding oxides or dealkylation of alkylamines or alkylsulfides when a hydroxyl group is added to the carbon adjacent to the heteroatom (Scheme 1.4). It is believed that both reactions share a radical cation intermediate formed by initial oxidation of the heteroatom (Ortiz de Montellano, 1986). On the other hand, the cytochrome P-450-catalyzed O-dealkylation of ethers proceeds by the direct carbon hydroxylation rather than initial oxidation of the heteroatom.

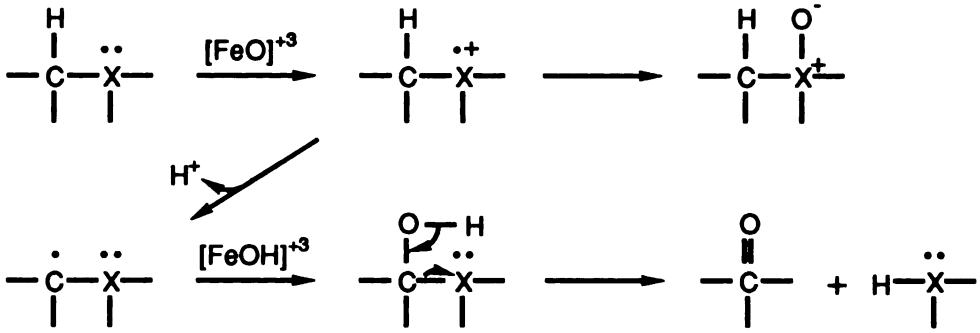

Scheme 1.4 Mechanisms for the oxidation and dealkylation of heteroatom by cytochrome P-450. The X indicates a nitrogen or a sulfur.

Olefin epoxidation

Cytochrome P-450-catalyzed epoxidations are usually stereospecific but retention of stereochemistry does not rule out a nonconcerted mechanism. Although the mechanism of P-450-catalyzed olefin epoxidation is not fully understood, a stepwise mechanism appears to be favored. The evidence for this is provided by the destruction of the heme group by terminal olefins and the rearrangements that occur during their oxidation (Ortiz de Montellano, 1986). Terminal olefins oxidized by P-450 cause the destruction of the enzyme in addition to being converted to the epoxides. Since the epoxide metabolites of destructive olefins do not inactivate the enzyme, they are not responsible for the heme alkylation (Scheme 1.5). Hence, epoxidation and heme alkylation must diverge prior to formation of the epoxide. Production of the epoxide and the corresponding aldehyde or ketone is common in the epoxidation of olefins catalyzed by P-450. The oxidation of trichloroethylene produces trichloroacetaldehyde as well as trichloroethylene oxide. The aldehyde is not derived from the epoxide because the synthetic epoxide does not rearrange to the aldehyde under physiological conditions (Henschler et al., 1979; Miller & Guengerich, 1982). This result indicates that chlorine migrates prior to formation of the epoxide (Scheme 1.6). *Trans*-1-phenyl-1-butene is oxidized to 1-phenyl-1- and 1-phenyl-2-butanone as well as *trans*-1-phenyl-1-butene-1,2-oxide (Liebler & Guengerich, 1983).

The oxidation of styrene by microsomal P-450 yields styrene oxide and phenylacetaldehyde (Mansuy et al., 1984), although the latter has not been detected in our system (Ortiz de Montellano et al., 1987). The aldehyde and ketone products are again not obtained from rearrangement of the epoxide.

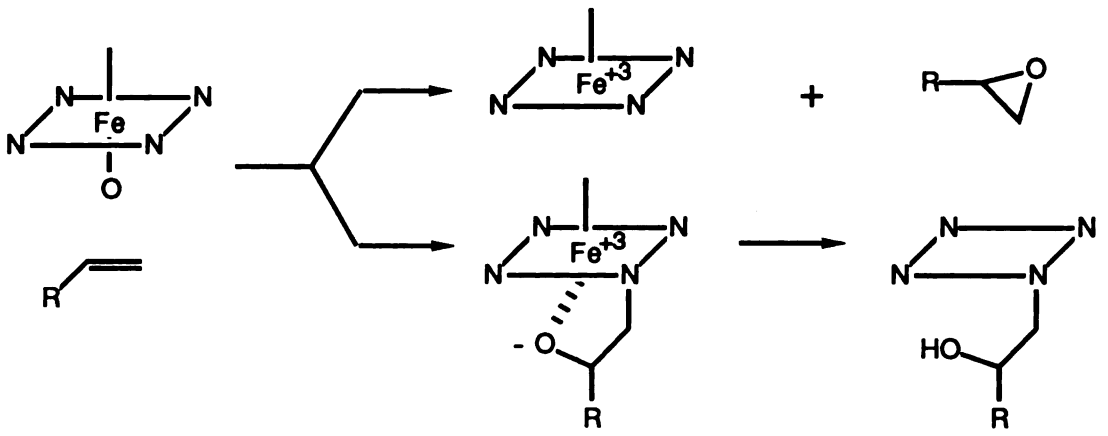

Scheme 1.5 Heme alkylation observed during the epoxidation of terminal olefins.

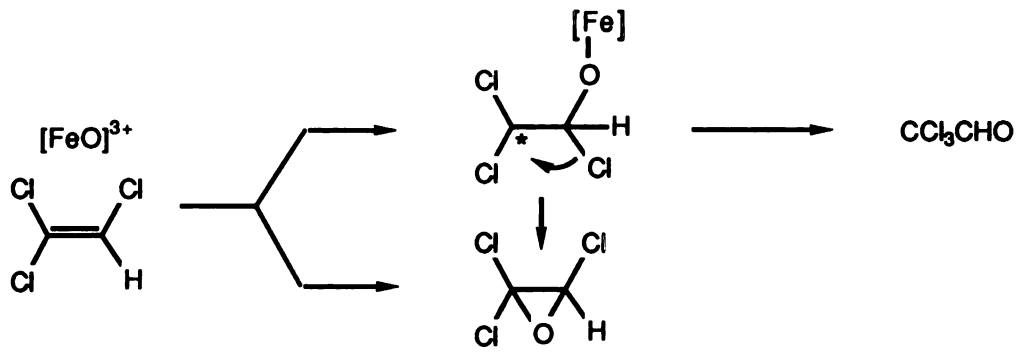

Scheme 1.6 Rearrangement observed during the oxidation of trichloroethylene. The asterisk stands for a radical or cationic center.

The above evidence for a nonconcerted mechanism suggests that there should be points at which the reaction diverges between either the epoxide and the N-alkylated heme or the epoxide and the aldehyde. Possible intermediates are a radical species which partitions to the epoxide or N-alkylated heme, and a cationic intermediate which rearranges

to the aldehyde (Scheme 1.7). An electron transfer from the olefin to the activated oxygen complex may result in an intermediate preceding a radical or a cationic species. Bruice's group suggested from porphyrin model studies that an olefin-derived charge transfer complex leads to formation of the epoxide and other side products (Castellino & Bruice, 1988). The epoxide and alkylated heme can also be formed via metallacyclobutane intermediates which derive either from a radical intermediate or directly from the activated enzyme and the olefin (Ortiz de Montellano, 1986). Although Ostovic and Bruice argued from computer graphics docking experiments against metallacycles as the intermediate in the epoxidation of olefins by sterically hindered porphyrin derivatives (Ostovic & Bruice, 1989), there are some studies in which the metallacyclic intermediates have been proposed. Sharpless and coworkers proposed a metallacyclic intermediate in the epoxidation of olefins by chromyl chloride (Sharpless et al., 1977). Groves and Watanabe observed the

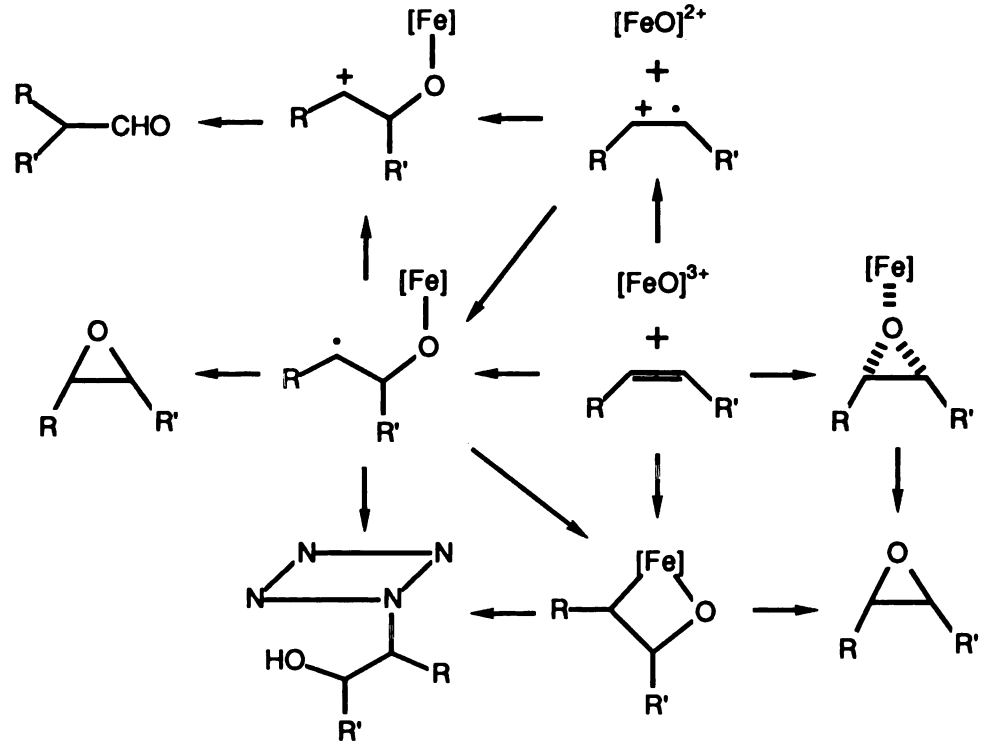

Scheme 1.7 Alternative mechanisms for the oxidation of the olefin

formation of a reversible intermediate in the epoxidation of olefins by iron tetramesitylporphyrin in the presence of *meta*-chloroperbenzoic acid. This intermediate was proposed to be an olefin π-complex or an oxametallacycle (Groves & Watanabe, 1986). Groves also proposed the presence of the metallacyclic intermediate in the epoxidation of *trans*-[1-^{2}H]propylene by reconstituted cytochrome P-450. This reaction caused exchange of the terminal hydrogen with the aqueous medium (Groves et al., 1986). The epoxidation of unlabeled propylene in D_2O gave higher than 80% *trans*-[1-^{2}H]propylene oxide and *trans*-[1-^{2}H]propylene in H_2O produced 95% unlabeled propylene oxide. Groves et al. explained the H/D exchange using a metallacyclic intermediate that equilibrates with an iron carbene complex. The iron carbene complex then produces the epoxide and N-alkylated heme (Scheme 1.8). The proposed mechanism also supports a nonconcerted mechanism for the olefin epoxidation. The evidence to date thus shows that cytochrome P-450 probably catalyzes a nonconcerted epoxidation reaction.

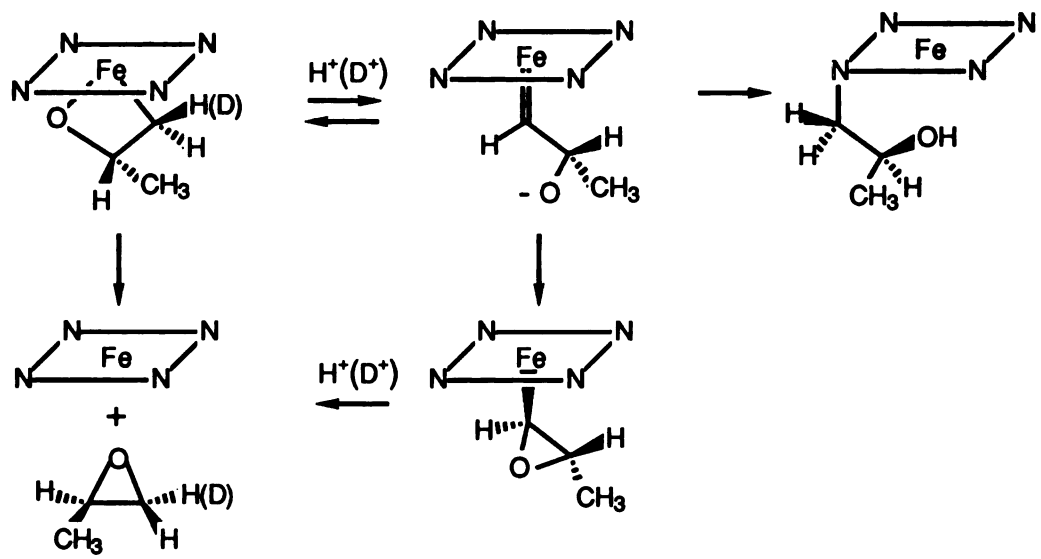

Scheme 1.8 Stereospecific H/D exchange from the aqueous medium during the epoxidation of propylene by reconstituted cytochrome P-450. The prosthetic heme is symbolized by the iron in a square of four nitrogens.

However, heme alkylation is not caused by all olefins. Monosubstituted, unconjugated olefins alkylate the heme and thus inactivate the P-450 during their catalytic oxidation to the epoxide (Ortiz de Montellano & Reich, 1986). Spectroscopic and ^{18}O studies of the heme adducts show that the terminal carbon is bound to a porphyrin nitrogen and the internal carbon to the activated oxygen. Scheme 1.7 shows the possible mechanisms for the formation of the alkylated heme. The olefin stereochemistry is retained during both the epoxidation and heme alkylation reactions. The oxidation of *trans*-[1-^{2}H]-1-octene with microsomal enzyme shows that the oxygen is delivered equally to both faces in the epoxidation reaction but only to the *re* face in formation of the N-alkylated heme (Ortiz de Montellano et al., 1983b). This is consistent with view that the epoxide metabolite does not participate in the heme alkylation.

The oxidation of terminal acetylenes by P-450 results in formation of the corresponding acetic acids via the corresponding ketene intermediates and also in alkylation of the heme group (Komives & Ortiz de Montellano, 1987). The fact that the activated oxygen is bound to the terminal carbon in the metabolite whereas it is bound to the internal carbon in the alkylated heme indicates that the oxygen is delivered to the π-bond after or during the step that leads to partitioning between metabolite formation and heme alkylation.

PROPOSAL

Although the hemoproteins contain the same prosthetic group, the active species formed by their reaction with the two electron oxidant H_2O_2 are not identical, presumably due to differences in the heme iron environment of the different hemoproteins. Since the active species of cytochrome P-450 has not been defined, it is of interest to study the globin-catalyzed redox reactions that are analogous to cytochrome P-450 reactions, and the formation of heme-bound products of myoglobin because similar products are formed by cytochrome P-450 with some suicide substrates. Although redox catalysis is not a natural function of the globins, the autooxidation of ferrous myoglobin yields metmyoglobin, which can react with H_2O_2 generated *in situ*. The reaction may cause damage to the cell.

The protein radical (Tyr 103) generated from the reaction of metmyoglobin with H_2O_2 is involved in various reactions. Therefore, the role of the protein radical in such reactions was studied to investigate the general nature of myoglobin, confirm the site of the protein radical, and extend the knowledge on other hemoproteins, including cytochrome P-450. The mechanism of epoxidation of styrene by chloroperoxidase and H_2O_2 was compared to those of cytochrome P-450 and myoglobin to determine if chloroperoxidase has a P-450-like active site and if the protein radical is required for the epoxidation reaction catalyzed by myoglobin.

CHAPTER 2

The epoxidation of styrene

2.0 Introduction

Olefins are oxidized *in vivo* to epoxides by cytochrome P-450 and the resulting epoxides are further metabolized by epoxide hydrolases and glutathione transferases (Ortiz de Montellano, 1985). Olefin epoxidation is one of the reactions catalyzed specifically by P-450 and not by most other hemoproteins. Therefore, this reaction has been used to differentiate cytochrome P-450 from other hemoproteins. The reaction can be used as a probe of the structure and mechanism of the enzyme because the origin of the epoxide oxygen and the stereochemistry of the epoxidation reaction provide information on the mechanism of the reaction.

Chemical models have provided insights concerning the mechanism of the epoxidation reaction that can be useful in understanding the enzymatic reaction. Olefins can be epoxidized chemically by peracids such as *meta*-chloroperbenzoic acid. Scheme 2.1 shows the proposed mechanism for the peracid oxidation reaction (Bartlett, 1957).

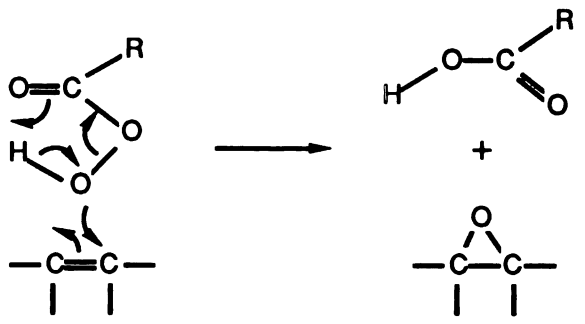

Scheme 2.1 One-step mechanism for the chemical epoxidation by peracids

Substituents on the double bond affect the rate of the reaction. For instance, electron donating groups increase the rate of the reaction. The reactivity of the π bond is altered by conjugation such that the epoxidation of conjugated olefins is slower than that of isolated olefins. Also, α,β-unsaturated ketones fail to give epoxides with peracids due to the electron withdrawing effect of the carbonyl group on the π bond. The chemical epoxidation of olefins occurs by both concerted and nonconcerted mechanisms. A concerted mechanism in which the carbon-oxygen bonds are formed simultaneously, but not necessarily at the same rate, leads to the retention of stereochemistry. The stereochemistry is also retained in an epoxide formed by a nonconcerted mechanism if the rotation about the carbon-carbon bond is slower than epoxide ring closure. The epoxidation of olefins by peracids likely proceeds by a concerted mechanism (Berti, 1973) whereas metal-catalyzed epoxidations are commonly thought to proceed by nonconcerted mechanisms (Groves, 1980; Mimoun, 1981).

Cytochrome P-450 enzymes, which have a cysteine as the fifth heme ligand, most efficiently catalyze the epoxidation of olefins. Although the mechanism of P-450-catalyzed olefin epoxidation is poorly defined, the reaction appears to proceed by a nonconcerted mechanism. The primary evidence for this is provided by the destruction of the heme caused by terminal olefins and the rearrangements that accompany their oxidation (Ortiz de Montellano, 1986) (Schemes 1.5 and 1.6). The oxidation of 1-octene by microsomal cytochrome P-450 results in formation of the corresponding epoxide and alkylation of a porphyrin nitrogen (Ortiz de Montellano et al., 1983b). In contrast to monosubstituted, unconjugated olefins, styrene, a conjugated olefin, is a good substrate because it does not inactivate the enzyme (Ortiz de Montellano & Reich, 1986).

Chloroperoxidase, which, like P-450, has a cysteine heme ligand, has also been shown to epoxidize styrene (McCarthy & White, 1983; Geigert et al., 1986). Classical peroxidases such as horseradish peroxidase, which have a histidine as the fifth heme ligand, do not catalyze epoxidation reactions. Horseradish peroxidase catalyzes those

reactions only in the presence of phenol or glutathione, which mimics the role of the protein in protein-mediated cooxidation (Ortiz de Montellano & Grab, 1986; Ortiz de Montellano & Grab, 1987). The axial heme ligand thus may play a major role in determining the reactivity of the prosthetic heme group. However, the globins have a histidine as the fifth heme ligand yet are able to catalyze styrene epoxidation (Ortiz de Montellano & Catalano, 1985). The H_2O_2-dependent oxidation of styrene by myoglobin produces styrene oxide and benzaldehyde as metabolites. However, the globins have diverse catalytic abilities, which is not unexpected because they normally do not catalyze redox reactions. For this reason, the globins may not be the best model of the effect of the fifth heme ligand on the epoxidation reaction. Therefore, 11-microperoxidase, which derives from cytochrome c by peptic digestion, was studied as a model hemoprotein to determine the effect of the fifth heme ligand on catalysis because it has both a histidine fifth heme ligand and minimal control of the protein over the heme prosthetic group. Microperoxidase does, in fact, catalyze the H_2O_2-dependent epoxidation of styrene (Mashino et al., 1990). The results obtained to date therefore suggest that the fifth heme ligand is not the main factor regulating the ability of the enzyme to catalyze olefin epoxidation.

The H_2O_2-dependent epoxidation of styrene by horse myoglobin was reexamined because Groves and Stern showed that *cis*-β-methylstyrene is epoxidized by manganese [Mn(IV)=O] porphyrins in a nonstereoretentive manner (Groves & Stern, 1987). The globins are oxidized by H_2O_2 to the ferryl oxygen [Fe(IV)=O] complex and a protein radical. Based on the results of Ortiz de Montellano and Catalano, the protein radical appears to participate directly by a cooxidation mechanism and indirectly by a ferryl oxygen transfer in the formation of styrene oxide (Scheme 1.1) (Ortiz de Montellano & Catalano, 1985). Seventy eight percent of the styrene oxide is formed by the former mechanism and the rest of the epoxide by the latter. In order to avoid the complexity caused by excess H_2O_2, 1.5 equivalents of H_2O_2 were added to myoglobin to allow the enzyme to undergo a single turnover. The hydroxyl radical can be formed prior to the protein radical by the

mechanism proposed by George and Irvine (George & Irvine, 1952). It can also be formed by the Fenton reaction because free ferrous iron released from the globins by peroxides may react with excess H_2O_2 (Gutteridge, 1986; Harel et al., 1988; Hebbel & Eaton, 1989). The hydroxyl radical will react with any reactive species in the vicinity due to its extremely high reactivity (redox potential: +2.33 V at pH 7.0) (Koppenol, 1976; Pryor, 1986; Sawyer & Nanni, 1981). For instance, the reaction of benzene with the hydroxyl radical produces phenol and biphenyl (Sangster, 1971). If the ferryl oxygen complex alone catalyzes the epoxidation reaction, styrene oxide and benzaldehyde will be generated from the incubation of styrene with the ferryl oxygen [Fe(IV)=O] complex. This can be determined by comparing the product yield obtained from the incubation of the ferryl oxygen complex with styrene to that from the standard incubation of the ferryl complex/protein radical pair with styrene. Alternatively, the protein radical or hydroxyl radical may be necessary in the epoxidation reaction. Whether it is the protein radical or hydroxyl radical that participates in the epoxidation reaction can be determined by initiating the reaction with styrene after the decay of the hydroxyl radical because the half life of the hydroxyl radical is very short relative to that of the protein radical.

The ability of the enzyme to catalyze olefin epoxidation thus may be controlled by the machinery around the ferryl oxygen: cytochrome P-450 has a lipophilic, open active site so the substrates can approach the ferryl oxygen; horseradish peroxidase has polar active site residues that stabilize the ferryl oxygen and may interfere with the approach of the olefin. The active sites of most hemoproteins are not well defined because their crystal structures are not known. However, active site models based on indirect studies have been proposed. The active site model of P-450IIB1 suggests that pyrrole ring B of the heme group is protected by the protein (Fig. 2.1) (Kunze et al., 1983), a proposal supported by the X-ray structure of $P\text{-}450_{cam}$ (Poulos et al., 1985). The active site model of horseradish peroxidase is based on the enzyme's reaction with phenylhydrazine (Ator & Ortiz de Montellano, 1987). Only the δ-meso carbon and the 8-methyl group of the heme prosthetic

group are modified in the reaction, suggesting that the substrates only have access to the δ-*meso* heme edge (Fig. 2.1). Since chloroperoxidase catalyzes the epoxidation of olefins, an atypical reaction for a peroxidase, and little is known about its active site structure, the epoxidation of styrene by chloroperoxidase was studied.

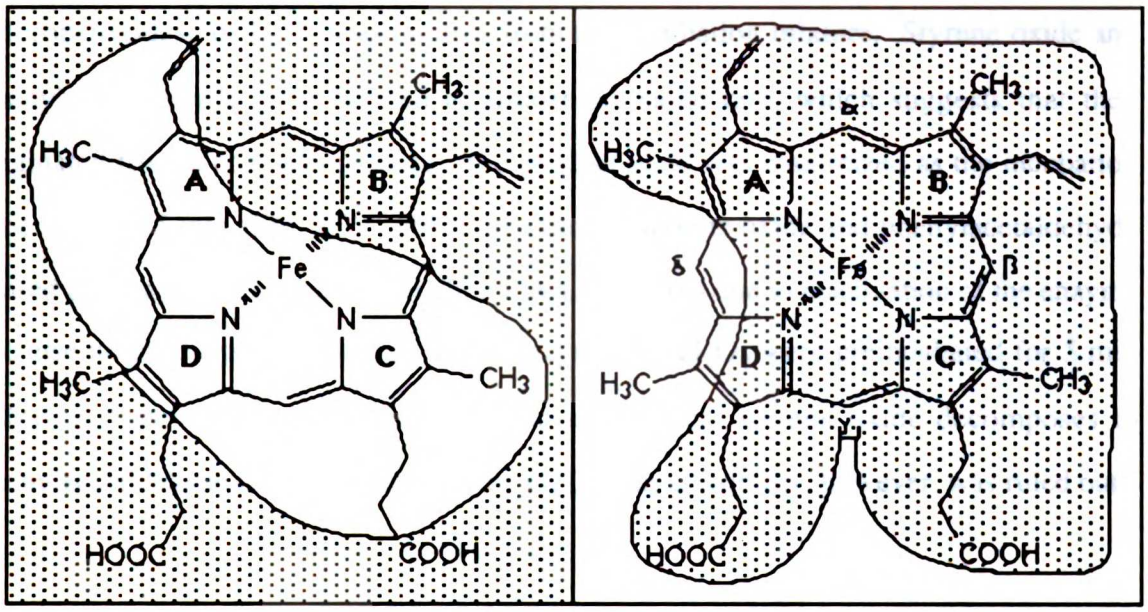

Fig. 2.1 Active site model of cytochrome P-450IIB1 (left panel), in which pyrrole ring B is protected by the protein, and active site model of horseradish peroxidase (right panel), in which only the δ-*meso* heme edge is available to the substrate.

2.1 Oxidation of styrene by chloroperoxidase

Incubation of styrene with chloroperoxidase and H_2O_2 resulted in the rapid production of nearly equal amounts of styrene oxide and phenylacetaldehyde (Ortiz de Montellano et al., 1987). Benzaldehyde, which is expected to be formed if styrene is oxidized by the cooxidative mechanism, was not detected in this system (Ortiz de Montellano & Catalano, 1985; Ortiz de Montellano & Grab, 1986; Ortiz de Montellano & Grab, 1987). Product formation was detected by gas-liquid chromatography. The retention time of each compound under the given conditions was: styrene, 5.83;

phenylacetaldehyde, 9.65; styrene oxide, 10.34; 2-undecanone (internal standard), 16.86 min. Benzaldehyde would have been detected at 7.41 min if it had been formed. The ratio of the peak area of styrene oxide to that of 2-undecanone was converted to the amount of styrene oxide from a standard curve (Fig. 2.2). Both the enzyme and H_2O_2 were required for the reaction because neither styrene oxide nor phenylacetaldehyde was formed if chloroperoxidase or H_2O_2 was omitted from the incubation mixture. Styrene oxide and phenylacetaldehyde were formed at almost the same rate, which suggests that they originated from a common process. The product yield was maximized as the incubation time reached 5 min (Fig. 2.3). The production of styrene oxide and phenylacetaldehyde ceased and stayed at the same level after 5 min. This was due to inactivation of the enzyme because no products were formed if the enzyme and H_2O_2 were preincubated for 5 min before styrene was added. There is a possibility that styrene oxide decomposes to phenylacetaldehyde during the analysis by GLC. The possibility, however, was ruled out

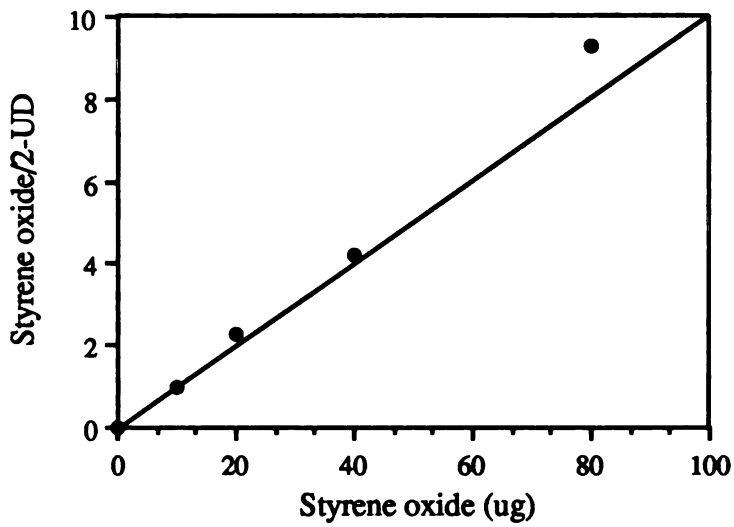

Fig. 2.2 Standard curve for the quantitation of styrene oxide. The y-axis indicates the ratio of peak area of styrene oxide to that of 2-undecanone as determined by gas-liquid chromatography. The amounts (μg) of styrene oxide used for the reaction are shown on the x-axis.

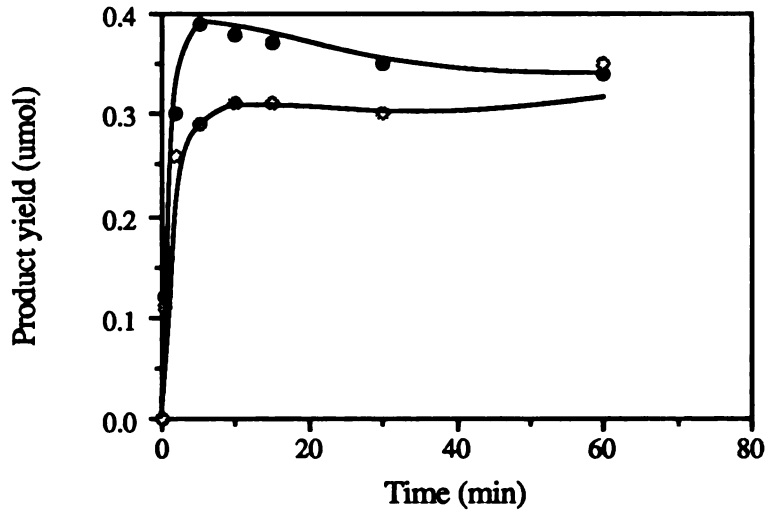

Fig. 2.3 Dependence of the chloroperoxidase-mediated formation of styrene oxide (•) and phenylacetaldehyde (o) on the incubation time. A 10 mM concentration of H_2O_2 and a 5 mM concentration of styrene were used in these experiments. Each data point is the average of the two independent values. The details of the incubations and product analyses are provided in the Experimental Chapter.

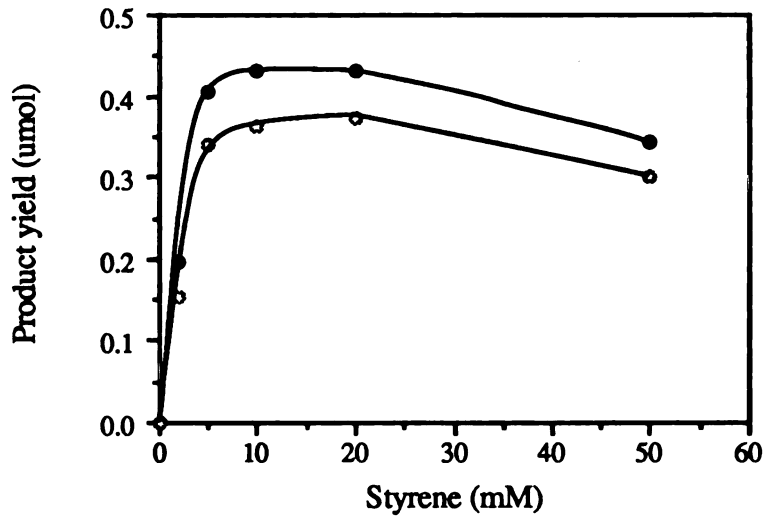

Fig. 2.4 Dependence of the chloroperoxidase-mediated formation of styrene oxide (•) and phenylacetaldehyde (o) on the concentration of styrene. A 10 mM concentration of H_2O_2 and an incubation time of 5 min were used in these experiments. Each data point is the average of two independent values.

by the fact that no phenylacetaldehyde was formed if styrene was replaced by styrene oxide in the standard incubation. The formation of both products depended in the same way on

the styrene concentration, the formation of both having been slightly inhibited at styrene concentrations higher than 20 mM. Product yield reached a maximum at styrene concentrations in the 5-10 mM range (Fig. 2.4). When the H_2O_2 reached 10 mM, the product yield also reached a maximum (Fig. 2.5). With higher concentrations of H_2O_2, the formation of both products was reduced, suggesting that the enzyme may have been inactivated.

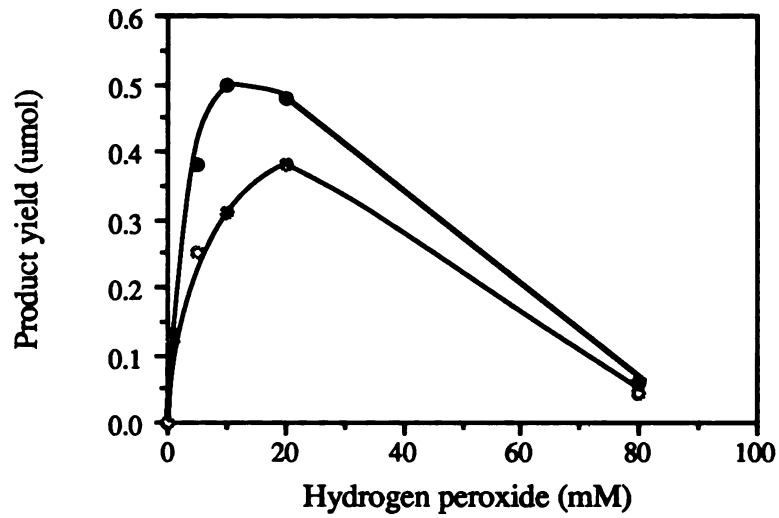

Fig. 2.5 Dependence of the chloroperoxidase-mediated formation of styrene oxide (•) and phenylacetaldehyde (o) on the H_2O_2 concentration. A 5 mM concentration of styrene and an incubation time of 5 min were used in these experiments. Each data point is the average of two independent values.

2.2 Origin of the oxygen in styrene oxide

^{18}O-labeled H_2O_2, made from $^{18}O_2$ by the known procedure (Sawaki & Foote, 1979), was shown by gas chromatography-mass spectrometry of the epoxide produced from menadione to contain 75 atom % ^{18}O. When styrene was epoxidized by chloroperoxidase and $H_2{}^{18}O_2$, 74% ^{18}O-labeled styrene oxide was obtained: m/z, 120 (26%):122 (74%) (Fig. 2.6). On the other hand, styrene oxide obtained from a standard incubation using normal H_2O_2 had no molecular ion peak at m/z 122. The oxygen of the styrene oxide thus derives quantitatively from the peroxide.

The oxygen of phenylacetaldehyde isolated from the oxidation of styrene by chloroperoxidase and $H_2{}^{18}O_2$ did not seem to derive from the peroxide because the aldehyde did not have the molecular ion peak at m/z 122 (Fig. 2.6). The oxygen of the aldehyde, however, is easily exchanged with that of the aqueous medium, which makes it difficult to determine the source of the oxygen in phenylacetaldehyde.

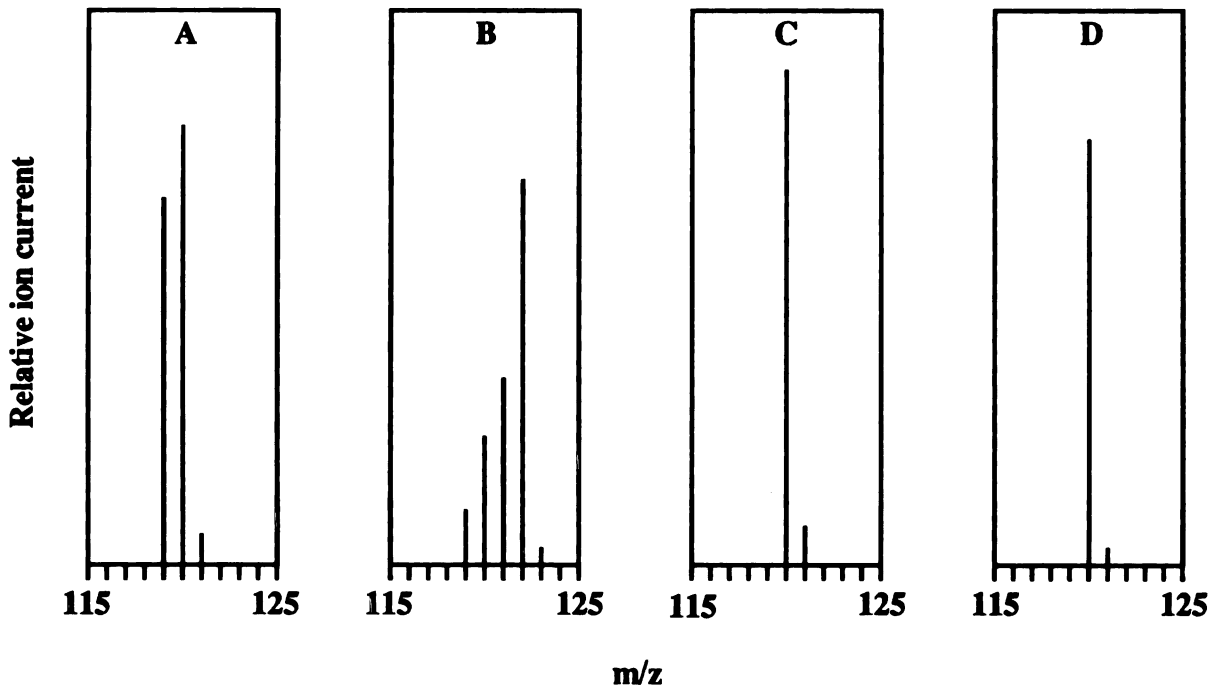

Fig. 2.6 Molecular ion region of the mass spectra of (A) styrene oxide and (C) phenylacetaldehyde isolated from incubations of styrene with chloroperoxidase and $H_2{}^{16}O_2$; (B) styrene oxide and (D) phenylacetaldehyde isolated from incubations of styrene with chloroperoxidase and $H_2{}^{18}O_2$.

2.3 Stereochemistry of the epoxidation of styrene by chloroperoxidase

Unlabeled styrene oxide obtained from standard incubations showed peaks at 7.3 (phenyl protons), 3.87 (benzylic proton), 3.15 (*trans* proton), and 2.81 ppm (*cis* proton) in the 500 MHz NMR spectrum. The latter three protons appeared as doublets of doublets (J_{ct} = 5.6, J_{bc} = 2.5 and J_{bt} = 4.1 Hz; c = *cis*, t = *trans* and b = benzylic). When labeled styrene oxide was obtained from a reaction in which styrene was replaced by *trans*-[1-

^{2}H]styrene, the *trans*-proton (3.15 ppm) was not observed (Fig. 2.7). The benzylic and *cis*-protons, whose integration ratio was 1:1, appeared as simple doublets due to the much smaller values for ^{2}H-H than H-H coupling. The epoxidation of *trans*-[1-^{2}H]styrene by chloroperoxidase and H_2O_2 is thus stereoretentive because it yields only *trans*-[1-^{2}H]styrene oxide.

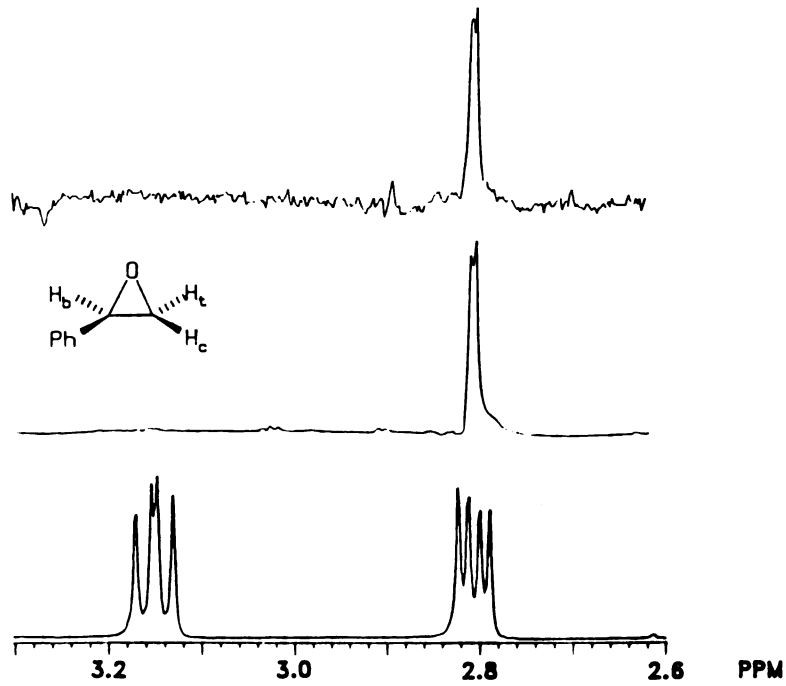

Fig. 2.7 Stereochemistry of epoxidation of *trans*-[1-^{2}H]styrene by chloroperoxidase and H_2O_2. The region of the NMR spectrum of the styrene oxide containing the signals for the terminal epoxide protons is shown: (top tracing) product formed from *trans*-[1-^{2}H]styrene by microsomal cytochrome P-450, (middle tracing) styrene oxide formed from *trans*-[1-^{2}H]styrene by chloroperoxidase, and (bottom tracing) authentic, unlabeled, styrene oxide. The protons responsible for the signals in the spectrum of unlabeled styrene oxide are identified in the inset structure as H_t (3.15 ppm) and H_c (2.81 ppm).

2.4 Stereochemistry of the epoxidation of styrene by rat liver microsomes

Styrene was oxidized to its epoxide by purified, reconstituted cytochrome P-450IIB1. Neither phenylacetaldehyde nor benzaldehyde was detected. More styrene was turned over at 37°C than at room temperature.

A large scale incubation of styrene was carried out using rat liver microsomes. Since microsomes contained epoxide hydrolase, the epoxide hydrolase inhibitor, 1,2-epoxy-3,3,3-trichloropropane, was used in these studies. The styrene oxide isolated from large scale incubations of *trans*-[1-^{2}H]styrene with the microsomal enzyme showed NMR peaks at 7.3 (phenyl protons), 3.87 (benzylic proton), and 2.81 ppm (*cis* proton) (Fig. 2.7). The olefinic protons appeared as doublets. Hence, the epoxidation of styrene by cytochrome P-450 proceeds with complete retention of the olefin stereochemistry. This is consistent with the result obtained with chloroperoxidase and H_2O_2.

2.5 Oxidation of olefins by 11-microperoxidase

The oxidation of styrene by microperoxidase and H_2O_2 yielded styrene oxide, phenylacetaldehyde and benzaldehyde. The yield of styrene oxide was slightly higher at pH 7 than at pH 6. The formation of products was maximal as the enzyme concentration reached 107 μM and decreased at higher concentrations, which suggests that the enzyme may have aggregated or been inactivated at higher concentrations (Fig. 2.8). The rates of formation of metabolites decreased in the order of styrene oxide > phenylacetaldehyde > benzaldehyde. The optimal incubation time ranged between 2 and 5 min. The yield of products went up to a maximum as the H_2O_2 concentration reached 10 mM (Fig. 2.9). Further increases in the H_2O_2 concentration resulted in a decrease in the yield, presumably because of peroxide-dependent inactivation of the catalyst. Stereochemistry can be determined by gas-liquid chromatography if styrene is replaced by *cis*-stilbene. Preliminary studies indicated that the incubation of *cis*-stilbene with microperoxidase and H_2O_2 resulted in the production of *trans*-stilbene and *cis*-stilbene oxide. The GLC retention times under the given conditions were 11.05 min for *cis*-stilbene oxide and 14.84 min for *trans*-stilbene. The oxidation of *cis*-stilbene with microperoxidase did not depend much on the incubation time beyond the first 10 min. The heme chromophore at 400 nm

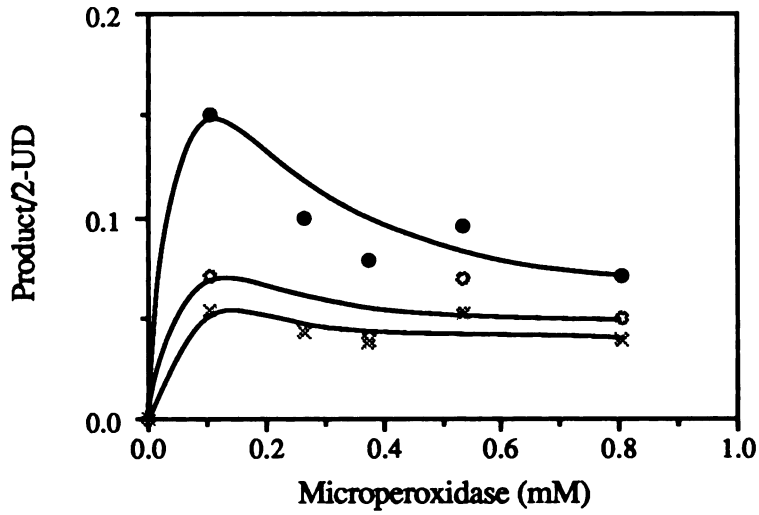

Fig. 2.8 Dependence of the microperoxidase-mediated formation of styrene oxide (•), phenylacetaldehyde (o) and benzaldehyde (x) on the concentration of the enzyme. The H_2O_2 and styrene concentrations were 10 and 5 mM, respectively. The y-axis represents the ratio of the peak area of product to that of 2-undecanone as determined by GLC.

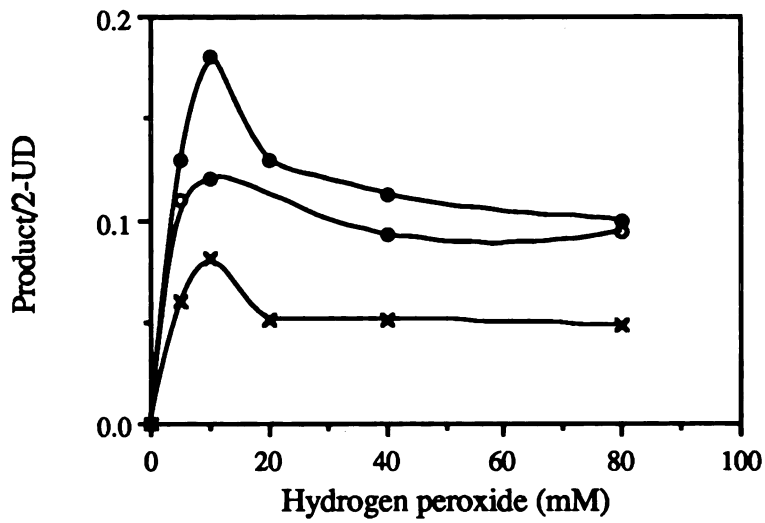

Fig. 2.9 Dependence of the microperoxidase-mediated formation of styrene oxide (•), phenylacetaldehyde (o) and benzaldehyde (x) on the H_2O_2 concentration. Microperoxidase (107 μM) and styrene (5 mM) were used in these experiments. The y-axis shows the ratio of peak area of product to that of 2-undecanone as determined by GLC.

was bleached within 30 seconds after the enzyme (107 μM) was added to the incubation mixture containing substrate (5 mM) and H_2O_2 (10 mM) (Fig. 2.10).

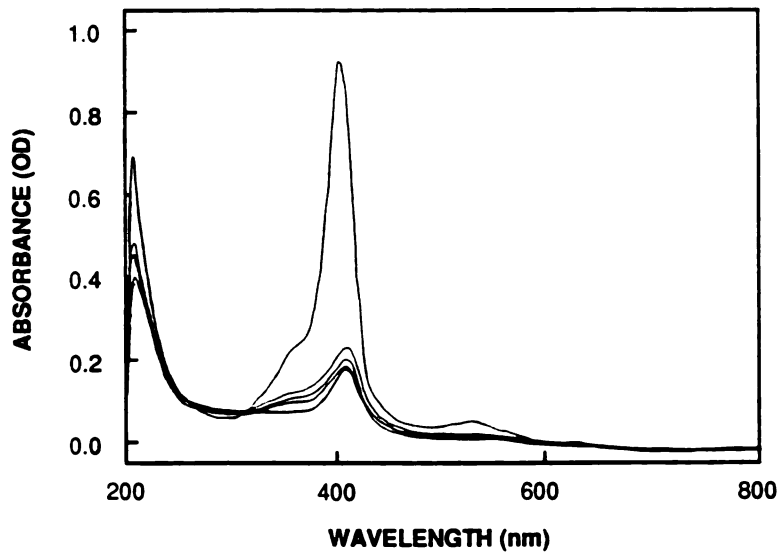

Fig. 2.10 Changes in the electronic absorption spectrum during the incubation of *cis*-stilbene by microperoxidase and H_2O_2. The line with the highest Soret band intensity is the spectrum of native microperoxidase. The other spectra, in order of decreasing Soret band intensity, were taken 1, 11, 26, and 90 min after the incubation was initiated. An incubation time of 10 min was used in the standard incubation. The concentrations of *cis*-stilbene, H_2O_2 and microperoxidase were 5 mM, 10 mM and 107 μM, respectively.

2.6 The reaction of the myoglobin [Fe(IV)=O] species with styrene

The EPR spectrum of horse metmyoglobin gave a single signal centered at g = 6, which indicated a high spin ferric hemoprotein. Addition of H_2O_2 to metmyoglobin yielded new signals at g = 2.004 and at g = 2.027 with a concomitant decrease of the signal at g = 6 (Fig. 2.11). The low field signal at g = 2.027 was smaller than that at 2.004. When myoglobin (300 μM) was treated with 1.5 equivalents of H_2O_2 (quantitated by iodometric titration) at 0°C, the protein radical decayed rapidly as a function of time (Fig. 2.12, A). When styrene (10 mM) was present in the reaction mixture, the protein radical decayed in the same pattern as that obtained when styrene was absent but the intensity of

the EPR signal was weaker (Fig. 2.12, B). In both cases, the half life of the protein radical was close to 1 min (Fig.2.12, B). The protein radical signal lasted for about 30 min, however, even though the intensity drastically decreased by 5 min after it was formed.

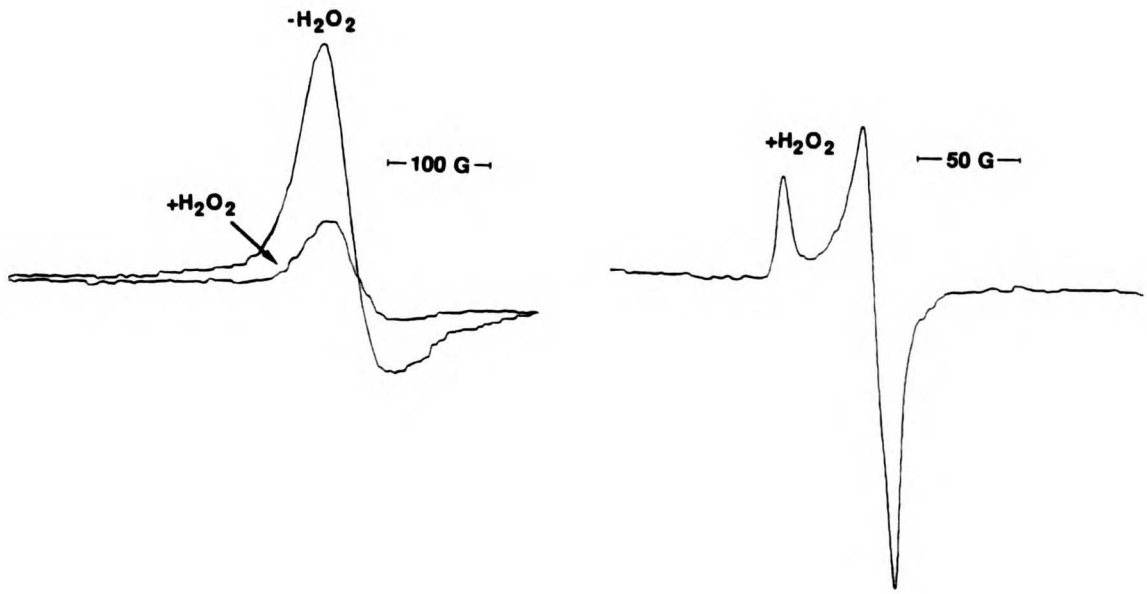

Fig. 2.11 The EPR spectra of horse myoglobin before and after addition of hydrogen peroxide (left trace, g = 6 region; right trace, g = 2 region).

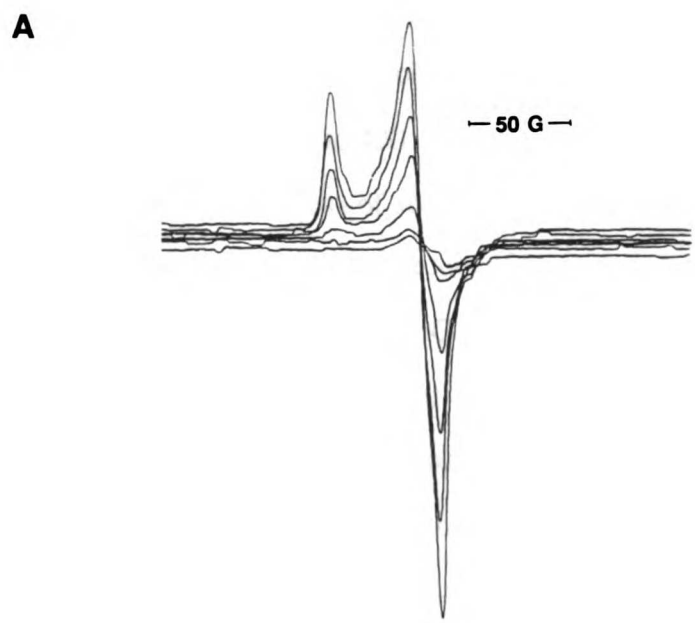

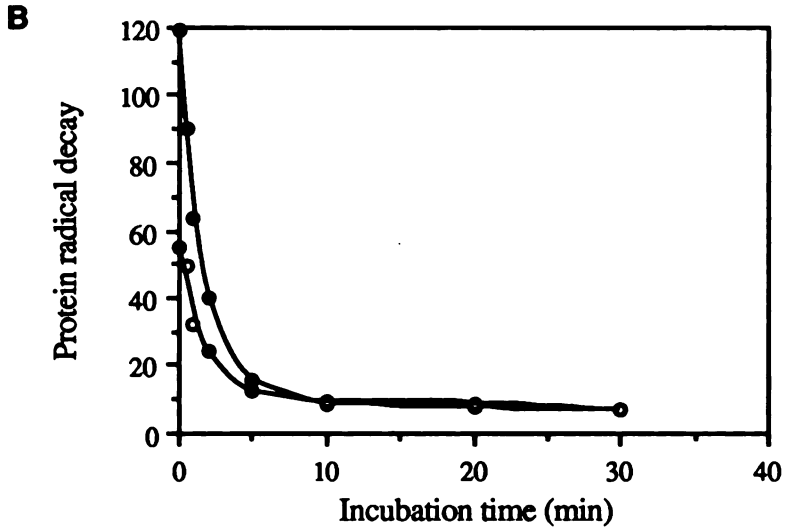

Fig. 2.12 (A) The decay of the protein radical observed 0, 0.5, 1, 2, 5, 10 and 30 min after addition of H_2O_2 (g = 2 region). (B) Plot of the protein radical decay vs. incubation time at 0°C. The incubation mixture contained myoglobin (300 μM) with H_2O_2 (450 μM) in the absence (•) and in the presence of styrene (o). The decay of the protein radical was measured by the decrease of the peak to peak height of EPR signal at g = 2.004.

Addition of sodium dithionite to metmyoglobin gave reduced myoglobin [Fe(II)] whose electronic absorption spectrum showed a shift of the Soret band from 408 to 430 nm and collapse of the two visible bands at 502 and 632 nm to a band at 558 nm (Fig. 2.13). Two-electron oxidation of reduced myoglobin by H_2O_2 produced the [Fe(IV)=O] species in which the Soret band was shifted to 420 nm and the visible band split into two bands at 546 and 578 nm. A three fold excess of sodium dithionite was used to ensure complete reduction. Consequently, a 10 to 12-fold excess of H_2O_2 was used to convert the [Fe(II)] to the [Fe(IV)] species. After purification by G-25 column chromatography, the absorption spectrum of the protein was nearly identical to that prior to purification (Fig. 2.13). It seems likely that the ferryl species was very stable during the chromatographic step. Once the ferryl species was formed, its reaction with styrene gave the same result whether in the presence or absence of oxygen. Traces of styrene oxide and benzaldehyde were barely

detected by gas-liquid chromatography and were probably due to slow recycling of the ferric species (Fig. 2.14, A).

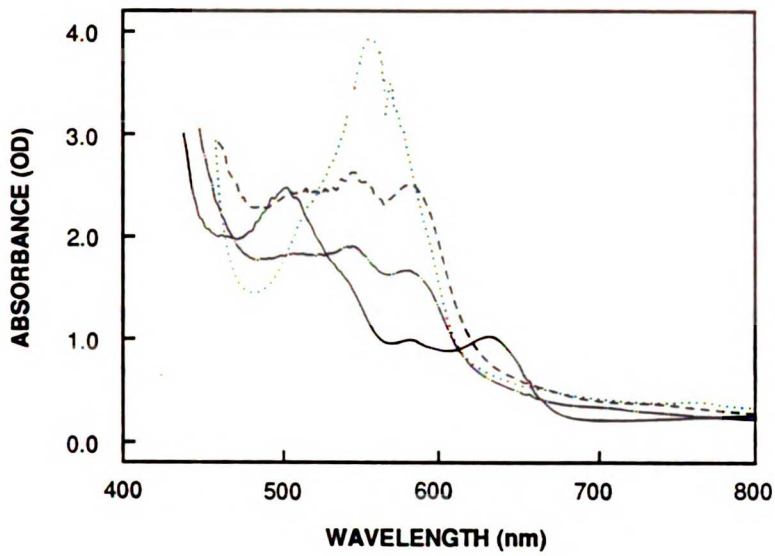

Fig. 2.13 Changes in the electronic absorption spectrum during the reduction followed by the oxidation of metmyoglobin. The spectra of native myoglobin (—), metmyoglobin + sodium dithionite (····), ferrous myoglobin + H_2O_2 (– –), and the ferryl enzyme purified by a G-25 column (–·–) are shown.

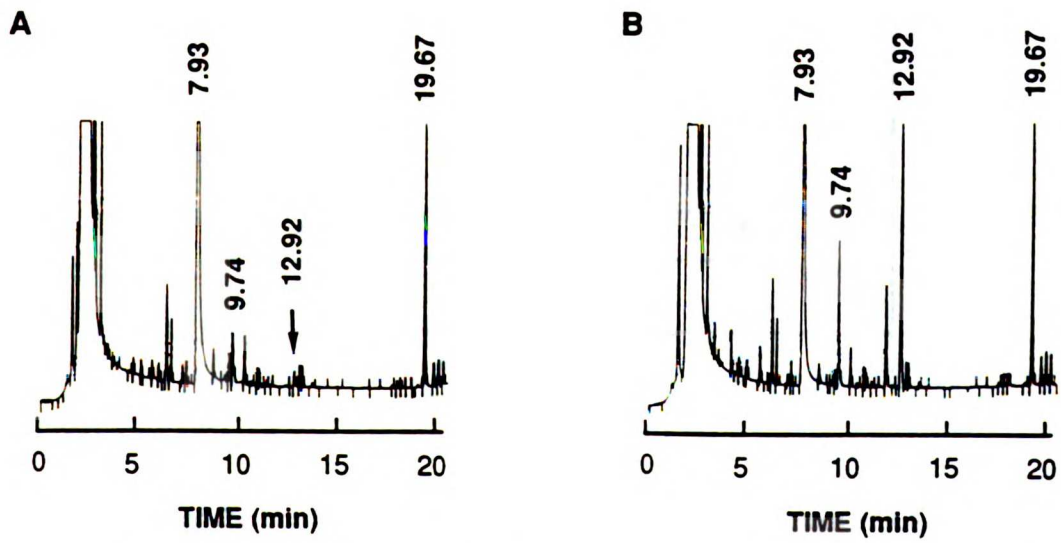

Fig. 2.14 Gas-liquid chromatographic analysis of the products obtained from (A) the reaction of the ferryl oxygen species with styrene and (B) the standard incubation (metmyoglobin + H_2O_2 + styrene). The retention time: styrene, 7.93; benzaldehyde, 9.74; styrene oxide,12.92; 2-undecanone, 19.67 min. The peaks at 6.34, 6.57 and 10.36 min are also shown in control incubations.

A myoglobin solution (300 μM) was allowed to stand at 0°C for 0, 0.5, 1, 2, 5, 10, 20 and 30 min after addition of 1.5 equivalents of H_2O_2 to determine the relationship between the protein radical decay and the decrease in product yield. Complete formation of the ferryl oxygen species required 1 or 2 min after myoglobin and H_2O_2 were mixed. Since only 1.5 equivalents of H_2O_2 were used to oxidize the ferric myoglobin, the enzyme must have undergone no more than a single turnover. The intensity of the absorption of the ferryl species decreased slightly by the end of the incubation with styrene, but the ferryl species did not return to the ferric state, presumably due to low turnover of styrene. Styrene oxide was not formed if either myoglobin or H_2O_2 was deleted from the reaction mixture but the formation of benzaldehyde was observed in both control experiments. A trace of benzaldehyde (0.03%) was present in the styrene, but benzaldehyde was also generated in the reaction of styrene with myoglobin or H_2O_2. Hence, it was not feasible to quantitate the amount of benzaldehyde produced from the reaction of myoglobin with

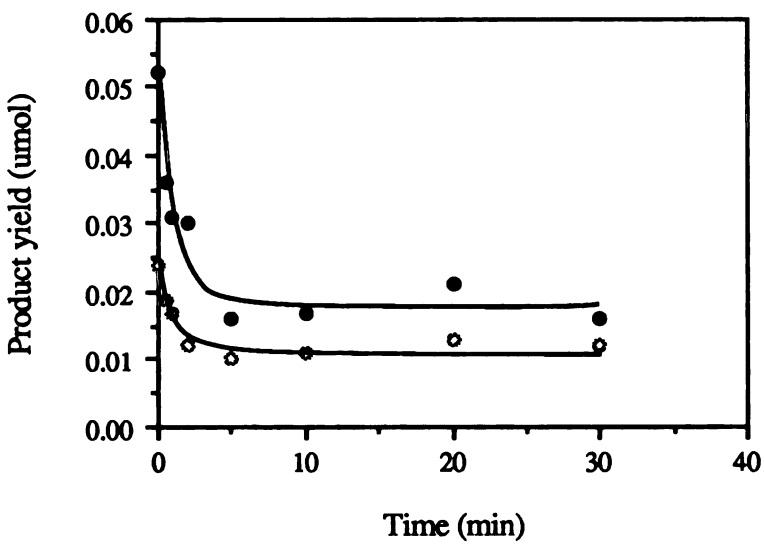

Fig. 2.15 Plot of the product yield vs. the time between addition of H_2O_2 and styrene. After myoglobin (300 μM) was mixed with 1.5 equivalents of hydrogen peroxide, the mixture was allowed to stand at 0°C for a given time before styrene was added. The formation of styrene oxide (•) and benzaldehyde (o) is shown.

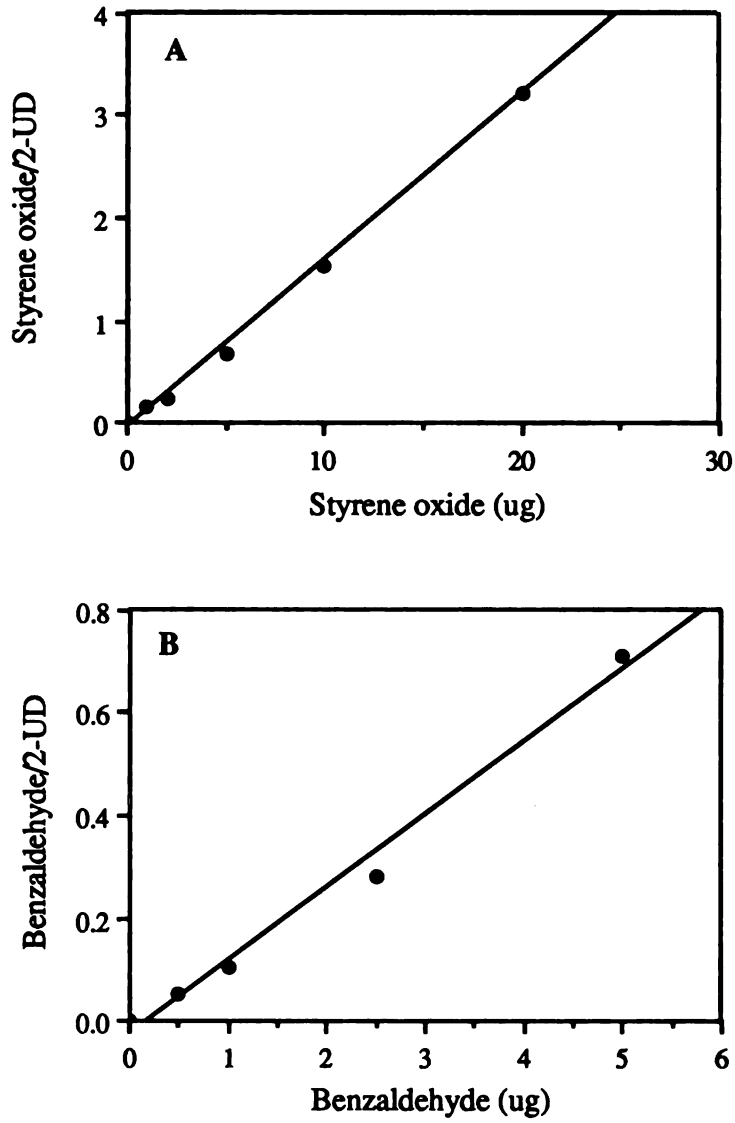

Fig. 2.16 Standard curve for the quantitation of styrene oxide (A) and benzaldehyde (B). The y-axis indicates the ratio of peak area of product to that of 2-undecanone as determined by gas-liquid chromatography. The amounts (μg) of styrene oxide or benzaldehyde used for the reaction are shown on the x-axis.

styrene. Nevertheless, the formation of styrene oxide and benzaldehyde was gradually suppressed as the time between addition of H_2O_2 and styrene increased (Fig. 2.15). Product yield was obtained from a standard curve of the ratio of the peak area of styrene

oxide (benzaldehyde) to 2-undecanone versus the known amount of styrene oxide (benzaldehyde) (Fig. 2. 16).

2.7 Discussion

Chloroperoxidase epoxidizes styrene in a time- (Fig. 2.3), styrene- (Fig. 2.4), H_2O_2- (Fig. 2.5), and enzyme-dependent manner. The formation of products decreases after 5 min of incubation due to peroxide-dependent inactivation of enzyme (Fig. 2.3). This is also supported by the demonstration that no product is formed when styrene is added to the reaction mixture after myoglobin and H_2O_2 are preincubated for 5 min. Geigert and coworkers also observed that chloroperoxidase is completely inactivated within, at most, several minutes after the epoxidation reaction starts (Geigert et al., 1986). Since styrene does not inactivate the enzyme, the inactivation must be caused by H_2O_2. Caution should be taken, however, because inactivation of chloroperoxidase may depend on the ratio of the peroxide to enzyme concentrations. The oxidation of styrene by chloroperoxidase and H_2O_2 produces styrene oxide and phenylacetaldehyde but not benzaldehyde. This result suggests that the chloroperoxidase-catalyzed epoxidation does not proceed by a cooxidative mechanism because the formation of benzaldehyde from styrene implies such a mechanism (Ortiz de Montellano & Catalano, 1985). In the epoxidation of styrene catalyzed by chloroperoxidase, the epoxide oxygen derives quantitatively from the peroxide (Fig. 2.6) and the stereochemistry of the olefin is completely retained (Fig. 2.7). The epoxidation catalyzed by chloroperoxidase thus clearly proceeds by a ferryl oxygen transfer mechanism (Ortiz de Montellano et al., 1987).

The oxidation of *trans*-[1-^{2}H]octene by microsomal cytochrome P-450 results in formation of the epoxide with retention of stereochemistry (Ortiz de Montellano et al., 1983b). The stereochemistry of epoxidation of conjugated olefins such as styrene by cytochrome P-450 had not been determined, however. Since the epoxidation of styrene by chloroperoxidase proceeds with retention of stereochemistry, the stereochemistry of the

same reaction by cytochrome P-450 was examined. As expected, the olefin stereochemistry is completely retained. Chloroperoxidase and cytochrome P-450 thus catalyze an epoxidation reaction in which the ferryl oxygen (Hager et al., 1972) is transferred to the olefin with retention of stereochemistry (Scheme 2.2).

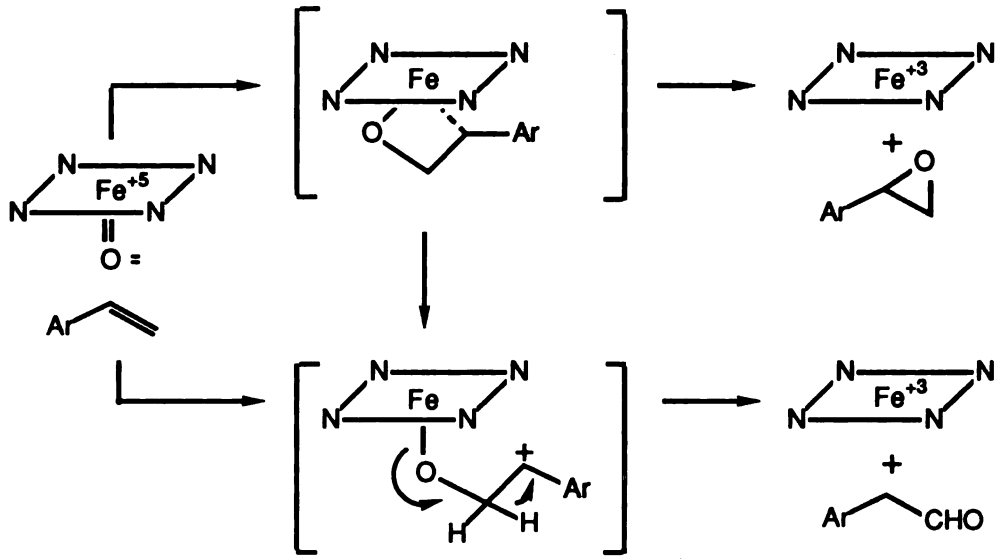

Scheme 2.2 Hypothetical mechanism for the formation of styrene oxide and phenylacetaldehyde in the oxidation of styrene by chloroperoxidase and cytochrome P-450. The prosthetic heme is indicated by the iron in a square of four nitrogens. The intermediate drawn with a dashed line could be a free radical or a metallacyclooxetane with a fully formed carbon-iron bond.

The chloroperoxidase-catalyzed oxidation of styrene produces styrene oxide and phenylacetaldehyde as reported previously for cytochrome P-450 (Liebler & Guengerich, 1983; Mansuy et al., 1984). Although the microsomal cytochrome P-450-catalyzed reaction is reported to produce a low yield of aldehyde (33:1 styrene oxide:phenylacetaldehyde ratio) (Mansuy et al., 1984), phenylacetaldehyde has not been detected in our incubations. The molar ratio of styrene oxide to phenylacetaldehyde produced by chloroperoxidase is 1.17-1.27:1, which is much lower than that produced by cytochrome P-450 (Ortiz de Montellano et al., 1987). The high yield of phenylacetaldehyde may be caused by the polar active site of chloroperoxidase because the

formation of a cationic transition state should be favored by a polar environment (Scheme 2.2). It has been shown in control studies that phenylacetaldehyde is not derived from isomerization of the styrene oxide in the reactions catalyzed by chloroperoxidase (Ortiz de Montellano et al., 1987), cytochrome P-450 (Mansuy et al., 1984), or model metalloporphyrins (Groves & Myers, 1983; Collman et al., 1986). The cationic intermediate resulting in aldehyde formation derives from the radical intermediate or directly from the ferryl oxygen complex and styrene. Although the mechanism of the production of phenylacetaldehyde is not clear, phenylacetaldehyde is probably generated by 1,2 rearrangement of a hydrogen in the cationic intermediate, a reaction analogous to the NIH shift.

Chloroperoxidase is a peroxidase that catalyzes the H_2O_2-dependent one-electron oxidation of classical substrates like horseradish peroxidase but also catalyzes a ferryl oxygen transfer like cytochrome P-450. Chloroperoxidase and cytochrome P-450 have a cysteine thiolate as the fifth heme ligand whereas classical peroxidases such as horseradish peroxidase have a histidine ligand. The globins, which have a histidine as the fifth ligand, also support the H_2O_2-dependent epoxidation of styrene. However, in order to better define the effect of the fifth heme ligand on the epoxidation reaction, 11-microperoxidase, which has a histidine fifth heme ligand, was examined. The products formed by microperoxidase and chloroperoxidase were compared: styrene oxide, phenylacetaldehyde and benzaldehyde were formed from the former but only the first two products from the latter. The formation of benzaldehyde suggests that the oxidation may occur, at least partially, via a protein-mediated cooxidative mechanism in which the stereochemistry is not retained. Due to the low yield of the epoxide, a large scale incubation (at least 10 ml) is required for ^{18}O studies to determine the origin of the epoxide oxygen and the olefin stereochemistry. Hence, styrene was replaced by *cis*-stilbene because the determination of olefin stereochemistry could be done by gas-liquid chromatography and *cis*-stilbene has a lower oxidation potential ($E_{1/2}$ = 1.54 V vs. standard calomel electrode) than that of styrene

($E_{1/2}$ = 2.1 vs. sce) (Heimbrook et al., 1986; Catalano, 1987). Absorption spectra were taken during the incubation of *cis*-stilbene by microperoxidase and H_2O_2 and approximately 70% of the heme disappeared within 1 min of the incubation (Fig. 2.10). This observation is supported by the structure of the hemepeptide, since the heme prosthetic group of microperoxidase is exposed to the medium whereas those of other hemoproteins are buried in a heme binding pocket. The microperoxidase-catalyzed oxidation of *cis*-stilbene produces *trans*-stilbene as well as *cis*-stilbene oxide, presumably by a mechanism similar to that of the bleomycin-catalyzed reaction (Heimbrook et al., 1986). The oxidation of *cis*-stilbene by bleomycin and an oxidant under aerobic conditions results in several oxidative products, including *cis*-stilbene oxide, deoxybenzoin, and benzaldehyde. Under anaerobic conditions, the yield of benzaldehyde decreases with a concomitant increase in the formation of *trans*-stilbene but little effect on the formation of *cis*-stilbene oxide (Heimbrook et al., 1986). Benzaldehyde, however, is not formed even when air or oxygen is bubbled into the microperoxidase incubation mixture. The formation of *trans*-stilbene increases under aerobic conditions, however, but deoxybenzoin, which is expected to be formed by oxygen transfer, is not detected. The finding that benzaldehyde is produced from styrene but not from *cis*-stilbene suggests that the steric or lipophilic properties of the substrates may play a role in the oxidation outcome. In contrast to our result, Mashino and coworkers have observed only styrene oxide and phenylacetaldehyde (molar ratio, 1:2.5) from the H_2O_2-dependent oxidation of styrene, and *cis*-stilbene oxide, diphenylacetaldehyde and *trans*-stilbene oxide (molar ratio, 2:1:trace) from the oxidation of *cis*-stilbene by 11-microperoxidase (Mashino et al., 1990). The result obtained from the oxidation catalyzed by microperoxidase, along with that of the globins, indicates that a cysteine thiolate heme ligand is not required for catalysis of epoxidation reactions.

Metmyoglobin (300 μM) catalyzes the H_2O_2 (450 μM)-dependent oxidation of styrene to styrene oxide and benzaldehyde. In the standard incubation, six moles of myoglobin (0.3 μmol) is used to epoxidize one mole of styrene (0.052 μmol) (Fig. 2.14, B

and Fig. 2.15). The protein radical decays rapidly as a function of time and then its decay levels off 5 min after H_2O_2 is added to myoglobin, which parallels the rate of decrease in the product yield (2.12 and 2.15). The protein radical is still detected 30 minutes after it is generated, even though its intensity is very weak. This could be explained by the formation of a stable protein radical which may not be identical to the initial radical but can still epoxidize styrene. Since the hydroxyl radical is very short-lived ($t_{1/2}$ at 37°C = 10 nsec in the presence of 1 M linoleate: (Pryor, 1986)), it decays much faster than the protein radical. The half life of the protein radical is approximately 1 min but may range between 30 seconds and 1 minute if the initial radical decay is considered. Davies reported that the protein radical decays with a half life of 30 seconds when myoglobin (1 mM) is rapidly mixed with an equivalent of H_2O_2 (Davies, 1991). When styrene is added to the system after the hydroxyl radical should have disappeared, the styrene is still epoxidized. Therefore, the hydroxyl radical does not appear to participate in the oxidation of styrene. The protein radical is thus required for the oxidation of styrene and this result strongly supports the proposed mechanism (pathways A and B, Scheme 1.1).

Cytochrome P-450 catalyzes oxygen transfer reactions. The fact that horseradish peroxidase does not catalyze ferryl oxygen transfer supports the proposal that substrates do not have access to the ferryl oxygen in horseradish peroxidase and thus react with the heme edge (Ator & Ortiz de Montellano, 1987). Chloroperoxidase, like cytochrome P-450, transfers its ferryl oxygen to styrene but, like horseradish peroxidase, catalyzes the one-electron peroxidation of guaiacol. Chloroperoxidase thus functions as both a peroxygenase and a peroxidase. Chloroperoxidase has a P-450-like active site but differs from P-450 in that it readily catalyzes peroxidative reactions. Myoglobin catalyzes the epoxidation of styrene in that part of the epoxidation proceeds by a mechanism similar to that of cytochrome P-450 and the rest possibly by a cooxidative mechanism (Ortiz de Montellano & Catalano, 1985). However, the protein radical is required for both of the epoxidation reactions catalyzed by myoglobin.

CHAPTER 3

H_2O_2-induced damage to myoglobin

3.0 Introduction

Hemoproteins are, in some cases, destroyed by substrates. These suicide substrates bind to the hemoprotein and are catalytically turned over to produce reactive species which irreversibly alter the enzyme and impair its catalytic activity. The irreversible inactivation of the cytochrome P-450 enzymes has been extensively studied and is known to be caused by covalent modification of the protein, the heme group or possibly covalent binding of the heme group to the protein (Osawa & Pohl, 1989; Ortiz de Montellano, 1990).

Protein modification of cytochrome P-450 has been observed in the reaction with chloramphenicol and sulfur compounds such as parathion. Chloramphenicol is oxidized to an oxamyl chloride that reacts with a lysine residue in the protein (Halpert & Neal, 1980; Halpert, 1981; Halpert, 1982; Halpert et al., 1983). This modification apparently blocks electron transfer from the reductase to the cytochrome P-450 since NADPH oxidase activity and reduction of P-450 are inhibited, whereas cumene hydroperoxide- or iodosobenzene-dependent deethylation of 7-ethoxycoumarin is not affected (Halpert et al., 1983).

Some aspects of the modification of the cytochrome P-450 heme group have been well defined by studies of P-450 inactivation by terminal olefins, terminal acetylenes, monosubstituted hydrazines, 1-aminobenzotriazole, and 4-alkyl-1,4-dihydropyridines (Ortiz de Montellano & Correia, 1983). The cytochrome P-450-catalyzed reaction of terminal, unconjugated olefins results in heme alkylation paralleled by epoxidation. Terminal acetylenes also alkylate the enzyme while being converted to the corresponding acetic acid derivatives. The characterization of alkylated heme adducts obtained in these terminal olefin and acetylene incubations indicates that the terminal carbon is bound to nitrogen and the internal carbon to the activated oxygen. However, whereas it can be

shown that the terminal carbon is bound to the activated oxygen in the metabolites of terminal acetylenes, it is not possible to do so in the metabolites of terminal olefins due to the symmetry of the epoxide (Ortiz de Montellano, 1985; Ortiz de Montellano & Reich, 1986). Monosubstituted hydrazines inactivate the enzyme by alkylating the pyrrole nitrogens, in some cases via the formation of transient iron-aryl or probably iron-alkyl complexes. 1-Aminobenzotriazole is oxidized to benzyne that inactivates the enzyme by forming an N,N-bridged species (Campbell & Rees, 1969; Ortiz de Montellano & Mathews, 1981; Ortiz de Montellano et al., 1984). 1,4-Dihydropyridines having primary, unconjugated alkyl groups at the 4-position also alkylate the pyrrole nitrogens (Augusto et al., 1982a). Dihydropyridines are oxidized to radical cations which release alkyl radicals from the 4-position in order to aromatize the pyridine ring. The resulting alkyl radicals are responsible for the heme alkylation.

Covalent binding of the prosthetic heme group to the protein has been postulated to be another mechanism for the irreversible destruction of cytochrome P-450 enzymes. Substrates that cause this type of destruction include CCl_4, AIA (2-isopropyl-4-pentenamide), secobarbital, fluroxene, 1-octene, vinyl chloride, vinyl bromide, 3,5-*bis* (carbethoxy)-2,6-dimethyl-4-ethyl-1,4-dihydropyridine, phenylhydrazine, hydrogen peroxide and cumene hydroperoxide. The incubation of radiolabeled rat liver microsomes with CCl_4 results in covalent binding of the heme group to the protein both *in vivo* and *in vitro* (Davies et al., 1985; Davies et al., 1986b). Heme-radiolabeling studies show that 31% and 28% of the total P-450 heme are covalently bound to microsomal proteins *in vitro* and *in vivo*, respectively (Davies et al., 1986b; Davies et al., 1985). A substantial amount of the covalently bound products from both the *in vivo* and *in vitro* reactions is bound to P-450. AIA also destroys up to 44% of phenobarbital-induced cytochrome P-450 *in vitro*, of which 50% is converted to heme-bound protein adducts and 50% to N-alkylated heme adducts (Davies et al., 1986a). Sixty four percent of the heme-derived products is bound to cytochrome P-450. Secobarbital inactivates cytochrome P-450 by both alkylating the

heme moiety and forming covalent heme-derived adducts with the protein *in vitro* (Lunetta et al., 1989). Both AIA and secobarbital also form small amounts of heme-derived protein adducts *in vivo* (Bornheim et al., 1987; Lunetta et al., 1989). Hydrogen peroxide or cumene hydroperoxide generates heme-derived protein-bound products in microsomal P-450 (Guengerich, 1978). The covalently bound adducts to cytochrome P-450 are not well defined because it is not known if heme, a modified heme or a heme degradation product is the bound species (Ortiz de Montellano, 1990). However, it is likely that the substrates are oxidized to radical or radical cationic intermediates by cytochrome P-450, and the resulting intermediates cause the covalent binding of the heme group to the protein. Alternatively, heme degradation products may be involved in the covalently bound adduct because the heme is degraded by peroxide to methylvinylmaleimide and propentdyopents which act as Michael acceptors. This is supported by the demonstration that glutathione and 2-mercaptoethanol readily attack the double bond of methylvinylmaleimide to give adducts (Schaefer et al., 1987).

Myoglobin is another hemoprotein in which covalent binding of the heme group to the protein is observed. The reaction of sperm whale metmyoglobin with $BrCCl_3$ under reducing conditions yields a covalently bound heme-protein adduct along with three soluble heme adducts (Osawa et al., 1989). Proteolytic digestion of the heme-derived protein yields a heme-hexapeptide that can be further digested to a heme-histidine adduct. Mass spectrometric analysis of these adducts indicates that the proximal iron ligand, His 93, is bound to a heme moiety modified by a CCl_2 group (Osawa et al., 1990). Further NMR analysis confirms that the His 93 and CCl_2 group are attached to the internal and terminal carbons of the heme 2-vinyl group, respectively (structure D, Fig. 4.1). A mechanism has been proposed in which the imidazole nitrogen of His 93 reacts with a cationic intermediate obtained from trichloromethylvinyl heme, an intermediate in the reaction of $BrCCl_3$ with heme (Osawa et al., 1991). This reaction has been proposed as a model for the CCl_4-

induced covalent binding of the heme to cytochrome P-450 because the CCl_3 radical is generated in both the P-450 and myoglobin reactions.

The reaction of equine metmyoglobin with H_2O_2 at pH 4.5 results in covalent binding of up to 20% of the heme group to the protein (Catalano et al., 1989), which is consistent with the report that more heme is retained by the protein after reaction at low pH than high pH (Fox et al., 1974). The nature of the crosslink between the heme group and protein has been studied (Catalano et al., 1989). Amino acid composition analysis suggests that 50% of the tyrosine content disappears after treatment of myoglobin with H_2O_2 at pH 7.4, which is consistent with the results of earlier studies by Rice and coworkers (Rice et al., 1983). Tryptic digestion followed by HPLC analysis of the apoprotein obtained from H_2O_2-treated and untreated myoglobin shows that the heme-associated peptide is generated only in the H_2O_2-treated protein (Catalano et al., 1989). Moreover, the intensity of a peptide containing aromatic residues (peptide A) greatly decreases after treatment of the protein with H_2O_2. Amino acid analysis and N-terminal amino acid sequencing have confirmed that peptide A has the amino acid sequence YLEFISDAIIHVLHSK. It is of some interest that the tyrosine content of the residual peptide A that is isolated decreases by 50% after treatment of myoglobin with H_2O_2. Mass spectrometric and amino acid composition data on the heme-peptide indicate that the heme is covalently attached to peptide A via Tyr 103 (Catalano et al., 1989). Covalent binding of the heme group to Tyr 103 presumably arises by reaction of the heme group with the protein radical. The reaction of metmyoglobin with H_2O_2, which produces a Compound II-like chromophore, forms a ferryl oxygen species and a protein radical (George & Irvine, 1956; King & Winfield, 1963; Yonetani & Schleyer, 1967). EPR studies by King and coworkers suggest that the protein radical of myoglobin is formed first at a phenylalanine or histidine residue close to the iron atom on the distal side of the porphyrin and then is rapidly transferred to a tyrosine residue (King et al., 1967) (Scheme 3.1).

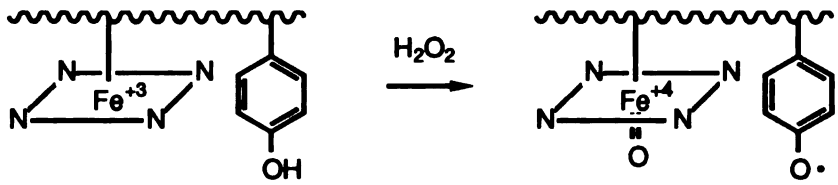

Scheme 3.1 The oxidation of metmyoglobin by H_2O_2 to a ferryl oxygen species and a protein radical, probably Tyr 103. An iron in a square of four nitrogens stands for the prosthetic heme group and the wavy line for the protein surface.

A protein radical has been detected by EPR in the reaction of H_2O_2 with sperm whale myoglobin (Gibson et al., 1958; King et al., 1967), horse myoglobin (King & Winfield, 1963; King et al., 1967; Yonetani & Schleyer, 1967), horse hemoglobin (King et al., 1967) and human hemoglobin (Shiga & Imaizumi, 1975; Tomoda et al., 1978). A tyrosine residue has been proposed as the site of the protein radical formed in the reaction of myoglobin with hydroperoxide (Tew & Ortiz de Montellano, 1988; Miki et al., 1989). Rice and coworkers have shown that the reaction of sperm whale myoglobin with H_2O_2 results in a decrease in the tyrosine content and the formation of myoglobin dimers (Rice et al., 1983). Tew and Ortiz de Montellano demonstrated that the dimerization occurs between Tyr 103 of one myoglobin and Tyr 151 of the other. This result supports the proposal that Tyr 103 is the primary site of the protein radical. Miki and coworkers have implicated Tyr 151 as one of the radical sources in the reactions of sperm whale myoglobin with ethyl hydroperoxide and irridate (Miki et al., 1989).

There is further evidence to support the formation of a protein radical. A major fraction of the epoxide oxygen derives from molecular oxygen in the epoxidation of olefins by metmyoglobin and H_2O_2 (Ortiz de Montellano & Catalano, 1985; Catalano & Ortiz de Montellano, 1987). A peroxyl radical produced by addition of oxygen to the protein radical has been proposed as the species that epoxidizes the olefin. Its formation is supported by recent EPR evidence for a putative DMPO-trapped peroxyl radical generated during the reaction of horse metmyoglobin (300 μM) with an equivalent of H_2O_2 (Davies, 1990). A

tyrosine-derived peroxyl radical, if generated, would probably exhibit a $t_{1/2}$ of ~7 sec analogous to a lipid peroxyl radical (Pryor, 1986). The proposal that a peroxyl radical mediates the epoxidation of styrene is very attractive because the H_2O_2-dependent epoxidation of styrene is catalyzed by horseradish peroxidase only in the presence of 4-methylphenol (Ortiz de Montellano & Grab, 1987).

Precedents exist for protein radicals as viable intermediates in enzymatic processes. Catalytic tyrosine radicals have been observed in ribonucleotide reductase (Ehrenberg & Reichard, 1972; Reichard & Ehrenberg, 1983; Ashley & Stubbe, 1985), prostaglandin H synthase (Kulmacz et al., 1987) and photosystem II (Barry & Babcock, 1987). Protein radicals residing at undetermined sites have been reported in cytochrome c peroxidase (Yonetani, 1976; Edwards et al., 1987; Goodin et al., 1987) and pyruvate formate-lyase (Knappe et al., 1984).

The reaction of myoglobin with H_2O_2 has been the focus of some attention because it may be associated with pathological process such as reperfusion injury (Hebbel & Eaton, 1989; Galaris et al., 1989). Myoglobin is the main hemoprotein of muscle and its function is to transport and store molecular oxygen intracellularly (Millikan, 1939; Wittenberg, 1970). However, oxymyoglobin can autooxidize to metmyoglobin and superoxide, the latter of which is dismutated to H_2O_2 (Wallace et al., 1982; Tajima & Shikama, 1987). The reaction of metmyoglobin with H_2O_2 may cause damage to the cell. Although the actual products or oxidants which cause the damage are not known, heme-bound apomyoglobin may be involved in the cellular destruction. The heme site covalently bound to Tyr 103 of myoglobin has been investigated to gain a better understanding of the peroxide-induced damage to myoglobin and, in turn, the potential damage to cellular constituents. The myoglobin reaction is also relevant to the nature of the heme-derived adducts of cytochrome P-450. In addition, the roles of the tyrosine residues of myoglobin in protein crosslinking have been studied using mutants resulting from site directed

mutagenesis of Tyr 146 and 151. Finally, the protein modification in the reaction of metmyoglobin with H_2O_2 in the presence of styrene has been studied.

3.1 The site of attachment of the heme group to the protein

3.1.1 Is the heme attached to the protein via the heme vinyl group?

Incubation of horse myoglobin with H_2O_2 for 30 min at 0°C decreased the intensity of the Soret absorbance but the heme prosthetic group extracted from the protein with acidic 2-butanone was spectroscopically identical to heme itself. A quantitative amount of heme was removed from the H_2O_2-untreated myoglobin but a small amount of heme remained in the H_2O_2-treated myoglobin. The incubation was carried out at pH 4.5 and 7.4 and the results indicated that more heme was retained after incubation at low pH (Table 3.1). If it

Table 3.1

Non-extractable heme content of peroxide-treated horse myoglobin

Reaction pH	Prosthetic group	$\lambda_{Soret}/\lambda_{280\,nm}$ $+H_2O_2$	$-H_2O_2$	Difference	Heme retention[a] (%)
4.5	Protoheme	0.97	0.08	0.89	18
4.5	Mesoheme	0.80	ND[b]	0.80	16
7.4	Protoheme	0.31	0.13	0.18	4
7.4	Mesoheme	0.22	ND[b]	0.22	4

[a]Heme retention is calculated from the $\lambda_{Soret}/\lambda_{280}$ ratio relative to the average for the myoglobin samples used in the study ($\lambda_{Soret}/\lambda_{280}$ = 4.99). The same value has been used to calculate the retention of mesoheme, although the true maximum value of $\lambda_{Soret}/\lambda_{280}$ is likely to be slightly different for the mesoheme.
[b]ND stands for not detectable.
Mesoheme was prepared as described in the Experimental Chapter or obtained commercially.

is assumed that the molar absorbance of the covalently bound product is identical to that of metmyoglobin, approximately 4-10% and 18-25% of the heme group was covalently bound to the protein after reaction with H_2O_2 at pH 7.4 and 4.5, respectively (Fig. 3.1).

Horse myoglobins reconstituted with protoheme and mesoheme were incubated with and without H_2O_2. After the prosthetic heme groups were removed with acidic 2-butanone, the residual amount of heme retained in the apoproteins was measured by comparing their Soret to 280 nm absorbance ratio with that of native myoglobin (Table 3.1). The apoproteins of the myoglobins incubated without H_2O_2 only contained a trace of Soret absorbance whereas the apoproteins from H_2O_2-treated myoglobins retained a much stronger Soret absorbance (Fig. 3.1). The intensity of the residual absorbance was nearly identical for both the protoheme and mesoheme-reconstituted metmyoglobins (Table 3.1).

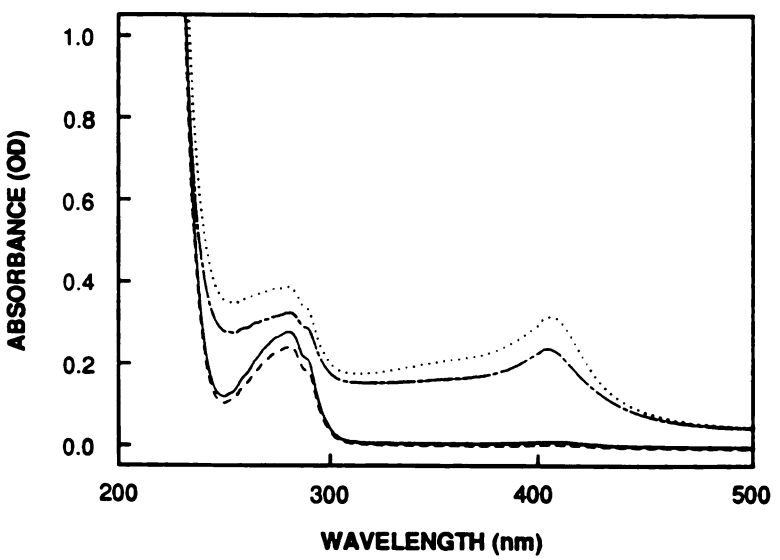

Fig. 3.1 Electronic absorption spectra of the apoproteins obtained by removal of the prosthetic group from protoheme-reconstituted myoglobin treated for 30 min at 0°C with H_2O_2 (····), without H_2O_2 (—) and from mesoheme-reconstituted myoglobin treated with H_2O_2 (–·–) and without H_2O_2 (– –) at pH 4.5. In each instance, the prosthetic heme group was removed to the extent possible with acidic butanone as described in the Experimental Chapter.

The spectrum suggests that the iron porphyrin chromophore remained intact in the residual heme associated with the apoprotein after heme extraction. This result was confirmed by the shift of the Soret maximum after addition of KCN. The Soret maximum shifted from 406 to 414 nm when KCN was added to the apoprotein of protoheme-reconstituted metmyoglobin treated with H_2O_2. A shift of the Soret band from 395 to 408 nm was similarly observed in the KCN-treated apoprotein from the reaction of mesoheme-reconstituted metmyoglobin with H_2O_2. These values were comparable to the 408 to 420 nm shift observed when KCN was added to native metmyoglobin. The results indicate that covalent binding of the heme group to the protein did not occur via the vinyl groups and did not significantly alter the parent heme chromophore.

3.1.2 Attempts to isolate the heme-peptide

Apoprotein was prepared after incubation of metmyoglobin in the presence and absence of H_2O_2 at pH 4.5. A tryptic heme-peptide, which was not detected in the reaction without H_2O_2, was obtained when the apoprotein of H_2O_2-treated myoglobin was digested with TPCK-treated trypsin (Fig. 3.2). The resulting tryptic heme-peptide was purified as a single peak by HPLC (Fig. 3.3), and its absorption spectrum exhibited a Soret maximum at 402 nm. When the tryptic heme-peptide was analyzed by 500 MHz ^1H NMR spectroscopy, only two of the four possible *meso* protons appeared (at 9.973 and 9.599 ppm) (Fig. 3.4). The two peaks were only seen when the *meso* proton-region was expanded, possibly because of the low resolution of the NMR spectrum. The tryptic heme-peptide was not fully soluble in the NMR solvent, a mixture of 100 µl of DMSO-d_6 and 300 µl of pyridine-d_5. Unfortunately, efforts to obtain a mass spectrum of the tryptic heme-peptide by LSIMS were not successful.

Digestion of the apoprotein of H_2O_2-treated myoglobin with other proteases were also carried out. Digestion with the nonspecific protease, elastase, gave the heme-peptide in the highest yield based on the HPLC profile. Therefore, the resulting heme-peptide with

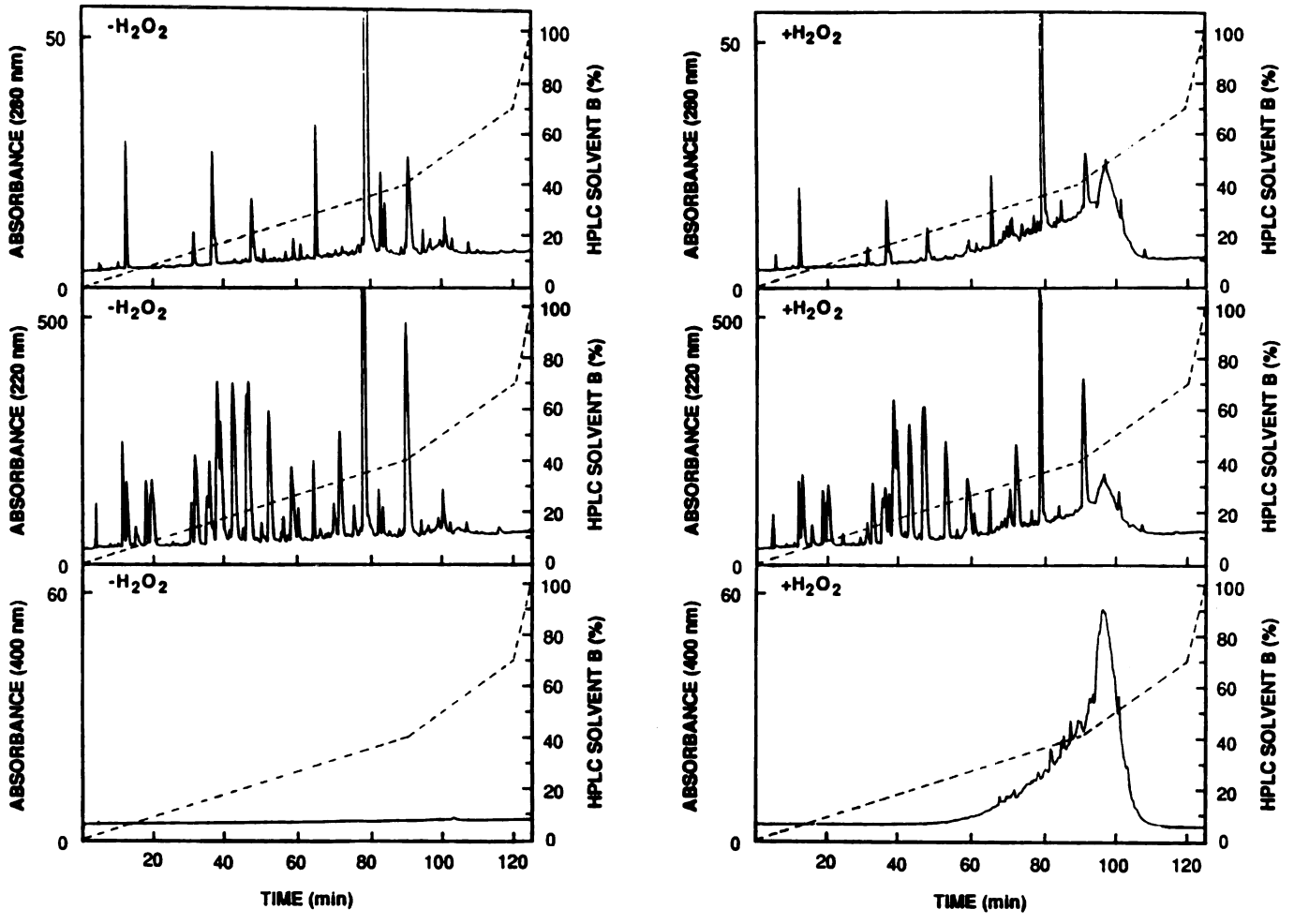

Fig. 3.2 HPLC peptide maps obtained from the trypsin-treated apoprotein of myoglobin incubated without H_2O_2 (left set) and with H_2O_2 (right set). Top traces were monitored at 280 nm, middle traces at 220 nm and bottom traces at 400 nm. The heme-peptide is eluted with a retention time between 93 and 100 min. The unreacted apoproteins are eluted at around 100 min. The dashed line indicates HPLC solvent B (%) gradient (solvent A: 0.1% trifluoroacetic acid in water; solvent B: 0.1% trifluoroacetic acid in acetonitrile).

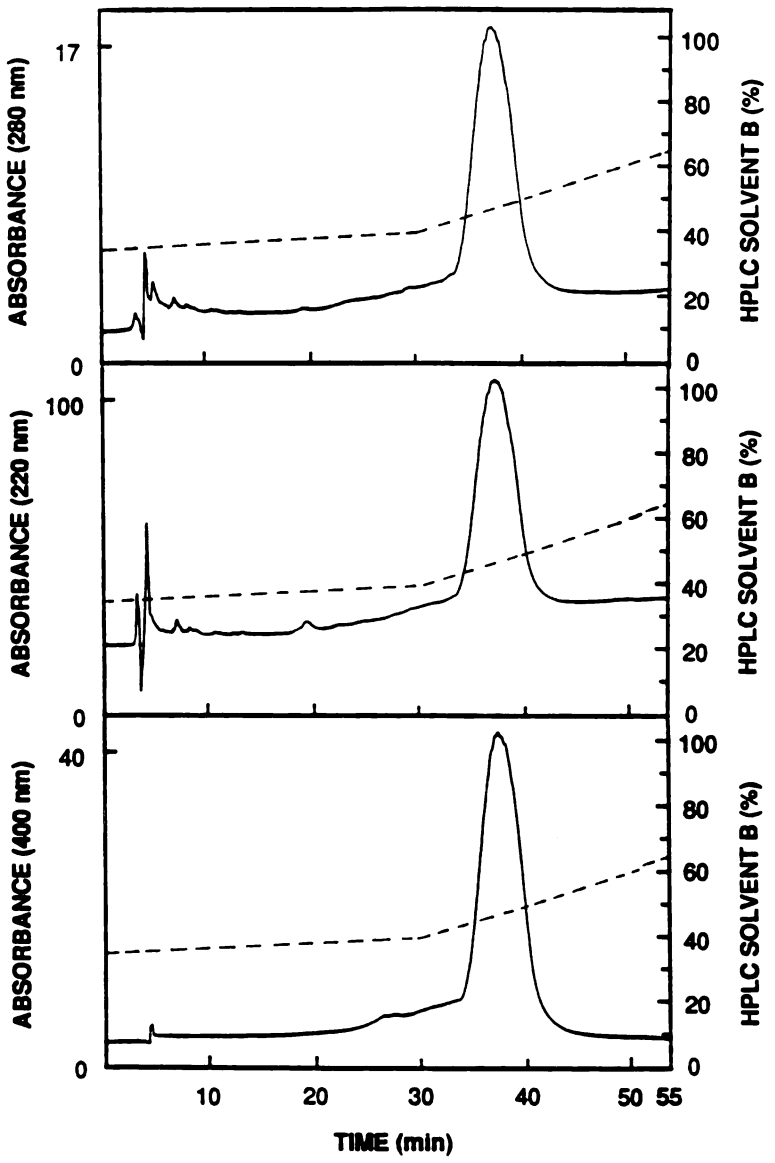

Fig. 3.3 HPLC chromatograms of the tryptic heme-peptide. Top trace was monitored at 280 nm, middle trace at 220 nm and bottom trace at 400 nm. HPLC solvent B gradient line is also shown (---). Solvent A contains 0.1% TFA in water and solvent B contains 0.1% TFA in acetonitrile.

absorption maximum at 398 nm was analyzed by both positive and negative LSIMS. The molecular ion and the fragments (nominal mass at m/z 586, 621, 812, 891 and 907 by positive mode; 513, 540, 810, 889, 905 and 1322 by negative mode) did not match with any calculated composition of the heme-peptide.

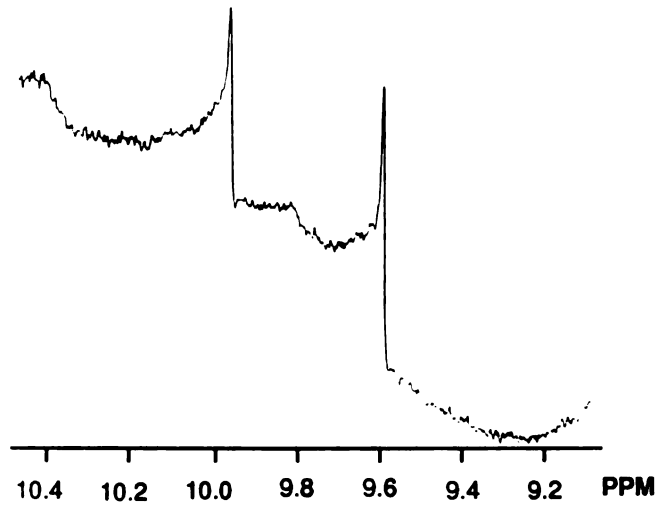

Fig. 3.4 500 MHz ^1H NMR spectrum of the tryptic heme-peptide in DMSO-d_6 and pyridine-d_5. The *meso* proton region only is shown.

3.1.3 Attempts to isolate the heme-bound protein

The apoprotein of H_2O_2-treated myoglobin contained approximately 20% residual heme. Efforts were therefore made to separate the heme-bound protein from the heme-free apoprotein by SDS-PAGE, IEF, HPLC, FPLC or gel filtration (Biogel column).

The heme-bound protein was not separated from the apoprotein by SDS-PAGE (20% acrylamide) due to the similarity in their molecular weights. High molecular weight bands were observed in the gel from the apoprotein of H_2O_2-treated myoglobin, presumably due to the formation of protein oligomers. Horse heart myoglobin has two isoelectric points, at 6.8 and 7.2, in IEF mix 3.6-9.3. The apoprotein should have a higher pI than that of the holoenzyme due to the presence of the two propionic acids in the heme group of the latter (Varadarajan et al., 1989). However, a separation based on this pI difference was not obtained in our system. The HPLC of the apoprotein of H_2O_2-untreated myoglobin showed a single peak which coeluted with the earlier one of the two peaks from the apoprotein of H_2O_2-treated myoglobin. A broad peak that retained the heme chromophore

appeared only in the H_2O_2-treated protein. When the apoprotein of H_2O_2-treated myoglobin was analyzed by FPLC, it eluted as two peaks. The latter peak containing the heme chromophore was shown by SDS-PAGE to contain a small amount of high MW bands as well as a monomer band whereas the earlier peak contained only the monomer (Fig. 3.5). This result was consistent with that obtained by gel filtration. The fraction retaining the heme chromophore contained a small amount of high MW bands as well as a monomer band. The heme-containing fractions and the corresponding fractions from the apoproteins of H_2O_2-treated and untreated myoglobins, respectively were digested with elastase and analyzed by HPLC. Peptide maps of both digests showed that there was a different peak with a retention time of 46 min, although the difference was significant only

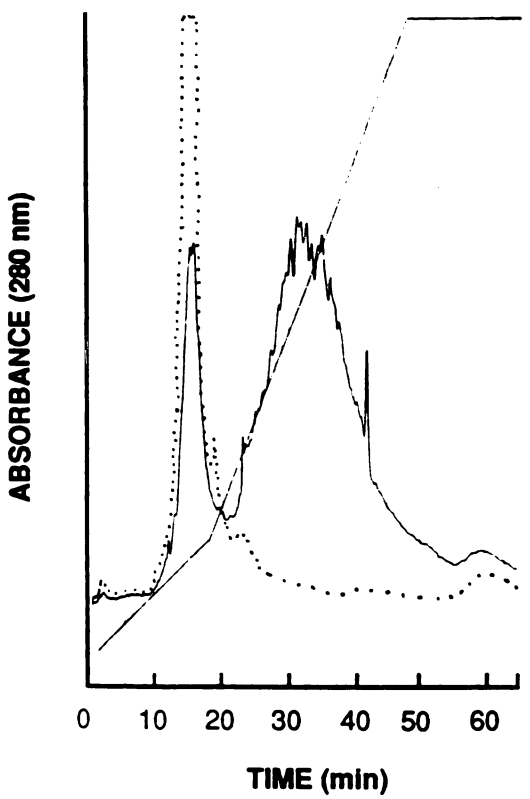

Fig. 3.5 FPLC chromatograms of the apoprotein of peroxide-untreated (···) and treated (—) myoglobins. FPLC solvent D (%) gradient is indicated by the diagonal line: solvent C-10 mM NH_4HCO_3 (pH 8.5); solvent D-700 mM NH_4HCO_3 (pH 8.5). The column was eluted using a step gradient of 0-20% solvent D over 20 min, 20-100% D over 30 min and 100 % D over 15 min

in the 400 nm region. The sharp peak at 46 min was present in much lower amount when the fraction containing only the monomer band was digested. However, characterization of this peak by mass spectrometry was not successful.

3.2 The roles of the tyrosine residues in peroxide-treated myoglobin

The reaction mixture of the recombinant myoglobin (MW ~ 17,946) with H_2O_2 showed a band at the position where a dimer (MW ~ 35,888) would run when analyzed by SDS-PAGE (Fig. 3.6). A comparable band was observed in the incubation of H_2O_2 with the Tyr146Phe mutant but not with the Tyr151Phe mutant. The wild-type and mutant enzymes only exhibited the monomeric protein when the reactions were carried out without H_2O_2.

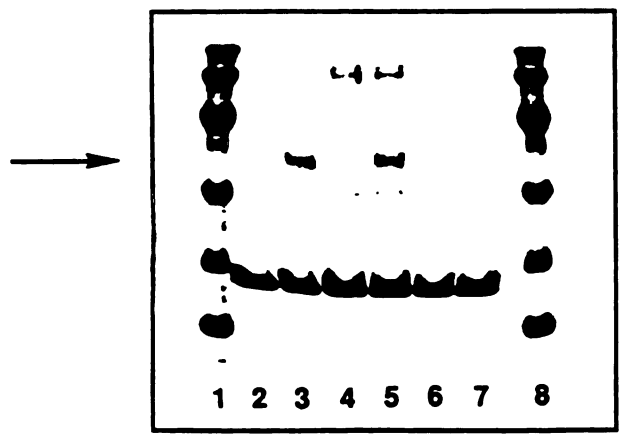

Fig. 3.6 SDS-PAGE (15% acrylamide) analysis of the cross-linking of recombinant sperm whale myoglobin. An arrow indicates the position of a dimer. Lanes from left to right: (1 and 8) molecular weight standards, (2) wild-type enzyme, (3) wild-type enzyme + H_2O_2, (4) Y146F, (5) Y146F + H_2O_2, (6) Y151F and (7) Y151F + H_2O_2.

3.3 Styrene-dependent protein modification

Heme extraction following incubation of metmyoglobin with H_2O_2 in the presence of styrene at pH 7.4 yielded apoprotein in which approximately 10% of the heme group was retained. The apoprotein obtained from a parallel reaction without H_2O_2 did not retain the

heme chromophore. Precipitation was observed during the final dialysis step after heme was extracted from the protein. However, significantly more precipitate was formed during dialysis with protein recovered from reaction with H_2O_2. The precipitates could be eliminated by either reducing the dialysis period or by centrifugation after dialysis. However, a peak due to a modified peptide did not appear on the peptide maps after V8 proteolysis of the soluble apoproteins. It seems likely that the modified protein precipitated out during the dialysis. The V8 protease-treated precipitates showed very similar HPLC chromatograms to those obtained when the apoproteins were used without prior removal of the precipitates. Most of the precipitates presumably derived from damage to the protein by H_2O_2. Hence, the apoprotein prepared without removal of the precipitate was used for the digestion with *Staphylococcal* V8 protease.

The HPLC data showed that there were a few differences in the peaks observed in the peptide region after digestion of the apoproteins from H_2O_2-treated and untreated myoglobins (Fig. 3.7). The differences in the heme-associated region were not investigated because they involved heme-bound peptides. A large scale experiment followed by preparative HPLC analysis showed similar peptide maps to those obtained from analytical experiments (Fig. 3.7 and 3.8). A peak with a retention time of 23.3 min disappeared and two other peaks appeared at 23.8 and 26.5 min when the apoprotein of H_2O_2-treated myoglobin was digested with V8 protease and analyzed by HPLC (Fig. 3.8). A small peak at 24.6 min disappeared but it may have been hidden under the peak at 23.8 min. The peaks eluting at 23.3 and 23.8 min were not identical, as confirmed by coinjection of the two peptides. Fractions eluting at 23.3 (-1), 24.6 (-2), 23.8 (+1) and 26.5 min (+2) were rechromatographed for mass spectrometric and amino acid composition analysis. The peak at 23.3 min was obtained in very pure form but the others were not as well purified by the HPLC system. The LSIMS mass spectra showed that peptides, -1 and +1 had the same protonated molecular ion at m/z 2315 (nominal mass), the value expected for a peptide containing Tyr 103 (Table 3.2). Although these two peptides were not

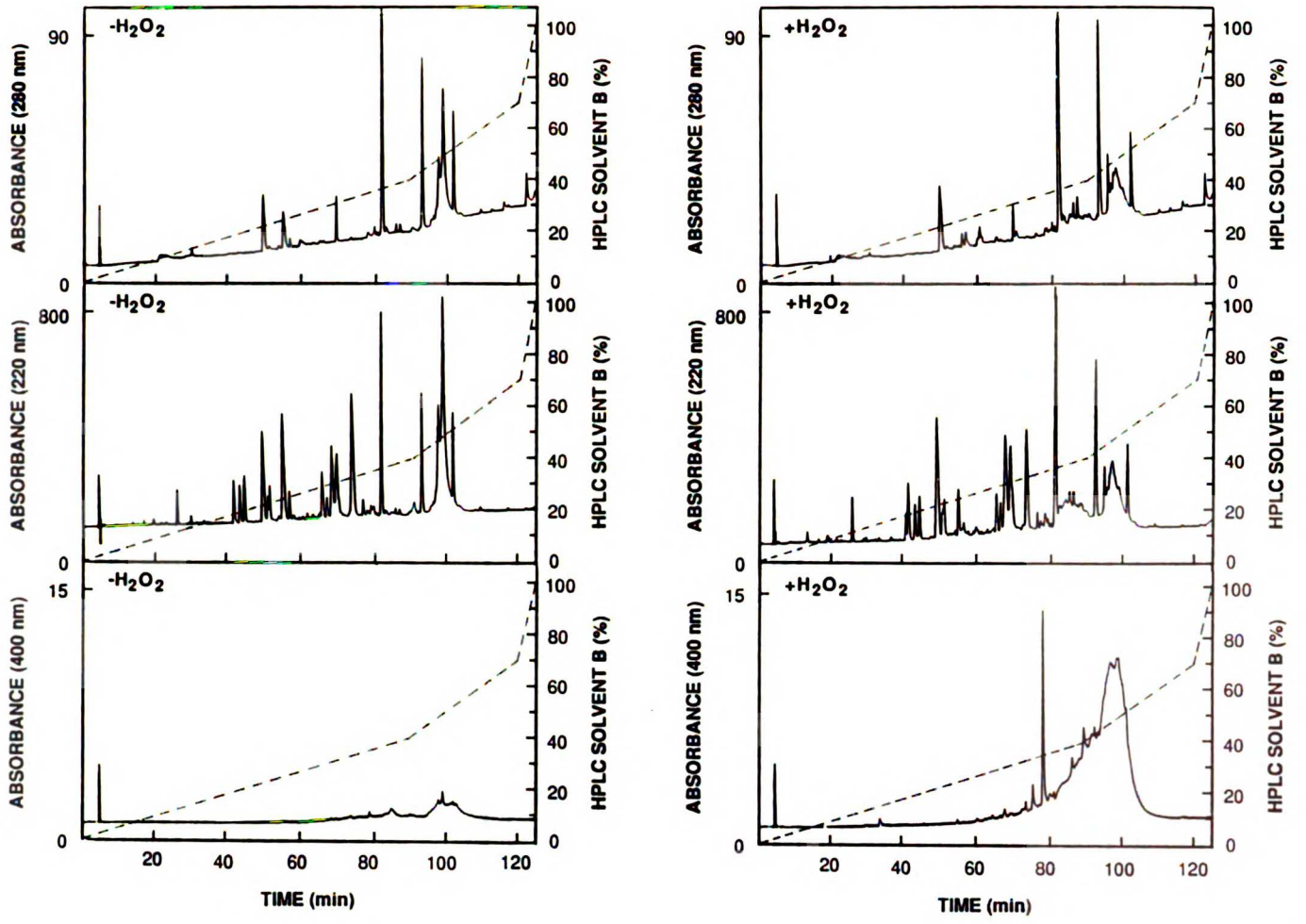

Fig. 3.7 HPLC peptide maps of V8 protease-treated apoproteins obtained from the myoglobins incubated without H_2O_2 (left set) and with H_2O_2 (right set) in the presence of styrene. Top traces were monitored at 280 nm, middle traces at 220 nm and bottom traces at 400 nm. HPLC solvent B gradient is indicated by the dashed line (solvent A: 0.1% trifluoroacetic acid in water; solvent B: 0.1% trifluoroacetic acid in acetonitrile).

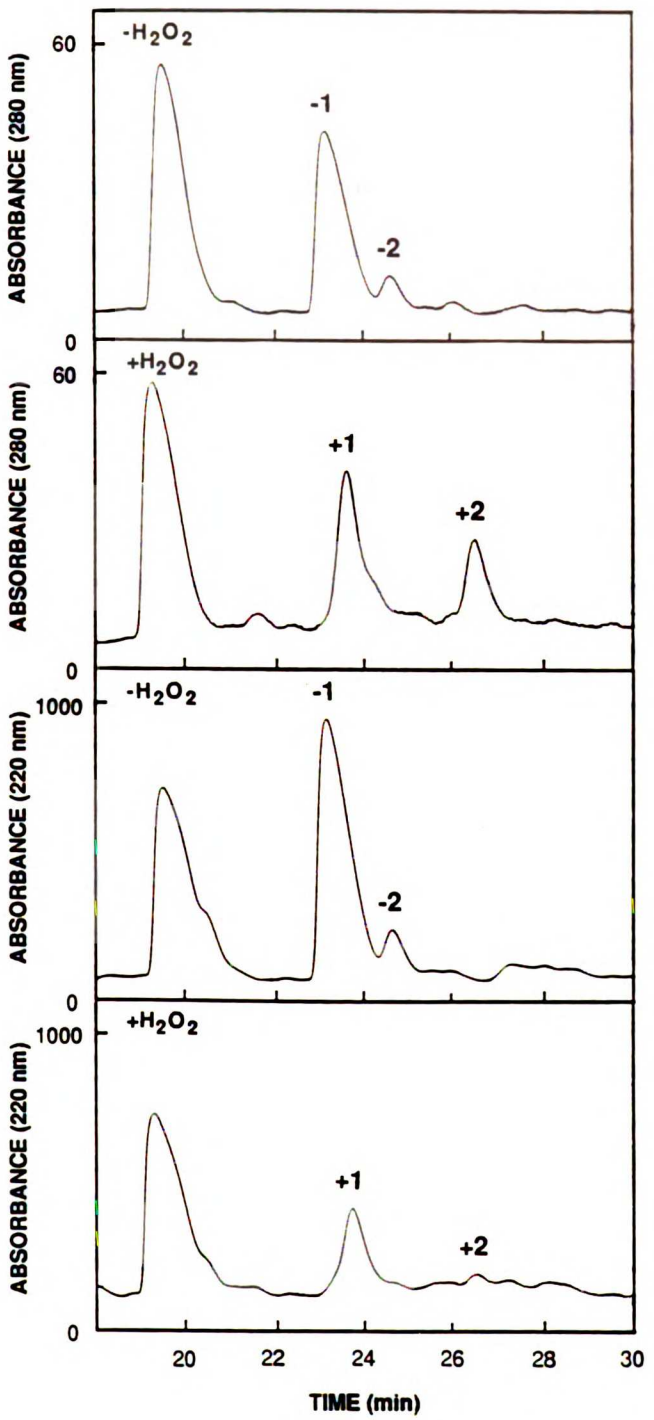

Fig. 3.8 Expanded region of HPLC peptide maps of V8 protease-treated apoproteins obtained from myoglobins incubated without H_2O_2 (-) and with H_2O_2 (+) in the presence of styrene. The top two traces were monitored at 280 nm and the bottom two traces at 220 nm. The peaks that eluted at 23.3, 24.6, 23.8 and 26.5 min are labeled as -1, -2, +1 and +2. The preparative column was eluted using a step gradient of 15-40% solvent B over 50 min, 40-70% B over 30 min and 70-100% B over 5 min.

identical, the unmodified peptide -1 must have been present in the peptide +1 because they eluted very closely on the HPLC chromatogram and the latter was not obtained in pure form. The peptide -2, which had a nominal MH^+ at 2515 and a fragment at 1451, may represent another peptide resulting from the proteolysis. The other peptide +2 had a nominal protonated molecular ion at 2214 and a fragment at 1186. The low molecular weight of the peptide +2 is not understood because this peptide was the major peak that appeared upon treatment with H_2O_2. The amino acid composition indicates that peptide -1

Table 3.2

Theoretical peptides and their masses* derived from the digestion of horse myoglobin with V8 protease

1	GLSDGE	576
2	WQQVLNVWGKVE	1485
3	ADIAGHGQE	896
4	VLIRLFTGHPE	1281
5	TLE	361
6	KFDKFKHLKTE	1420
7	AE	218
8	MKASE	564
9	DLKKHGTVVLTALGGILKKKGHHE	2579
10	AE	218
11	LKPLAQSHATKHKIPIKY(103)LE	2314
12	FISDAIIHVLHSKHPGNFGADAQGAMTKALE	3275
13	LFRNDIAAKYKE	1467
14	LGFQG	520

* Masses are reported as their nominal monoisotopic mass.

Table 3.3

Amino acid composition of peptides of interest derived from V8 protease-treated horse myoglobin

Amino Acid	Theoretical	-1	-2	+1	+2
Leu	3	3.1	3.7	2.5	2.7
Lys	4	3.9	4.0	4.0	4.0
Pro	2	2.0	1.7	1.4	2.0
Ala	2	2.0	3.0	1.7	1.8
Glu + Gln	2	2.1	3.1	2.1	2.7
Ser	1	1.0	1.1	0.7	0.9
His	2	2.0	2.0	1.7	1.5
Thr	1	1.0	1.6	1.1	1.4
Ile	2	1.9	1.8	1.4	1.2
Tyr	1	1.0	0.9	0.4	0.2
Asp + Asn	0	0.1	1.1	0.7	3.7
Phe	0	0	0	0.8	1.1
Val	0	0	0.6	0	0.2
Met	0	0	0	0	0.1

The numbers for -1 were determined when the average value of the contents of Thr, Ser and Tyr was set to 1. For the rest of the peptides, the content of Lys was set to 4.

was the parent peptide that disappeared with H_2O_2 treatment (Tables 3.2 and 3.3). The peptide -2 had a tyrosine residue but might have been contaminated with peptide -1, which was supported by the same mass unit obtained between them. The content of tyrosine greatly decreased in the two peptides, +1 and +2. However, N-terminal amino acid sequencing data showed that peptide +2 was a mixture of 3 peptides including a peptide

starting with L-K-P. The mass spectrometric and amino acid analysis data thus indicate that a peptide containing Tyr 103 is modified by treatment with H_2O_2 in the presence of styrene.

3.4 Discussion

The prosthetic heme group of horse myoglobin is only partially removed by acidic butanone after reaction of the hemoprotein with H_2O_2 at pH 4.5 or 7.4, more heme being retained by the protein after reaction at the lower pH (Fig. 3.1) (Fox et al., 1974). The residual heme group after heme extraction is bound to the protein because heme-labeled peptides are obtained by proteolytic digestion of the apoprotein of H_2O_2-treated horse myoglobin (Catalano et al., 1989). The chromophore of the apoprotein of H_2O_2-treated myoglobin and that of the heme-peptide isolated by HPLC after its tryptic digestion are similar to that of heme itself. The integrity of the heme chromophore is further supported by the Soret shift observed when cyanide is added to native myoglobin, the heme-bound apoprotein, and the heme-peptide. The spectroscopic data thus indicate that the conjugated structure of the heme group is not significantly disrupted by covalent binding to the protein. Furthermore, the mass spectrometric molecular ion of the heme-peptide is consistent with binding of the intact heme group to the apoprotein (Catalano et al., 1989).

The site of attachment of the heme group to the protein was unambiguously defined earlier as Tyr 103 but the site on the heme group covalently bound to Tyr 103 was not determined (Catalano et al., 1989). Although computer graphics analysis of horse heart myoglobin indicates that Tyr 103 resides close (5.42 Å: *ortho*-carbon of Tyr to vinyl carbon) to the 4-vinyl group (Evans & Brayer, 1988), the prosthetic group was found to bind equally well when mesoheme-reconstituted myoglobin (Fig. 3.9) was treated with H_2O_2. This result indicates that the vinyl groups are not required for covalent attachment (Fig. 3.1 and Table 3.1). This does not rule out the vinyl groups as the site of attachment in the native hemoprotein, but alternative sites must exist for covalent bond formation since

binding of the prosthetic group is not affected by the absence of the vinyl groups. It is apparent that the heme carboxyl groups are not involved in the heme-protein crosslink because an ester bond between a heme carboxyl group and Tyr 103 would be cleaved by the hydrolytic conditions employed in the amino acid analyses. It is highly unlikely that the heme group is covalently crosslinked to the protein via a heme methyl or propionic acid methylene group due to the low chemical reactivity of these sites. Substitution at the porphyrin ring positions other than the *meso* carbons is not attractive because it would

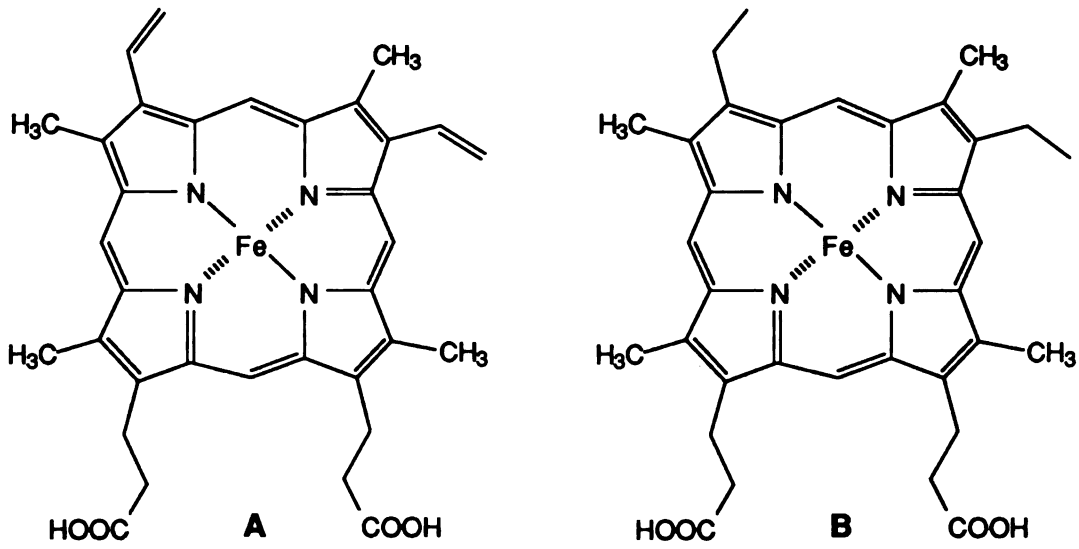

Fig. 3.9 Structures of the prosthetic groups of (A) protoheme- and (B) mesoheme-reconstituted myoglobins

disrupt the heme chromophore. It is most likely, therefore, that the protein is bound to the heme via one of the *meso* carbon atoms, although binding to a vinyl group may also occur when the vinyl groups are present. Although computer graphics analysis shows that the β-*meso* carbon resides 8.89 Å away from the *ortho*-carbon of Tyr 103 (Fig. 3.10), the tyrosine residue may move closer to the β-*meso* carbon due to a conformational change analogous to that required for formation of the trichloromethyl radical-derived heme-protein adduct (Osawa et al., 1991). *Meso* addition reactions have been demonstrated to occur

when alkyl and azide radicals are formed by the catalytic action of horseradish and *Coprinus macrorhizus* peroxidases (Ortiz de Montellano, 1987; Ator & Ortiz de Montellano, 1987; Ator et al., 1987; Depillis & Ortiz de Montellano, 1989).

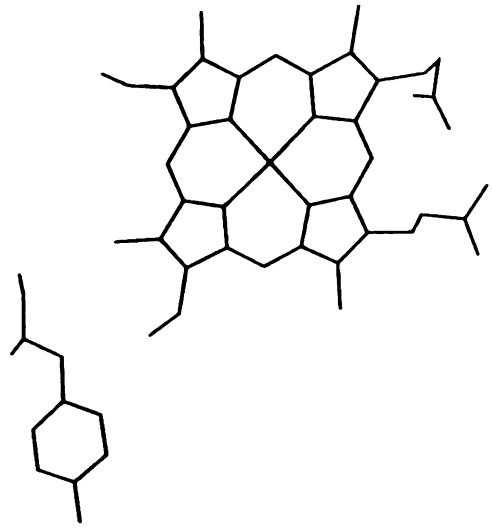

Fig. 3.10 Position of Tyr 103 relative to the prosthetic heme group in the crystal structure of horse myoglobin. The crystallographic coordinates are from a refinement to 2.8 Å resolution (Evans & Brayer, 1988).

A mechanism that is analogous to the reaction of phenyl or alkyl radical with horseradish peroxidase is proposed for covalent bond formation between Tyr 103 and the β-*meso* carbon (Scheme 3.2). Addition of the Tyr 103 radical to a Compound II-like ferryl species is highly plausible because alkyl radicals add to the δ-*meso* carbon of horseradish peroxidase Compound II with concomitant reduction of the iron from the ferryl to the ferric state. However, only 10-20% of the heme is covalently bound to the protein even though Tyr 103 resides close to the heme edge (Fig. 3.1 and Fig. 3.10). This may be explained by the absence of phenoxyl-bound heme adducts when horseradish peroxidase oxidizes phenols to phenoxyl radicals. Therefore, tyrosine radicals may not easily add to the heme edge in the case of myoglobin.

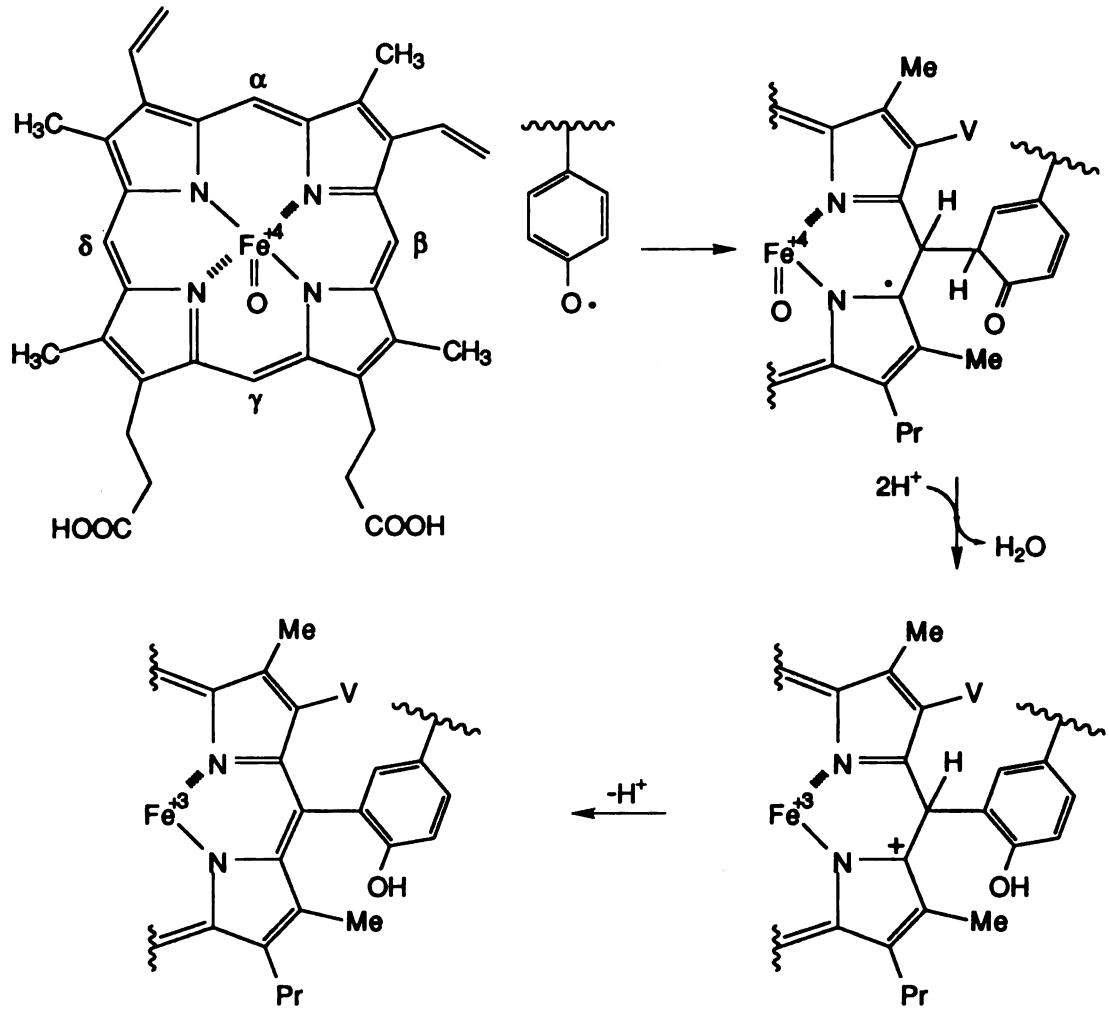

Scheme 3.2 Proposed mechanism for the covalent bond formation between Tyr 103 and the β-*meso* carbon of horse myoglobin.

If a *meso* position is involved in the heme-protein crosslink, characterization of the adduct should be possible by NMR studies. Analysis of the tryptic heme-peptide by NMR, however, has not been successful (Fig. 3.4). Mass spectrometric analysis also failed to give the molecular ion of the tryptic heme-peptide. Nor did mass spectrometric analysis of the elastase-treated heme-peptide provide information on its composition. Since the isolation of heme-peptide was time-consuming and its NMR analysis was not successful, undigested heme-bound protein was studied by NMR. The *meso* protons of the ferrous myoglobin·CO complex were well resolved in ^2H_2O at 9.88, 9.73, 9.67 and 9.18 ppm

whereas no *meso* protons were detected in the corresponding analysis of the heme-bound protein, probably due to the small amount of heme (20%) present in the sample. NMR analysis of a more concentrated sample was impossible because it was difficult to dissolve higher concentrations of the protein in ^2H_2O. It is likely that some of hydrophobic amino acid residues are exposed on the protein surface when the heme is bound to the apoprotein because the water solubility of the heme-bound protein is reduced. As an alternative, an effort was made to separate the heme-containing fraction (20%) from the apoprotein. Similar results were obtained by HPLC, FPLC or gel filtration (Biogel) column. The heme-containing fraction has high MW bands as well as a monomer band when analyzed by SDS-PAGE. However, it is not known from our data whether it is the high MW proteins or the monomeric protein that retains the heme group since they are not separated by the methods used.

The reaction of H_2O_2 with equine myoglobin produces a covalent bond between the heme group and Tyr 103 of the apoprotein, while that with sperm whale metmyoglobin results in dimerization due to formation of a bond between Tyr 103 of one monomer and Tyr 151 of the other (Catalano et al., 1989; Tew & Ortiz de Montellano, 1988). The dimerization of sperm whale myoglobin is confirmed by the reactions of recombinant sperm whale myoglobin and its Tyr146Phe mutant with H_2O_2 (Fig. 3.6). The fact that the absence of Tyr 151 prevents dimerization is consistent with the earlier results (Tew & Ortiz de Montellano, 1988).

The reaction of horse myoglobin with H_2O_2 forms a stable ferryl oxygen species and a Tyr 103 radical that rapidly decays. In the presence of styrene, the myoglobin-catalyzed epoxidation of the double bond may proceed by two different mechanisms, a ferryl oxygen transfer and a cooxidative mechanism (Ortiz de Montellano & Catalano, 1985) (Scheme 1.1). It has been proposed in the cooxidative mechanism that the Tyr 103 radical, which is relatively stable due to delocalization of the unpaired electron (Nonhebel et al., 1979), picks up molecular oxygen to form a peroxyl radical that catalyzes the epoxidation of styrene with

concomitant destruction of Tyr 103 (Scheme 3.3). The Tyr 103-containing peptide has been shown to be modified by mass spectrometry and the amino acid composition of the peptide obtained by proteolytic digestion and HPLC (Fig. 3.8 and Table 3.3). One or more peptides appear to be modified but the characterization of their structures has not been accomplished because it has not been possible to separate the modified peak from other peptides. It is likely that Tyr 103 is hydroxylated as a result of the reaction (Scheme 3.3), but the molecular weight of the new peptide is less than that of the unmodified peptide.

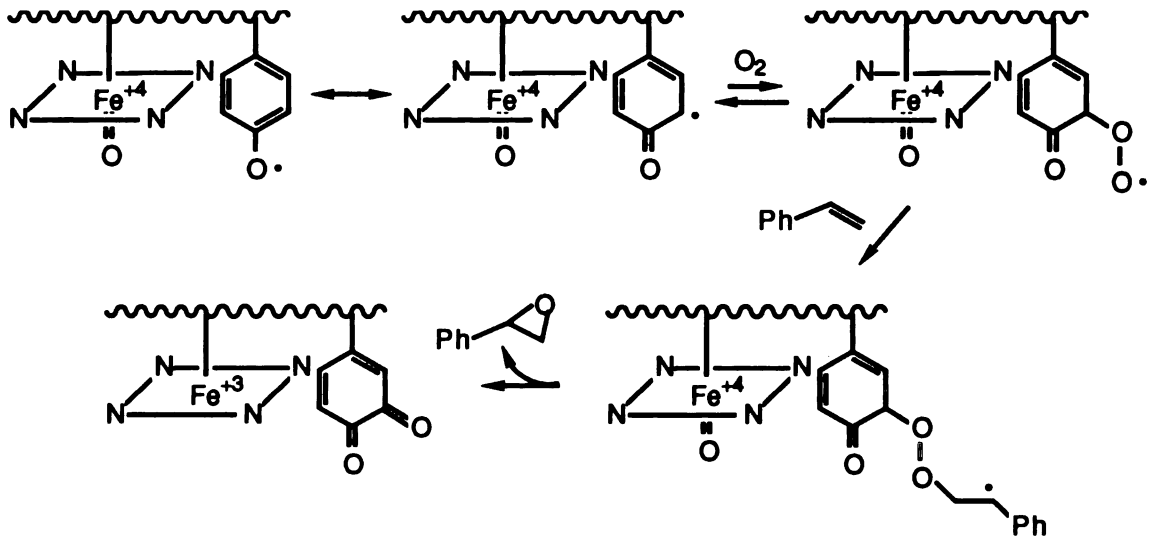

Scheme 3.3 Proposed mechanism for protein modification during the epoxidation of styrene catalyzed by myoglobin. The iron in the square of four nitrogens represents the prosthetic heme group and the wavy line the protein surface.

This can only be true if another site of the Tyr 103-containing peptide is also modified and is lost during the oxidation or the proteolytic digestion. It is unlikely that the product, styrene oxide, is involved in the protein modification because an amount of styrene oxide comparable to that produced in the reaction with H_2O_2 was added to the control reactions. The styrene is required for this protein modification, however, because the difference between the peptide maps of digests obtained from the apoproteins of H_2O_2-treated and untreated myoglobin is not observed if styrene is not present.

The protein radical generated from the reaction of horse metmyoglobin with H_2O_2 forms a covalent cross-link to the prosthetic heme group but, in the presence of the styrene, undergoes an alternative modification reaction. More work is required to identify the heme site of the covalently bound product and the structure of the modified protein.

CHAPTER 4

γ-*Meso* substitution of the heme prosthetic group of horse myoglobin by alkylhydrazines

4.0 Introduction

Hemoprotein-catalyzed oxidation of substrates frequently produces free radicals. The resulting radicals, in many cases, inactivate the hemoproteins by adding to the iron atom, pyrrole nitrogens, pyrrole carbons, vinyl groups or *meso* carbons of the prosthetic heme group (Ortiz de Montellano, 1990).

Oxidation of phenylhydrazine by oxyhemoglobin has elicited much attention because the protein is precipitated as a green hemoglobin which has a similar composition to that of Heinz bodies (Beaven & White, 1954; Itano & Matteson, 1982). Heinz bodies, which lead to hemolytic anemia, are water-insoluble precipitates that result from oxidative denaturation of hemoglobin in the erythrocyte. Phenylhydrazine is known as a very effective chemical inducer of Heinz bodies and as a cause of hemolytic anemia (Webster, 1949; Beutler, 1969; Itano et al., 1977). However, the ring substituents on phenylhydrazine affect the rate of the reaction and in turn, the severity of the anemia, with *ortho*-alkyl and halogen atoms decreasing the rate of the reaction and *meta* and *para*-substituents increasing it (Itano et al., 1977; Itano & Matteson, 1982).

Phenylhydrazine is oxidized to a phenyl radical by oxyhemoglobin, as is shown by observation of the EPR signal of the DMPO-trapped phenyl radical (Goldberg & Stern, 1977; Hill & Thornalley, 1981; Augusto et al., 1982b) (Scheme 4.1). Phenyldiazene is an intermediate in the oxidation of phenylhydrazine to the phenyl radical. Kosower's group has synthesized phenyldiazene, which is relatively stable, and proposed the formation of a phenyl radical from its one-electron oxidation (Scheme 4.1) (Huang & Kosower, 1968; Kosower, 1971). The phenylhydrazyl radical seems to precede phenyldiazene because

Smith and Maples detected it in the oxidation of phenylhydrazine by oxyhemoglobin by fast-flow EPR (Smith & Maples, 1985). The splitting pattern of the EPR signal suggests that the radical resides on the internal nitrogen. It has been shown that the reaction of phenylhydrazine with oxyhemoglobin also generates the superoxide anion, its dismutation product, H_2O_2 and nitrogen (Goldberg et al., 1979; Cohen & Hochstein, 1964; Rostorfer & Totter, 1956). Peroxide is also formed from the autooxidation of phenylhydrazine.

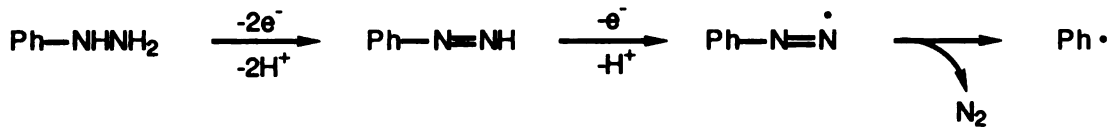

Scheme 4.1 The formation of phenyldiazene and the corresponding radical from the oxidation of phenylhydrazine by hemoproteins.

Alkyl and aryldiazene have been proposed to be formed prior to carbon radical formation. Mansuy's group isolated the iron (II)-methyldiazene complex from the oxidation of methylhydrazine by iron (III) mesotetraphenylporphyrin in the presence of limited amounts of oxygen. The reaction of iron (II) TPP and methyldiazene under anaerobic conditions yields the same complex as above. This complex has absorption maxima at 424, 528 and 560 nm in CH_2Cl_2 and unique methyldiazene peaks at -1.3 ($-CH_3$) and 7.83 ppm (-NH) in the NMR spectrum (Battioni et al., 1983). Further oxidation of this complex by oxygen or ferric chloride gives the iron (III)-methyl complex. Phenylhydrazine reacts with iron TPP in the same fashion as methylhydrazine. The iron (III)-phenyl complex is more stable than the methyl complex, but the iron (II)-phenyldiazene complex is very unstable, so its formation is only detected by its absorption at 426, 529 and 561 nm. The methyl and phenylhydrazine-treated globins yield similar intermediates to those obtained from the model porphyrin (Battioni et al., 1983). The direct reaction of methyldiazene with oxyhemoglobin yields the iron (II) methyldiazene complex with absorption maxima at 429, 528 and 555 nm (Mansuy et al., 1982). Further oxidation

of the iron (II)-methyldiazene intermediate with potassium ferricyanide or oxygen gives an iron (III)-methyl complex with absorption maxima at 437, 537 and 567 nm. Phenylhydrazine-treated hemoglobin gives the iron (III)-phenyl complex whose absorption maxima are at 430, 538 and 571 nm. Myoglobin reacts with methyl- and phenylhydrazine in the same manner as hemoglobin (Mansuy et al., 1982). The iron-phenyl complex of hemoglobin is reportedly formed *in vivo* after phenylhydrazine is administered to rats, and an iron-methyl complex of hemoglobin is detected in low yield upon *in vivo* treatment with methylhydrazine (Delaforge et al., 1986).

The formation of an iron-phenyl complex has been demonstrated in model studies with iron tetraphenylporphyrin (Ortiz de Montellano et al., 1982). The reaction of phenylmagnesium bromide with iron (TPP)Cl gives the iron-phenyl TPP with absorption maxima at 419 nm (ε = 108 $mM^{-1}cm^{-1}$ in THF) and 526 nm (ε = 10.13 $mM^{-1}cm^{-1}$). The iron-phenyl complex of TPP shows the *meta*-protons at 13.22, the *para*-proton at -25.52 and the *ortho*-protons of the phenyl ring at -80.67 ppm in the ^1H NMR spectrum. The formation of the iron-aryl complexes of hemoglobin and myoglobin has been demonstrated by ^1H NMR spectroscopy (Kunze & Ortiz de Montellano, 1983). The iron-*para*-tolyl complex obtained from *para*-tolylhydrazine-treated hemoglobin shows identical NMR chemical shifts to those of the synthetic iron-*para*-tolyl complex. The fact that addition of cyanide to the iron aryl complex of hemoglobin does not affect the NMR spectrum also provides strong evidence that the position of the sixth heme ligand is already occupied by the *para*-tolyl group.

Formation of iron-phenyl complexes of hemoproteins (Scheme 4.2) has been confirmed by the X-ray crystal structures of myoglobin (Ringe et al., 1984) and P-450_{cam} (Raag et al., 1990) after reaction with phenylhydrazine and phenyldiazene, respectively. The σ-phenyl complex of myoglobin is shown by the crystal structure to have the phenyl ring positioned in the plane perpendicular to the heme passing through the α and γ-*meso*

carbons. It is apparent from the structure that the side chains of His 64, Arg 45 and Val 68 move away to open a channel from the protein surface into the heme pocket.

Treatment of the iron-phenyl complex of TPP with acidic methanol produces N-phenyl TPP, which is identified by the high-field positions of the N-phenyl protons caused by the porphyrin ring current (Ortiz de Montellano et al., 1982). The dimethyl ester of the N-phenyl PPIX extracted from phenylhydrazine-treated hemoglobin has a Soret band at 430 nm and visible bands at 518, 550, 613 and 670 nm (Ortiz de Montellano & Kunze, 1981). The zinc complex has ^{1}H NMR peaks for the *para*-proton at 5.50, *meta*-protons at 4.95 and *ortho*-protons of the N-phenyl group at 2.02 ppm. The formation of the N-aryl adducts depends on the hydrazine used. The *meta*- and *para*-substituted phenylhydrazines form σ-aryl complexes and N-aryl adducts whereas *ortho*-substituted phenylhydrazines form much less stable σ-complexes and do not form N-aryl adducts (Ortiz de Montellano & Kerr, 1985). It is thought that the *ortho*-substituents interact sterically with the heme and prevent migration of the aryl group from the iron to the pyrrole nitrogen.

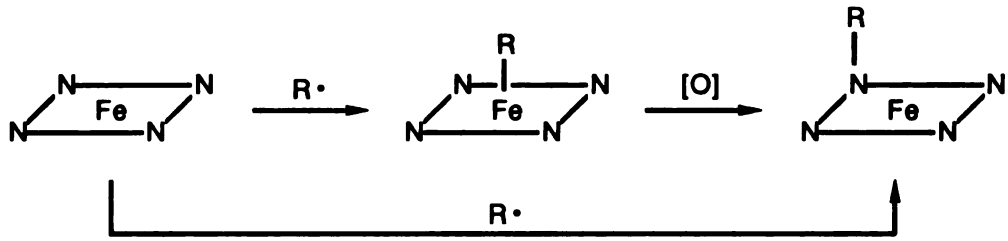

Scheme 4.2 The inactivation of hemoproteins by arylhydrazines and possibly alkylhydrazines. The iron in a square of four nitrogens indicates the heme prosthetic group and R stands for the aryl or alkyl group. In some cases the iron is removed after the migration of the aryl or alkyl group to a pyrrole nitrogen.

The absolute configurations of the N-ethyl PPIX isomers obtained from hemoglobin have been determined (Ortiz de Montellano et al., 1983a). The isomer ethylated on pyrrole ring C of the heme from hemoglobin has been assigned the R absolute configuration

because the ethyl group migrates to a pyrrole N on the same side of the porphyrin to which molecular oxygen is bound (Scheme 4.2).

The reaction stoichiometry is well established in the methemoglobin-catalyzed oxidation of phenylhydrazine. The reaction yields 5 benzenes, 6 H_2O_2 and 6 nitrogens per heme at the expense of 6 phenylhydrazines and 6 oxygens (Augusto et al., 1982b). Therefore, 1 phenylhydrazine must be associated with the inactivated heme group. It is apparent that six phenylhydrazines are required for the formation of one N-phenyl heme. However, enzyme inactivation does not necessarily depend on heme N-adduct formation because *ortho*-substituted phenylhydrazines inactivate the enzyme and form the iron-aryl complexes but do not give N-aryl heme adducts (Augusto et al., 1982b).

The reactions of the globins with alkylhydrazines are not so well defined as that with phenylhydrazine. Alkyl radicals are shown to be formed from the oxidation of alkylhydrazines by the globins (Augusto et al., 1982b). An iron-alkyl complex has not been observed in the aerobic reaction although an iron-methyl complex has been detected in the presence of limited amounts of oxygen (Augusto et al., 1982b; Battioni et al., 1983). Upon acidic extraction, heme is recovered from the methylhydrazine-treated globins whereas the iron-phenyl complex is converted to the N-phenyl PPIX isomers (Mansuy et al., 1982). However, the reaction of ethylhydrazine with hemoglobin provides N-ethyl heme adducts but in very low yield (Augusto et al., 1982b). N-Alkylprotoporphyrin IX isomers, resulting from the reactions of hemoproteins with alkylhydrazines, are known to inhibit ferrochelatase, the enzyme which catalyzes the insertion of the iron into PPIX in heme biosynthesis (Tephly et al., 1979; De Matteis et al., 1980; Ortiz de Montellano et al., 1980).

In addition to the globins and cytochrome P-450, catalase is inactivated by phenylhydrazine (Ortiz de Montellano & Kerr, 1983). A transient, protein-stabilized iron-phenyl complex is observed in which the phenyl group can be induced to migrate to a pyrrole nitrogen of the heme group. The reaction of ethylhydrazine with catalase produces

only N-ethyl PPIX isomers (Ortiz de Montellano & Kerr, 1983). Pyrrole rings C and D are preferentially alkylated in the catalase reaction.

Horseradish peroxidase is inactivated by phenylhydrazine in the presence of H_2O_2 (Ator & Ortiz de Montellano, 1987). Phenylhydrazine is first oxidized to phenyldiazene. An electron is then transferred from the diazene to Compound I to produce Compound II and the phenyldiazenyl radical. The phenyl radical produced from the diazenyl radical by elimination of nitrogen adds to the δ-*meso* carbon of Compound II to give, after electron-delocalization and deprotonation, the δ-*meso* phenyl heme adduct. A second product is formed by abstraction of a hydrogen atom by the phenyl radical from the 8-methyl group, followed by addition of water, to produce the 8-hydroxymethyl heme adduct (Ator & Ortiz de Montellano, 1987). Alkylhydrazines inactivate horseradish peroxidase in a similar manner. However, alkyl radicals only add to the δ-*meso* carbon of the prosthetic heme group but do not react with the 8-methyl group (Ator et al., 1987). An isoporphyrin intermediate with a characteristic band at 840 nm is proposed to be formed during the δ-*meso* addition reaction of the radicals. This intermediate is detected in the reactions of horseradish peroxidase with the alkylhydrazines but not with phenylhydrazine and azide (Ator et al., 1989).

The 3-oxopropyl and nitromethyl radicals generated from cyclopropanone hydrate and nitromethane by horseradish peroxidase also yield *meso*-alkylated heme adducts (Wiseman et al., 1982; Porter & Bright, 1983). The site of *meso*-alkylation is the δ-*meso* carbon in the former reaction. In addition to carbon radicals, the azidyl radical derived from azide has been shown to add to the δ-*meso* carbon of horseradish peroxidase prosthetic group (Ortiz de Montellano et al., 1988). Regiospecific addition to the δ-*meso* position is also observed in the reaction of the fungal peroxidase, *Coprinus macrorhizus* with phenylhydrazine and azide (Depillis & Ortiz de Montellano, 1989).

Recent work shows that the reaction of sperm whale myoglobin with $CBrCl_3$ under reductive conditions gives three soluble products and a heme-bound protein (Osawa et al.,

1989; Osawa et al., 1990; Osawa et al., 1991). In the latter, the proximal His 93 is covalently bound to the trichloromethyl-activated 2-vinyl group (structure D, Fig. 4.1) (Osawa et al., 1990; Osawa et al., 1991). The former products are those in which the 2-vinyl group is modified to a β-carboxyvinyl, 1,1,1-trichloromethyl-3,3,3-trichloropropyl or 1-hydroxy-3,3,3-trichloropropyl group (Fig. 4.1). Reductive debromination of $CBrCl_3$ by reduced myoglobin forms the trichloromethyl radical (Castro & Bartnicki, 1975; Bartnicki et al., 1978; Poyer et al., 1978; Kubic & Anders, 1981; Noguchi et al., 1982). The soluble products presumably arise via a common pathway leading to a cationic trichloromethyl intermediate. This intermediate is obtained by attack of the trichloromethyl radical on the 2-vinyl group followed by delocalization of an electron to the iron. The deprotonation of the cationic intermediate produces trichloromethylvinyl heme. Reductive dechlorination, electron transfer to the iron, addition of water and hydrolysis give a β-carboxyvinyl heme adduct (A). On the other hand, addition of a second trichloromethyl radical to the trichloromethylvinyl heme yields bis-trichloromethyl adduct (B). The third

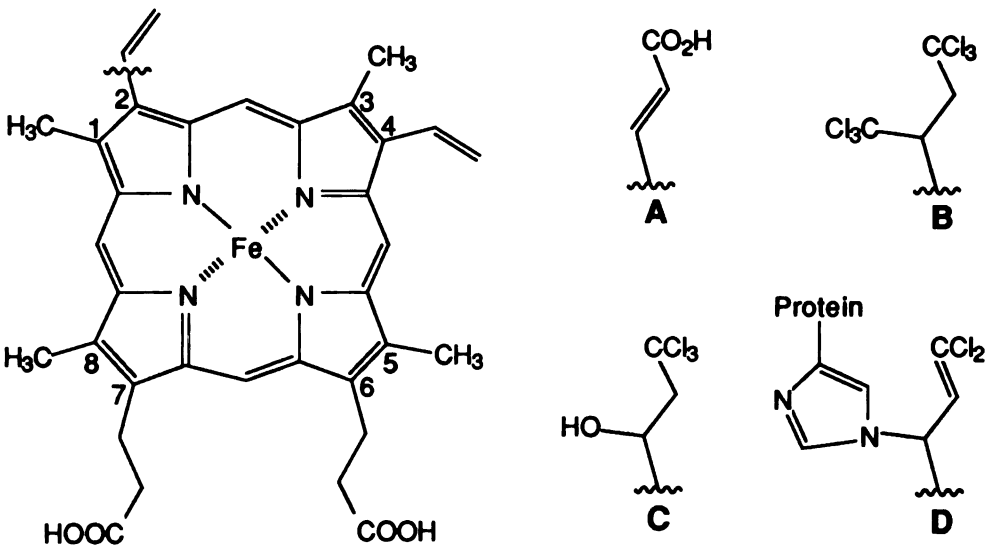

Fig. 4.1 Products obtained from the reaction of bromotrichloromethane with the prosthetic group of reduced myoglobin: (A) β-carboxyvinyl; (B) 1,1,1-trichloromethyl-3,3,3-trichloropropyl; (C) 1-hydroxy-3,3,3-trichloropropyl heme adducts; (D) heme-bound protein via His 93.

product (C) is formed by addition of water to the cationic trichloromethyl intermediate (Osawa et al., 1989). It is interesting to note that the radical does not detectably add to the iron atom or the pyrrole nitrogens, or to any other position of the heme prosthetic group.

It has been demonstrated that the 2-vinyl group is also modified when nitrite reacts with horse heart myoglobin in the presence of H_2O_2 at pH 5.5 (Bondoc & Timkovich, 1989). It is likely that the nitrite radical generated by electron transfer from nitrite to the protein adds to the heme 2-vinyl group and, following one electron transfer to the iron and loss of a proton, yields myoglobin with a nitro substitution on the vinyl group. This result is intriguing because the resulting nitrimyoglobin causes the greening effect in improperly cured meat.

The iron and nitrogen are the sites of modification in the cytochrome P-450 reactions whereas the δ-*meso* heme edge is the site modified in the horseradish peroxidase reactions. The H_2O_2-dependent reactions of alkylhydrazines with horse myoglobin was reexamined to see if the reaction occurs at the pyrrole nitrogen, the heme 2-vinyl group or some other position.

4.1 Reactions of horse metmyoglobin with alkylhydrazines

Incubation of myoglobin with methyl-, ethyl-, *n*-propyl-, *n*-butyl-, *tert*-butyl-, 2-phenylethyl-, and 2,2,2-trifluoroethylhydrazine caused time-dependent decrease of the Soret intensity at 408 nm (Fig. 4.2). However, in the reaction with methylhydrazine, the Soret band gradually shifted to 430 nm and a broad visible band appeared at around 540 nm after 5 min of incubation. At the end of a 30 min-incubation, the ratio of the Soret absorbance to that of the shoulder at 430 nm was approximately 2:1. In the case of 2-phenylethylhydrazine, the Soret band moved to 414 nm and two visible bands appeared at 544 and 580 nm. The reaction of myoglobin with 2,2,2-trifluoroethylhydrazine resulted in a shift of the Soret band to 430 nm and the appearance of new visible bands at 544 and 578 nm. When the Soret loss was plotted as a function of time, linear plots were not obtained

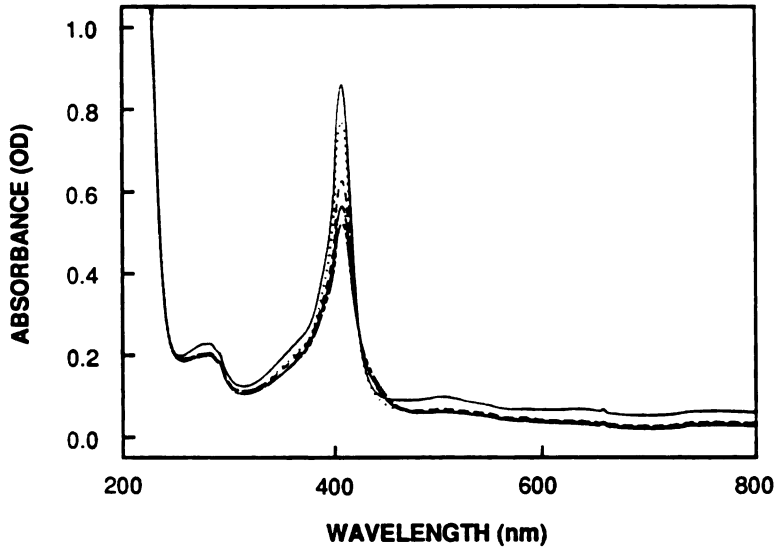

Fig. 4.2 Changes in the electronic absorption spectrum observed during the reaction of myoglobin with *n*-butylhydrazine. The intensity of the Soret band decreased as the reaction progressed. The spectra were taken 0, 2,10, 20 and 30 min after *n*-butylhydrazine was added.

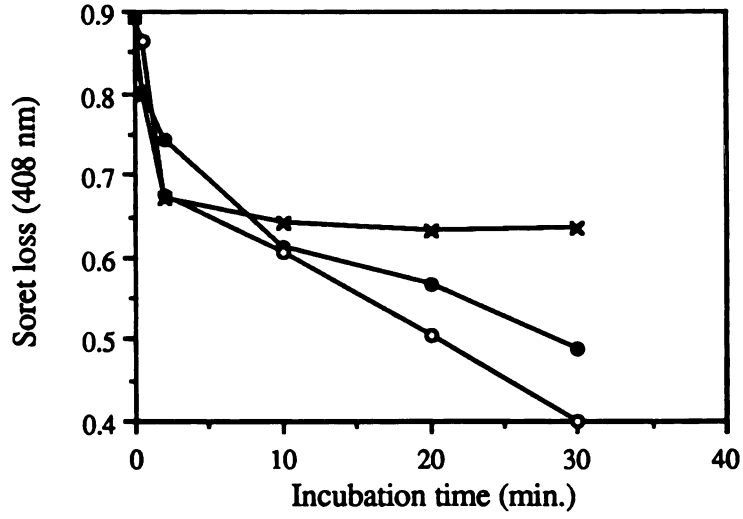

Fig. 4.3 Soret loss observed during the incubations of myoglobin with linear alkylhydrazines: ethyl (x), *n*-propyl (o) and *n*-butylhydrazine (•). Soret loss from the incubation with methylhydrazine is not included in the plot because the Soret band shifted to 430 nm during the incubation.

due to the complexity of the reaction process (Fig. 4.3). After the heme prosthetic group was extracted from reaction mixtures of myoglobin and alkylhydrazines, it was analyzed by reverse phase HPLC. The heme group was converted into less polar products by methyl-, ethyl-, *n*-propyl-, and *n*-butylhydrazine (Fig. 4.4). The HPLC retention times of these products increased in proportion to the chain length of the linear alkylhydrazine used (Fig. 4.5). The extent of conversion of the heme into products was highest for *n*-propylhydrazine and lowest for methylhydrazine. Prolonged incubation up to 1 hour produced higher yield of adducts but the heme group was also degraded in the reaction with *n*-propylhydrazine. The less polar products obtained from the reaction of myoglobin with linear alkylhydrazines exhibited Soret maxima at 405 nm (Fig. 4.6). However, analogous products were not detected in the reactions of myoglobin with 2-phenylethyl-, *tert*-butyl-, and 2,2,2-trifluoroethylhydrazine. Minor, more polar products were obtained with absorption in the 400 nm region with the latter two hydrazines. Traces of much less polar

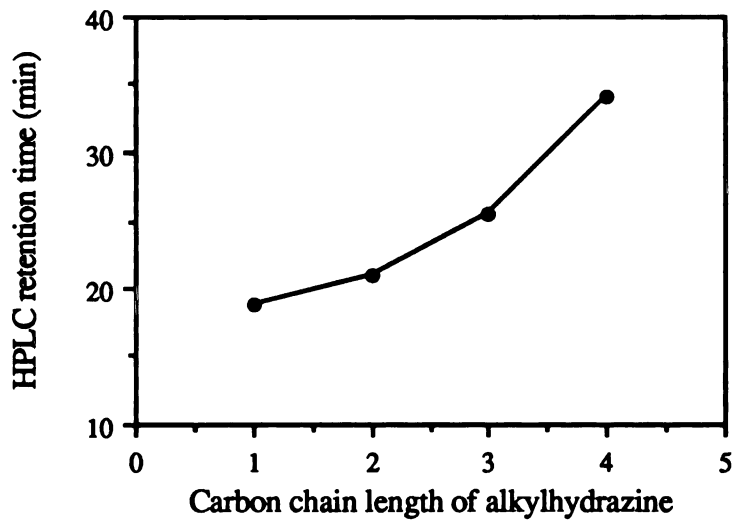

Fig. 4.5 Plot of the HPLC retention times of the alkyl heme adducts vs. the carbon chain length of the alkylhydrazine used to generate them. The alkylhydrazines are methyl (1), ethyl (2), *n*-propyl (3) and *n*-butylhydrazine (4), and the corresponding heme adducts are eluted at 16.73, 20.98, 25.46 and 34.17 min.

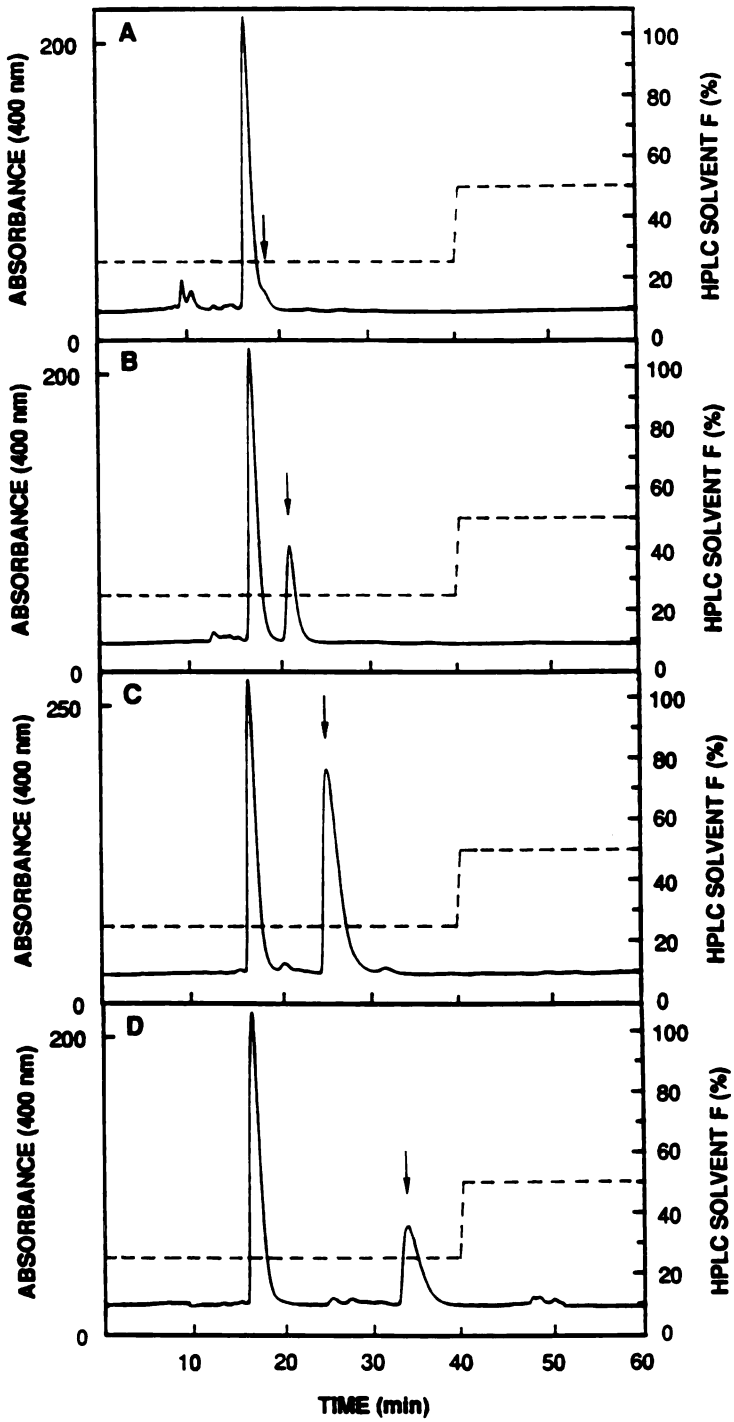

Fig. 4.4 HPLC chromatograms of the prosthetic groups extracted from myoglobin reacted with (A) methylhydrazine, (B) ethylhydrazine, (C) *n*-propylhydrazine and (D) *n*-butylhydrazine. Heme is eluted at 16.7 min and the modified hemes are indicated by arrows. N-Alkyl PPIX isomers appear with retention times around 50 min. The dashed line indicates HPLC solvent F (%). Solvent E contains 5:5:1 methanol:water:glacial acetic acid and solvent F contains 10:1 methanol:acetic acid.

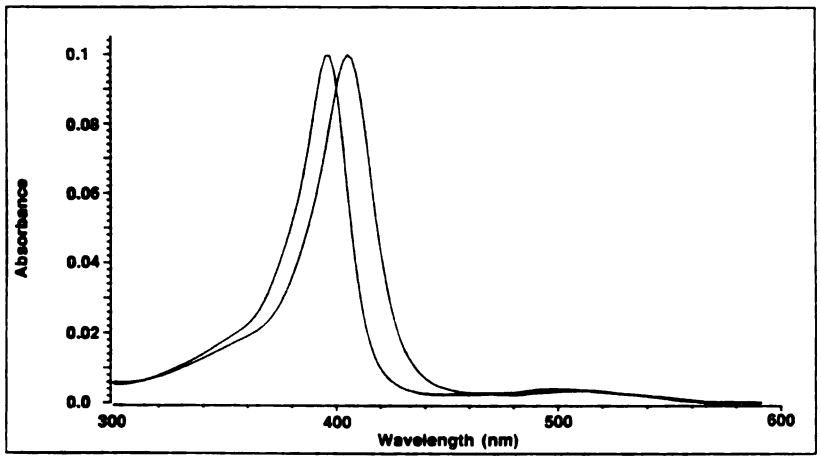

Fig. 4.6 Electronic absorption spectra of heme (left trace) and the *n*-butyl heme adduct (right trace). The spectra were taken in the HPLC solvent mixture (25% solvent F and 75% solvent E).

products that have similar retention times as the authentic N-methylprotoporphyrin IX isomers were also observed in the reactions with *n*-propyl and *n*-butylhydrazine.

When 0.04 M catalase was added to the incubation of myoglobin with *n*-butylhydrazine, it did not inhibit the reaction. With addition of 2 M catalase, the rate of Soret loss decreased and about a third as much adduct was obtained as in a standard incubation without catalase. Addition of 4 M catalase severely attenuated Soret loss and fully suppressed heme adduct formation (Fig. 4.7). This result paralleled that obtained from the reaction of myoglobin with ethylhydrazine.

Incubation of myoglobin with ethylhydrazine under anaerobic conditions completely prevented Soret loss and heme adduct formation unless 1 or 2 equivalents of exogenous H_2O_2 were added (Fig. 4.8). Addition of one equivalent of H_2O_2 to the metmyoglobin generated a Compound II-like spectrum in which the Soret band shifted from 408 to 418 nm and visible bands appeared at 550 and 578 nm. As ethylhydrazine was added, this spectrum immediately reverted to that obtained when exogenous H_2O_2 was not added (Fig. 4.2). The Soret band decreased as a function of time without changing its position.

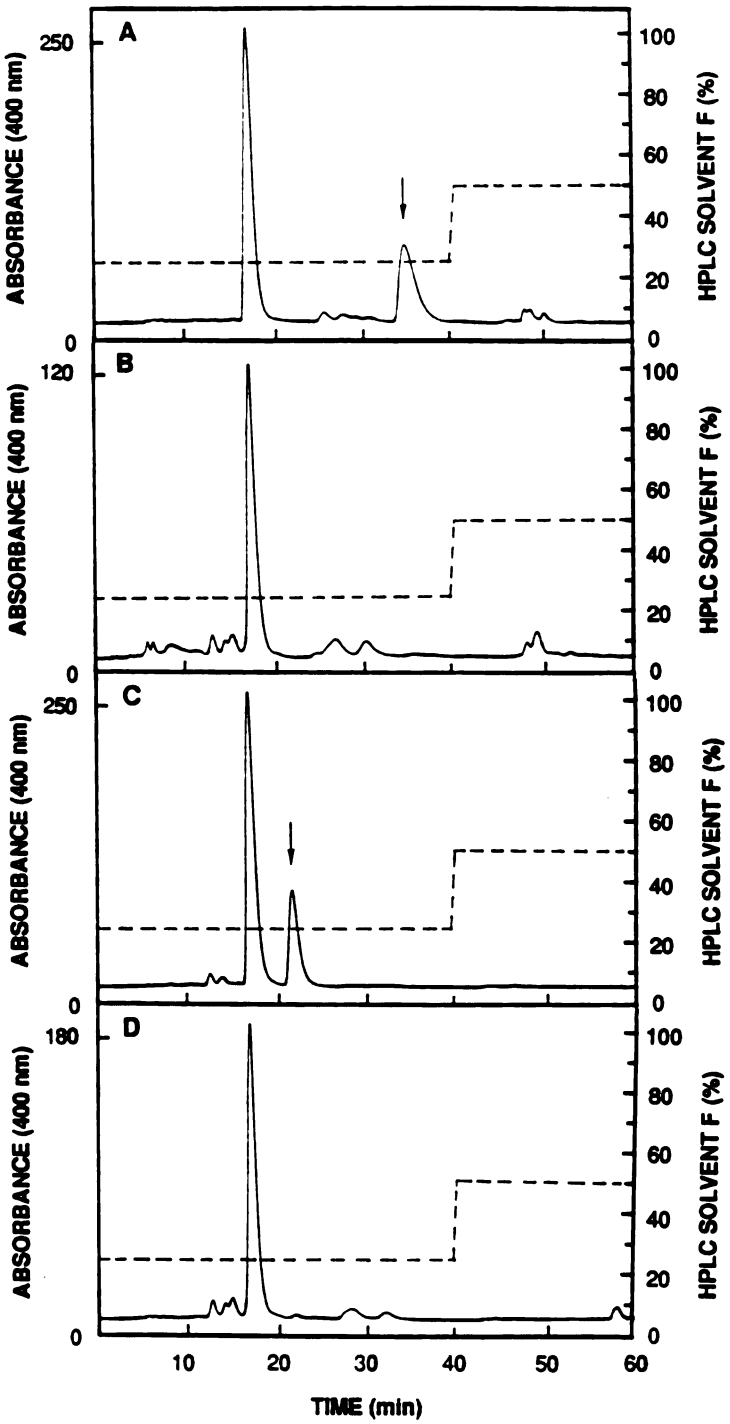

Fig. 4.7 HPLC chromatograms of the prosthetic groups isolated from the reactions of myoglobin with (A) *n*-butylhydrazine, (B)*n*-butylhydrazine + catalase, (C) ethylhydrazine, and (D) ethylhydrazine + catalase. Heme appears at 16.57 min and the modified hemes are indicated by arrows. The dashed line indicates HPLC solvent F(%). Solvents E and F are described in the legend to Fig. 4.4.

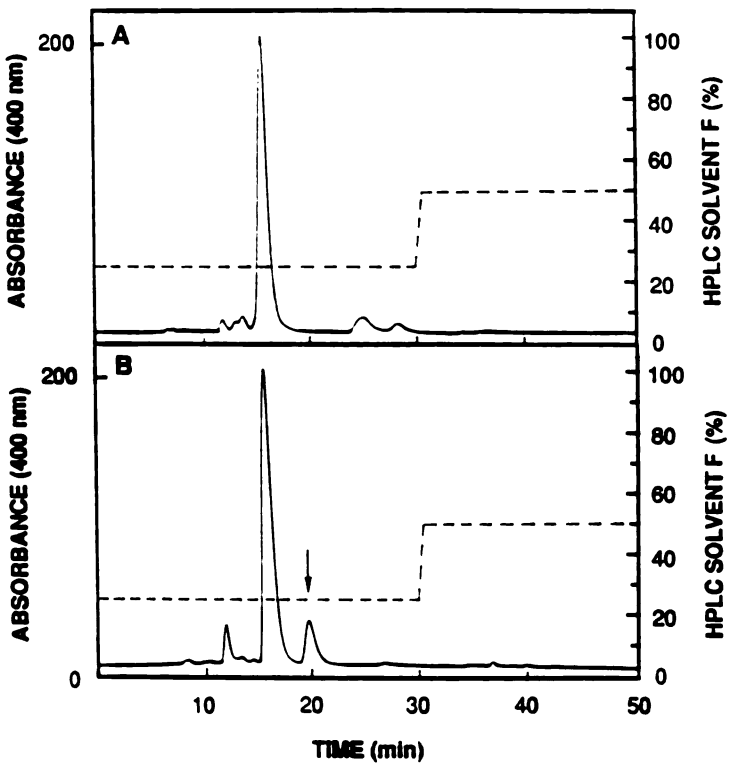

Fig. 4.8 HPLC chromatograms of the prosthetic groups extracted from myoglobin incubated with (A) ethylhydrazine and (B) H_2O_2 + ethylhydrazine under anaerobic conditions. Heme is eluted at 15.3 min and the ethylheme adduct at 19.2 min. The dashed line indicates HPLC solvent F (%). Solvent E is 5:5:1 methanol:water:glacial acetic acid and solvent F is 10:1 methanol:acetic acid.

Isoporphyrin formation was not observed in the reaction of alkylhydrazines with myoglobin. Myoglobin has a visible band at 835 nm that gradually shifted to 885 nm as reaction progressed (Fig. 4.9). However, a new band at 840 nm characteristic of an isoporphyrin intermediate was not detected.

The formation of heme-bound protein, which probably formed from the reaction of myoglobin with H_2O_2 generated *in situ*, was negligible (<2%). To measure this accurately, the reaction mixture was extracted with acidic 2-butanone to avoid the precipitate between the organic and aqueous layers formed if the extraction was done with acidic ether.

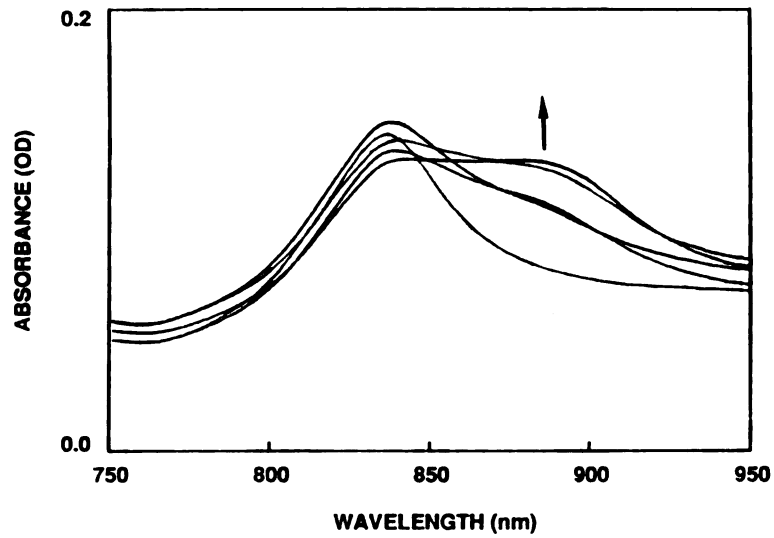

Fig. 4.9 Changes in the electronic absorption spectrum (750-950 nm) obtained 0, 0.5, 2, 10 and 30 min after *n*-butylhydrazine is added to myoglobin. Native myoglobin has a band at 835 nm.

4.2 Quantitation of *n*-butyl adduct formation

Unreacted heme and the *n*-butyl heme adduct were quantitated relative to mesoheme added as an internal standard. There was a possible disadvantage of this method in that mesoheme was more soluble in the HPLC solvent than heme or the *n*-butyl heme adduct. However, the extraction of heme by acidic 2-butanone followed by HPLC analysis suggested that there were no major products other than heme and the *meso* heme adduct. Thus, on the assumption that the extinction coefficients of both the heme adduct and mesoheme are the same as that of heme, it can be estimated that most of the heme lost was converted into the adduct.

4.3 EPR studies

The incubation of myoglobin with ethylhydrazine and POBN at room temperature resulted in the rapid appearance of a triplet of doublets in the EPR with $^{\alpha}N$ = 15.85 G and $^{\alpha}H$ = 2.75 G (Fig. 4.10). These signals were essentially identical to those of the spin

trapped ethyl radical in the same medium ($^{\alpha}N$ = 15.78 G and $^{\alpha}H$ = 2.73 G) (Augusto et al., 1982a). The signal was not observed if myoglobin or ethylhydrazine was omitted from the incubation (C and D, Fig. 4.10). Addition of 4 M catalase prevented appearance of the signal during the first 4 min, the time period in which the EPR spectra were usually measured. A small signal, however, was detectable after 4 min. Addition of 1 equivalent of H_2O_2 did not greatly increase the intensity of the signal but did increase it after prolonged incubation.

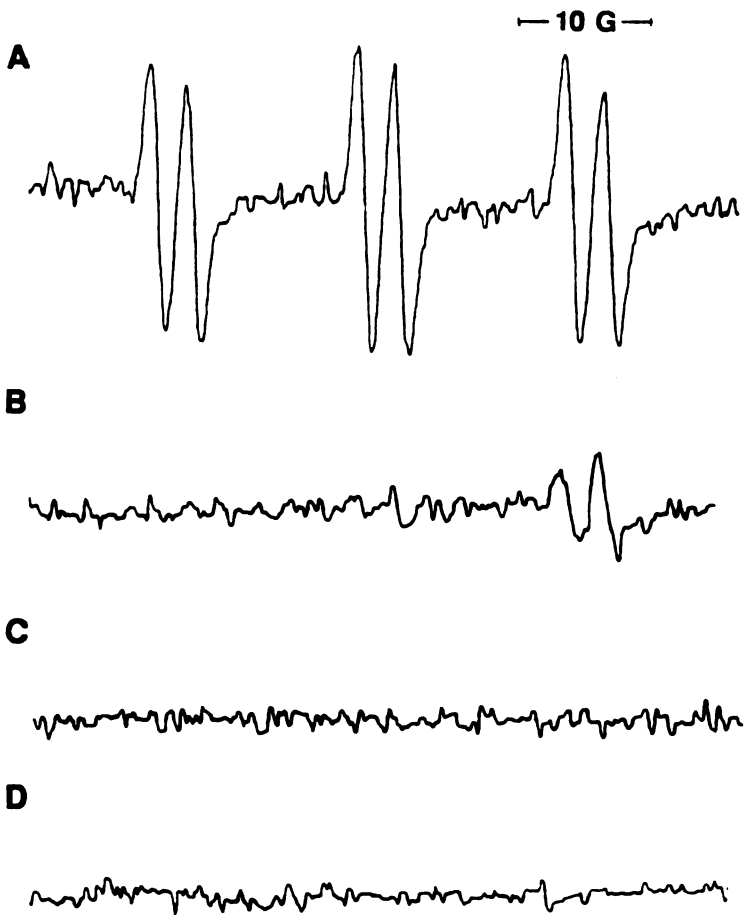

Fig. 4.10 EPR spectra obtained from the reaction of (A) myoglobin with ethylhydrazine at room temperature; (B), catalase + (A); (C), (A) - myoglobin; (D), (A) - ethylhydrazine. EPR spectrum obtained from the reaction of (A) + H_2O_2 is not shown because it is similar to that of (A). POBN was used as a radical spin trap. EPR conditions are described in the Experimental Chapter.

4.4 Characterization of the *n*-butyl heme adduct

The *n*-butyl heme adduct purified by reverse phase HPLC was esterified with acidic methanol to improve its solubility properties and facilitate its characterization by mass spectrometry. The iron was removed to improve the spectroscopic analysis. The demetallation was performed under argon gas to prevent reoxidation of the reduced heme adduct generated by treatment of the ferric porphyrin with ferrous sulfate. Since the reduced iron [Fe(II)] was less tightly held by the four nitrogens of the porphyrin ring, it was easily replaced by two protons. The resulting esterified, demetallated porphyrin had absorption maxima in $CHCl_3$ (relative molar absorbance) at 416 (100), 514 (13.9), 550 (9.9), 588 (9.3) and 642 nm (7.3) (Fig. 4.11). Its mass spectrum exhibited a protonated molecular ion at m/z 647 (Fig. 4.12) that corresponds to a structure composed of dimethyl protoporphyrin IX (590) and a butyl group (57). Zinc was added to the esterified demetallated porphyrin to prevent possible sample heterogeneity due to partial metallation

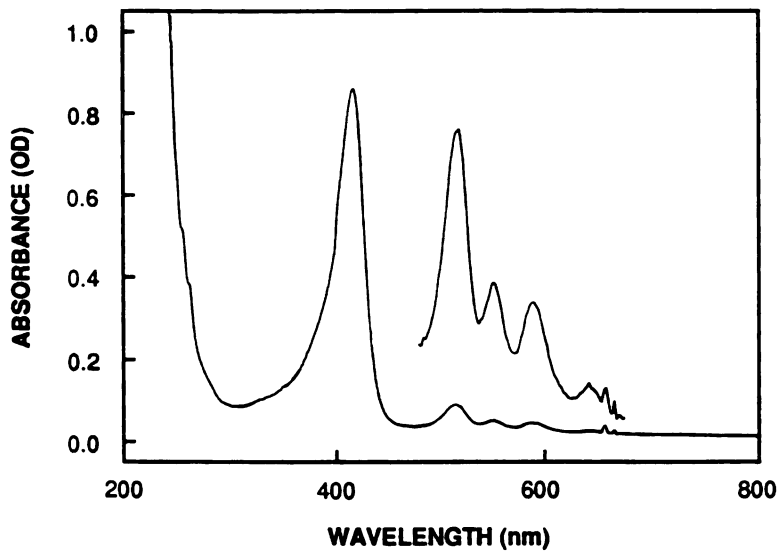

Fig. 4.11 Electronic absorption spectrum of the dimethyl ester of *n*-butyl PPIX in $CHCl_3$.

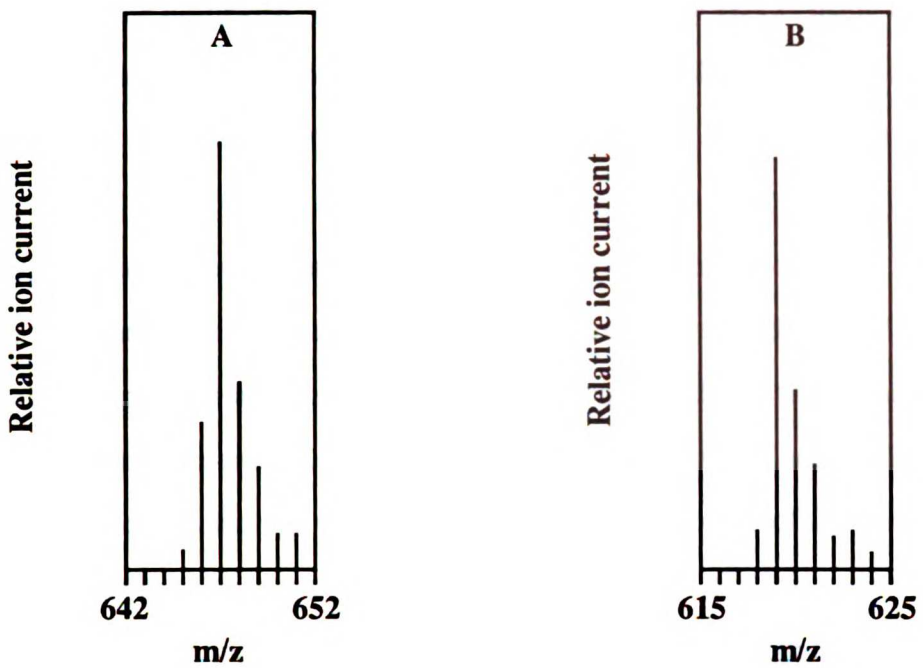

Fig. 4.12 Mass spectra of the dimethyl esters of (A) γ-*meso*-*n*-butyl PPIX and (B) γ-*meso*-ethyl PPIX.

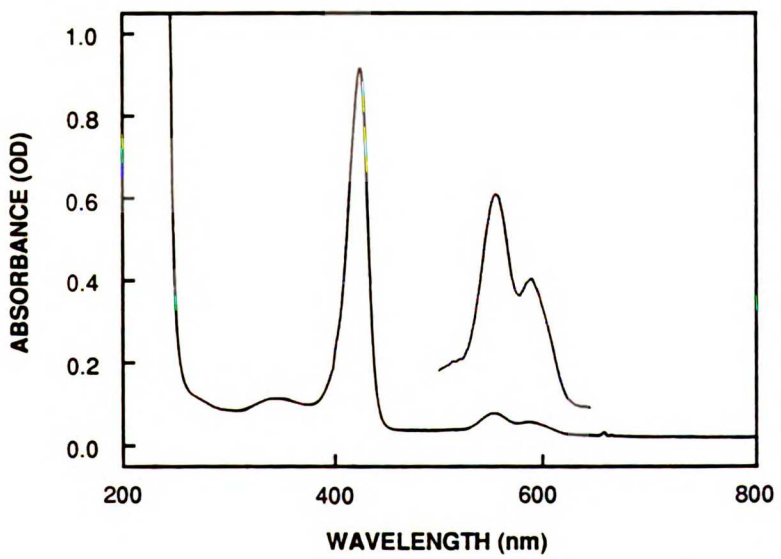

Fig. 4.13 Electronic absorption spectrum of the dimethyl ester of zinc γ-*meso*-*n*-butyl PPIX in $CHCl_3$.

or protonation of the porphyrin. The zinc complex purified by HPLC using a non-acidic HPLC solvent to avoid elimination of the zinc from the porphyrin exhibited absorption maxima in $CHCl_3$ (relative absorbance) at 422 (100), 552 (10.5), and 586 nm (8.2) (Fig. 4.13).

The site of attachment of the butyl group to the porphyrin was obtained by ^1H NMR analysis of the zinc complex. Relatively dilute solutions were used for NMR studies to avoid stacking interactions between the porphyrins which caused substantial variation in the chemical shifts of the *meso*, methyl and vinyl protons. The NMR spectrum unambiguously showed that the *n*-butyl group was attached to one of the *meso* positions because there were only three *meso* proton signals (Fig. 4.14). NMR signals were present for all the protons of the two vinyl groups, six methyl groups (two from the esterified

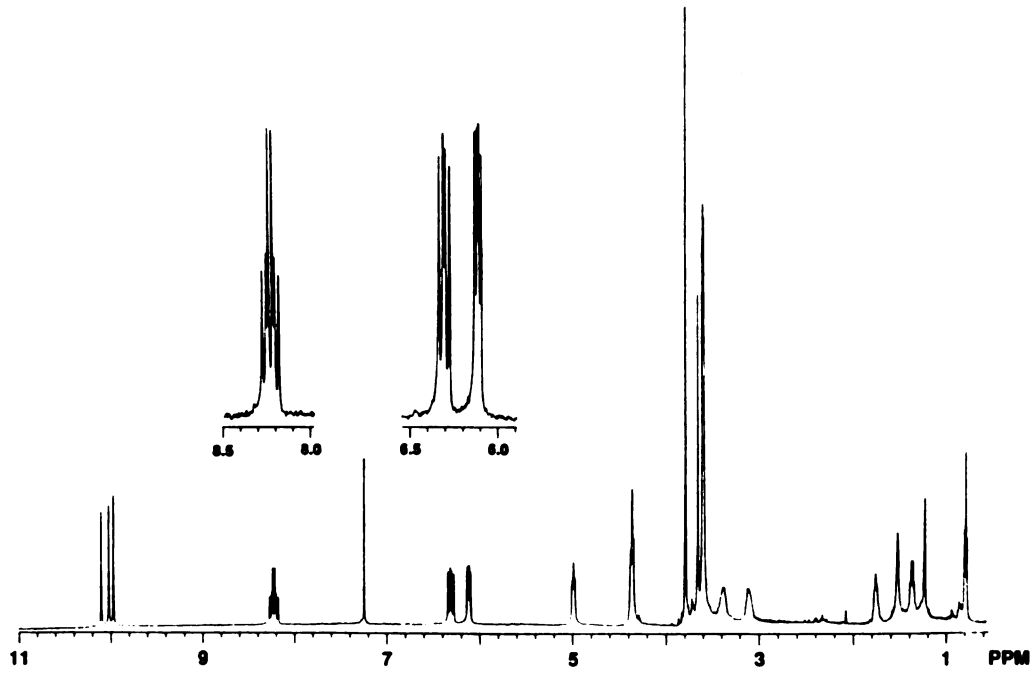

Fig. 4.14 ^1H NMR spectrum in C^2HCl_3 of dimethyl ester of zinc γ-*meso n*-butyl PPIX. Heme vinyl region is expanded and shown in the inset. The peak at 7.240 ppm is due to $CHCl_3$, that at 1.528 ppm to water, and at 1.229 ppm to an unidentified impurity.

carboxyls) and propionic acid methylene groups. This was confirmed by integrating all the protons. The *n*-butyl group was assigned by decoupling experiments. When the 1'-methylene (internal) protons of the butyl group were decoupled, the 2'-methylene protons collapsed to a triplet. In the case of decoupling of the 2'-methylene group, the 1'-methylene protons collapsed from a triplet to a singlet and the 3'-methylene protons to a quartet. When the 3'-methylene protons were decoupled, the 2'-methylene protons appeared as a triplet and the 4'-methyl protons as a singlet. This assignment of the *n*-butyl methylene (4.985, 1.749 and 1.381 ppm) and methyl (0.786 ppm) protons was further confirmed by one and two-dimensional NOE experiments which were carried out to assign the proton signals and to determine which of the four *meso* positions bears the *n*-butyl group (Table 4.1). These experiments established that the γ-*meso* proton was replaced by the *n*-butyl group. This was shown by the demonstration that irradiating the *n*-butyl internal methylene protons at 4.985 ppm enhanced the internal propionic acid proton peak at 4.357 ppm but not those of any of the methyl groups (Fig. 4.15). This result was also confirmed by NOESY experiments (Fig. 4.17). When the *n*-butyl internal methylene protons were irradiated, the enhancement of the external propionic acid proton signal was not significant in dilute samples (0.3-0.4 mg/350 μl C^2HCl_3) but was drastic in concentrated samples due to the stacking interactions. The assignment of the external propionic acid proton signals was also accomplished by a decoupling experiment. Decoupling of the internal propionic methylene protons at 4.357 ppm resulted in collapse of the external propionic acid proton signals from two sets of multiplets at 3.391 and 3.119 ppm to two doublets. The α-, β-, and δ-*meso* protons were identified by NOE with the neighboring methyl groups. The irradiation of the α-*meso* proton enhanced the intensity of the 3-methyl and the 2-internal vinyl groups and the irradiation of β-*meso* proton enhanced the 5-methyl and the 4-internal vinyl groups (Fig. 4.16). The intensity of the 1- and 8-methyl signals was enhanced when the δ-*meso* proton was irradiated (Fig. 4.15). The NOE experiments showed that the γ-*meso* position was the only one for which no proton

was detected. The isolated porphyrin is thus the dimethyl ester of γ-*meso*-(*n*-butyl)protoporphyrin IX.

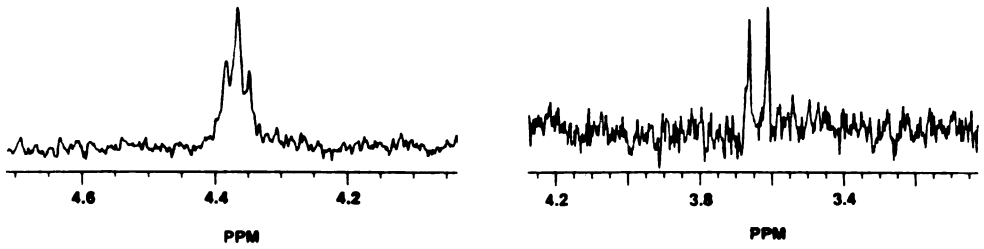

Fig. 4.15 Left trace: one dimensional NOE spectrum of the internal propionic acid proton at 4.357 ppm enhanced as the *n*-butyl internal methylene protons at 4.985 ppm of the γ-*meso* *n*-butyl adduct are irradiated. Right trace: NOE spectrum of the 1- and 8-methyl protons enhanced when the δ-*meso* proton at 10.024 ppm is irradiated.

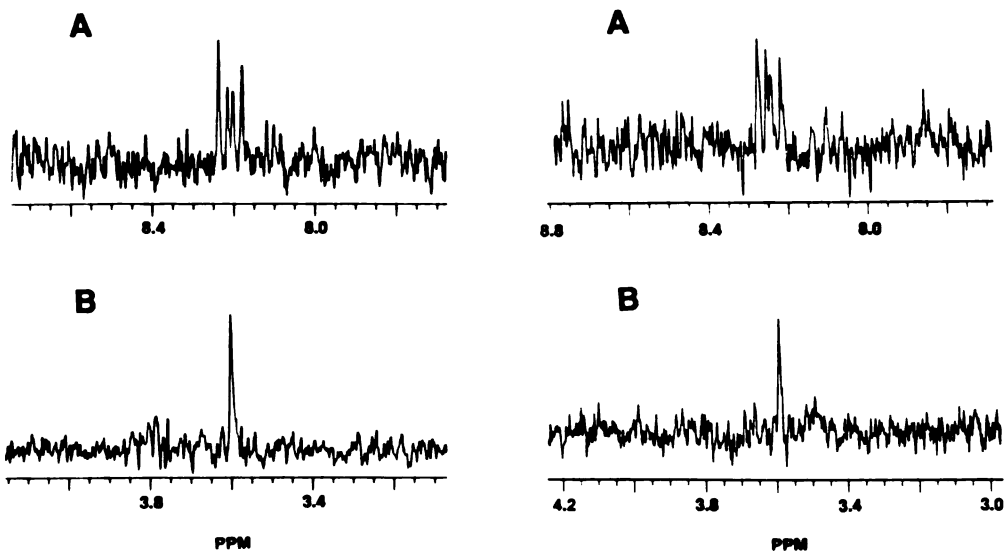

Fig. 4.16 Left trace: NOE enhancement of the 2-internal vinyl proton (A) and the 3-methyl protons (B) caused by the irradiation of the α-*meso* proton at 9.973 ppm. Right trace: NOE enhancement of the 4-internal vinyl proton (A) and the 5-methyl protons (B) caused by the irradiation of the β-*meso* proton.

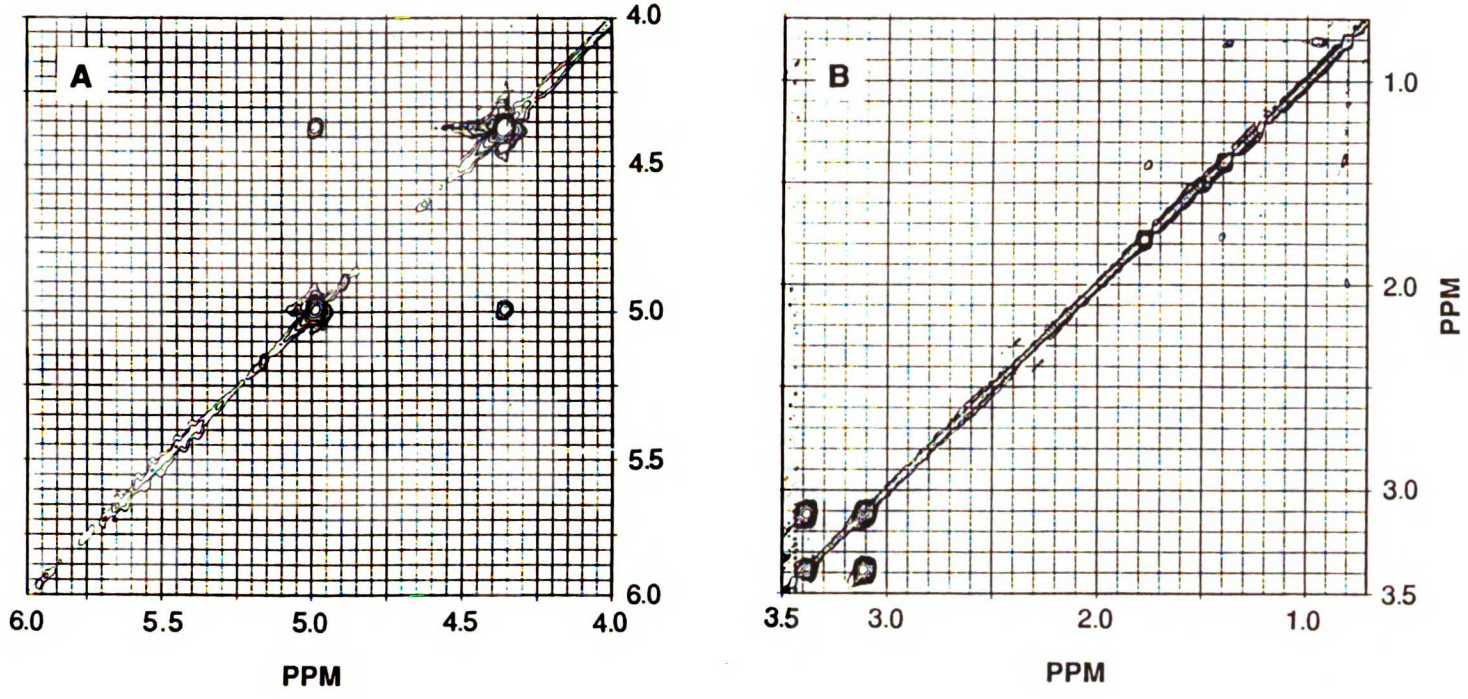

Fig. 4.17 Two dimensional NOE spectrum of the γ-*meso* *n*-butyl adduct. Regions from (A) 4.0 to 6.0 ppm and (B) 0.7 to 3.5 ppm are shown. Cross peaks are shown (A) between the internal propionic acid methylene protons at 4.357 ppm and the *n*-butyl internal methylene protons at 4.985 ppm and (B)between the external propionic acid protons at 3.391 and 3.119 ppm; between the 2'- and 3'-butyl methylene protons (1.749 and 1.381 ppm). The conditions for NOESY experiments are described in the Experimental Chapter.

Table 4.1

^{1}H NMR spectral assignments for the γ-*meso*-*n*-butyl adduct

proton	chemical shift (ppm)	NOE[a]
meso		
α	9.973	3-Me, 2-CH=CH_2
β	10.106	5-Me, 4-CH=CH_2
γ	-	-
δ	10.024	1-Me, 8-Me
-CH=CH_2		
4	8.230	
2	8.210	
-CH=CH_2		
trans 4	6.318 (J = 17.67 Hz)	
trans 2	6.294 (J = 17.67 Hz)	
cis 4	6.120 (J = 11.23 Hz)	
cis 2	6.107 (J = 11.23 Hz)	
-$CH_2CH_2CO_2Me$	4.357	1'-CH_2, 2'-CH_2, 3'-CH_2, 5-Me, 8-Me, -$CH_2CH_2CO_2Me$
-$CH_2CH_2CO_2Me$	3.391	
	3.119	
methyls		
1	3.659	
3	3.602	
5	3.592	
8	3.610	
ester	3.791	
ester	3.791	
γ-*meso*-butyl		
1'-CH_2	4.985	-$CH_2CH_2CO_2Me$, 2'-CH_2, 3'-CH_2, 4'-CH_3
2'-CH_2	1.749	
3'-CH_2	1.381	
4'-CH_3	0.786	

[a]Positions exhibiting NOE when the proton in the far left column is irradiated.

4.5 Characterization of the ethyl heme adduct

The demetallated, dimethyl esterified porphyrin from the reaction of myoglobin with ethylhydrazine exhibited absorption bands in $CHCl_3$ (relative absorbance) at 414 (100), 512 (14.4), 548 (10.1), 584 (9.4), and 640 nm (6.5). The mass spectrum of the porphyrin showed a monoprotonated molecular ion at m/z 619 which is in accord with addition of an ethyl group (29) to the esterified porphyrin (590) (Fig. 4.12). Its zinc complex had absorption maxima at 420 (100), 550 (12.9), and 580 nm (10.3). The spectra of the porphyrin and its zinc complex were very similar to those of γ-*meso*-(*n*-butyl)protoporphyrin IX. ^1H NMR studies showed that the isolated porphyrin was the dimethyl ester of γ-*meso*-ethylprotoporphyrin IX because there were only three *meso* protons whereas the vinyl and other groups remained intact (Fig. 4.18 and Table 4.2).

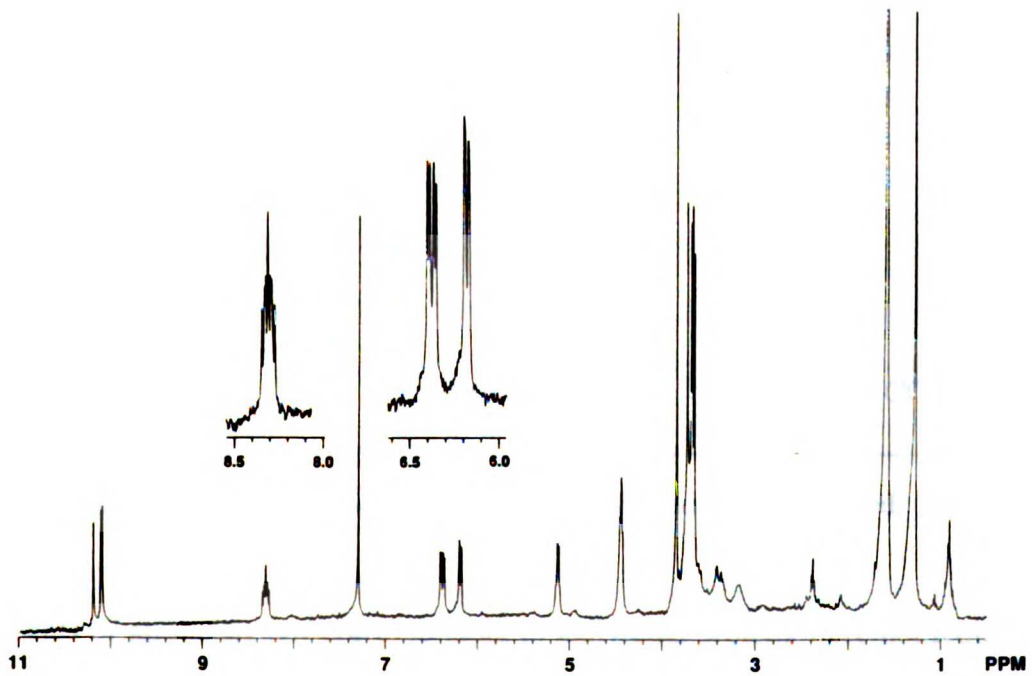

Fig. 4.18 ^1H NMR spectrum in C^2HCl_3 of the dimethyl ester of zinc γ-*meso* ethyl PPIX. Heme vinyl region is expanded and shown in the inset. The peak at 7.240 ppm is due to $CHCl_3$, that at 1.528 ppm to water, and that at 1.229 ppm to an unidentified impurity.

Table 4.2

^{1}H NMR spectral assignments for the γ-*meso*-ethyl adduct

proton	chemical shift (ppm)	NOE[a]
meso		
	10.135	
	10.056	
	10.038	
-CH=CH_2	8.273	
	8.238	
-CH=CH_2		
trans	6.331 (J = 17.69 Hz)	
trans	6.317 (J = 17.69 Hz)	
cis	6.131 (J = 11.40 Hz)	
cis	6.125 (J = 11.40 Hz)	
-$CH_2CH_2CO_2Me$	4.385	
-$CH_2CH_2CO_2Me$	3.352	
	3.112	
methyls		
	3.680	
	3.637	
	3.622	
	3.603	
ester	3.792	
ester	3.792	
γ-*meso*-ethyl		
1'-CH_2	5.068	-$CH_2CH_2CO_2Me$
2'-CH_3	0.856	

[a]Positions exhibiting NOE when the proton in the far left column is irradiated.

Assignments of all the signals corresponding to individual protons were not required to determine the site of attachment of the ethyl group because the irradiation of ethyl methylene protons at 5.068 ppm caused NOE enhancement of the internal propionic acid protons at 4.385 ppm but not those of any of the methyl protons (Fig. 4.19). The γ-*meso* proton is thus replaced by the ethyl group.

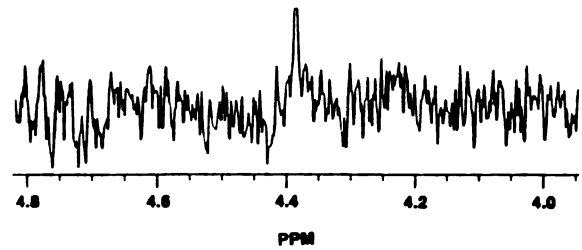

Fig. 4.19 NOE spectrum of the internal propionic acid protons at 4.385 ppm enhanced when the ethyl internal methylene protons at 5.068 ppm of the γ-*meso* ethyl adduct are irradiated.

4.6 Comments on NMR NOE and NOESY experiments

The structural identification of the γ-*meso*-ethyl- and γ-*meso*-butyl-heme adducts was accomplished by one and two-dimensional NOE (NOE and NOESY, respectively) experiments (Derome, 1987). The NOE depends on the dipolar coupling, which involves the direct magnetic coupling between nuclei through the space. The NOE is a change in intensity of one resonance when the transitions of another resonance are perturbed. The perturbation is obtained by saturating the latter resonance. The intensity inversely depends on the distance between the two groups and its change is determined by subtracting the unperturbed from the perturbed system. The saturated signal appears inverted in the difference spectrum. NOESY is a technique that detects the chemical exchange of one nucleus with another. Further NOE show the cross peaks between the exchanging sites.

4.7 Reaction of human hemoglobin with ethylhydrazine

Incubation of human hemoglobin with ethylhydrazine caused a slight biphasic, time dependent decrease in the intensity of the Soret band. Extraction and HPLC analysis of the prosthetic heme group, however, yielded no detectable trace of *meso*-ethylheme or any other identifiable heme adduct.

4.8 Discussion

The reactions of equine metmyoglobin with small, linear alkylhydrazines yield the γ-*meso*-alkyl substituted myoglobins. The Soret absorbance at 408 nm gradually decreases as a function of time during the incubation but its position remains unchanged despite the 7 nm-red shift of the heme chromophore caused by γ-*meso* alkyl substitution (Fig. 4.2). This may be explained by the fact that unreacted heme is the major product obtained after heme extraction and analysis by HPLC, so the Soret absorbance changes during the incubation may be masked. The formation of heme adducts has been demonstrated by HPLC analysis of the prosthetic group after reaction of myoglobin with methyl-, ethyl-, *n*-propyl-, and *n*-butylhydrazine (Fig. 4.4). The formation of the methyl heme adduct is the lowest and that of the *n*-propyl heme adduct is the highest. The latter suggests that the *n*-propyl radical probably fits better the reaction site with respect to both size and lipophilicity. The methyl adduct was not extensively studied due to its low yield. The ethyl- and *n*-butyl adducts were thus chosen to be characterized by electronic absorption, mass and ^{1}H NMR spectroscopy. The porphyrins isolated from two heme adducts are dimethyl esters of γ-*meso*-ethyl- and γ-*meso*-(*n*-butyl)protoporphyrin IX, respectively (Fig. 4. 20). Although methyl- and *n*-propyl adducts have not been extensively characterized, both have the same absorption spectra as the ethyl and *n*-butyl adducts, and their retention times are consistent with the gradual increase in lipophilicity expected from stepwise increase of the γ-*meso* alkyl chain length (Fig. 4.5).

The alkyl radical generated from the alkylhydrazine can be spin-trapped and detected by EPR during the incubation (Fig. 4.10). The stability of the free radical is in the reverse order of the dissociation energies of the alkyl-hydrogen bonds. The dissociation energies of the methyl, ethyl and *n*-propyl free radicals are 104, 98 and 98 kcal/mol, respectively (March, 1985). Despite the fact that the methyl free radical is the least stable, the reaction of myoglobin with methylhydrazine gives only a small amount of methyl adduct. This could be explained by formation of an iron-methyl adduct that reverts to heme rather than

producing a N-methyl heme adduct upon acidic extraction of the prosthetic group (Mansuy et al., 1982). However, this is contradicted by the finding that other small alkylhydrazines yield the γ-*meso* heme adducts rather than N-alkyl heme adducts. Alternatively, methyldiazene may be small enough to get easily into the heme site relative to other alkyldiazenes.

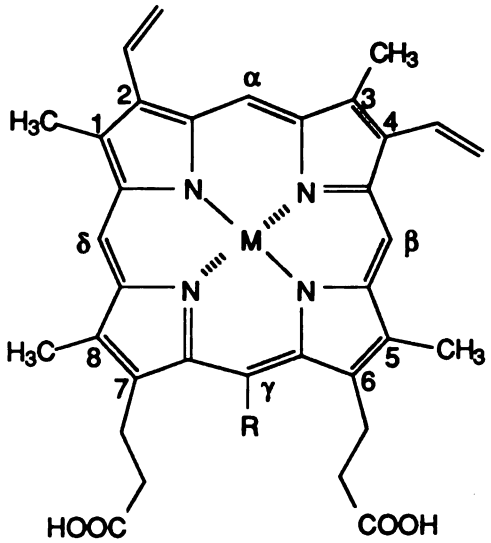

Fig. 4.20 Structures of the heme adducts resulting from the reactions with methylhydrazine (M = Fe, R = Me), ethylhydrazine (M = Fe, R = Et), *n*-propylhydrazine (M = Fe, R = *n*-Pr), and *n*-butylhydrazine (M = Fe, R = *n*-Bu), and of the zinc-complexed porphyrins derived from them (M = Zn).

The reactions of myoglobin with 2-phenylethyl-, *tert*-butyl-, and 2,2,2-trifluoroethylhydrazine do not form any heme-associated products. The failure to form an adduct with *tert*-butylhydrazine is not surprising because of the steric bulkiness. The γ-*meso* position is the most sterically hindered of the four *meso* positions due to the propionic acid side chains. This steric sensitivity and the high oxidizability of the *tert*-butyl radical ($E_{1/2}$ = 0.09 V vs. standard calomel electrode) may cause electron transfer to give the *tert*-butyl cation rather than the *meso* adduct (Griller & Wayner, 1989). The lack of reaction with 2-phenylethylhydrazine also probably is due to the steric demands of the γ-

meso position because a δ-*meso*-(2-phenylethyl)adduct is formed with horseradish peroxidase (Ator et al., 1989). In contrast, electronic effects are likely to be important in the reaction of myoglobin with 2,2,2-trifluoroethylhydrazine. The strong electron withdrawing effect of the three fluorines makes oxidation of this compound relatively difficult. Even if 1 equivalent of H_2O_2 is added to the incubation, the adduct is not formed, suggesting that lack of reaction is not simply due to slow autooxidative generation of H_2O_2. The 2-phenylethyl- and 2,2,2-trifluoroethylhydrazines seem to interact with the hemoprotein but in a different manner from the other alkylhydrazines because there are changes in the electronic absorption spectrum. Furthermore, minor and more polar products are formed in these cases which have the same retention time as the products resulted from peroxidative degradation of the heme group.

The pK_a values of small, linear alkylhydrazines are very similar: methyl, 7.87 (30°C); ethyl, 7.99 (30°C), 7.95 (25°C); *n*-propyl, 7.92 (25°C) and *n*-butylhydrazine, 7.82 (25°C). On the other hand, the pK_a of 2,2,2-trifluoroethylhydrazine is 5.38 (25°C) and of 2-phenylethylhydrazine 6.75 (25°C) (Krueger, 1975). At the incubation pH (7.4), approximately 72.5-78% of the linear alkylhydrazines and 0.95-18.3% of the latter two hydrazines are ionized. The internal nitrogen atom of monosubstituted hydrazines is protonated in the ionization state. However, the terminal nitrogen atom is protonated in the negatively substituted monoalkylhydrazines (Krueger, 1975). Since an eighty fold excess of the alkylhydrazine is used in the standard incubation, the pK_a differences do not appear to be the only factor that determines the reactivity of the alkylhydrazines.

The reaction of hemoglobin with ethylhydrazine does not form *meso* heme adduct but gives a very low yield of N-ethylprotoporphyrin IX (Ortiz de Montellano et al., 1983a). Similar products have been detected in the reactions of myoglobin and alkylhydrazines. The N-alkyl adducts were minor products, if formed, because the retention times of authentic N-methyl adducts were very similar to those of the minor products obtained from the reactions of myoglobin with *n*-propyl- and *n*-butylhydrazines (Fig. 4.4). It is thus clear

that the N-alkyl adducts are minor products in the reactions of both hemoglobin and myoglobin. Phenyl- and substituted phenylhydrazines, in contrast, react with myoglobin to give the iron-aryl complexes in high yields (Ringe et al., 1984; Ortiz de Montellano & Kerr, 1985). The aryl moiety shifts from the iron to a porphyrin nitrogen to give the four N-arylprotoporphyrin IX isomers when these complexes are denatured under aerobic, acidic conditions (Augusto et al., 1982b). Preliminary evidence suggests that *meso* adducts are formed as the minor products in this reaction. Saito et al. have reported that the reaction of oxyhemoglobin with phenylhydrazine yields a major green and a minor blue pigment, N-phenyl PPIX and β-*meso*-phenylbiliverdin, respectively (Saito & Itano, 1981). If the latter is not formed by addition of the phenyl radical to preformed biliverdin, β-*meso*-phenylbiliverdin should derive from β-*meso*-phenylheme. This would suggest that the regiochemistry of the reaction of phenylhydrazine with hemoglobin differs from that of the alkylhydrazines with myoglobin. Therefore, the reactions of myoglobin with arylhydrazines mainly produce the iron-phenyl adducts whereas those with alkylhydrazines yield the γ-*meso* heme adducts.

The fact that catalase completely suppresses the formation of γ-*meso* heme adducts suggests that H_2O_2 generated by autooxidation of the alkylhydrazines is required for the reaction (Fig. 4.7). This is confirmed by the observation that the anaerobic reaction of myoglobin with ethylhydrazine does not yield a *meso*-heme adduct but does if H_2O_2 is added (Fig. 4.8). The reaction thus appears to be catalyzed by the ferryl complex generated from the reaction of ferric myoglobin with H_2O_2 (King & Winfield, 1963; Yonetani & Schleyer, 1967). Addition of 1 equivalent of H_2O_2 to metmyoglobin produces a Compound II-like spectrum that is immediately converted by addition of ethylhydrazine to the spectrum obtained without the addition of exogenous H_2O_2. The ferryl complex may oxidize the alkylhydrazine to the corresponding alkyldiazene and remove one electron from the alkyldiazene to give the alkyldiazenyl radical that fragments to a molecule of nitrogen and an alkyl radical (Huang & Kosower, 1968; Kosower, 1971). EPR studies show that

alkyl radicals are formed in the reaction and their formation is affected by H_2O_2 and catalase in that it is accelerated by the former after prolonged incubation, and suppressed by the latter (Fig. 4.10). The fact that the reaction is probably catalyzed by the ferryl complex and the resulting alkyl radical adds to the γ-*meso* carbon of the prosthetic group has led us to propose two possible mechanisms (Scheme 4.3). Mechanism B is favored over A because the former mechanism can also be used to explain the formation of an iron-phenyl complex. An isoporphyrin has a transient absorption band at 840 nm and has been identified as an intermediate in the addition of radicals to the δ-*meso* carbon of horseradish peroxidase heme group (Ator et al., 1989). However, although metmyoglobin has a band at 835 nm which moves to 885 nm as the reaction progresses, a band at 840 nm is not detected in the myoglobin reaction (Fig. 4.9). The isoporphyrin, if formed, decays too rapidly to be detected. The isoporphyrin intermediates which are thought to be generated are also not detected in the δ-*meso* addition of phenyl and azidyl radicals to the heme of horseradish peroxidase (Ator et al., 1987; Ortiz de Montellano et al., 1988). However, the isoporphyrin intermediate is stable enough to be detected in the addition of alkylhydrazines to the δ-*meso* carbon of the heme of horseradish peroxidase (Ator et al., 1989). It is not known why the former is not stabilized while the latter is. In the case of the latter, the cationic isoporphyrin intermediate may be stabilized by a vicinal negative charge on the protein.

In some instances, the 2-vinyl group is the site of reaction in the modification of the heme group of myoglobin. The trichloromethyl radical reacts with the 2-vinyl group of the heme of sperm whale myoglobin under reductive conditions (Osawa et al., 1989). However, alkyl radicals react with the γ-*meso* carbon of the heme group of horse myoglobin under oxidative conditions (Choe & Ortiz de Montellano, 1991). Since the myoglobins obtained from both species (whale and horse) have very similar heme and substrate binding sites (Takano, 1977a; Evans & Brayer, 1988), the contribution of this factor to the reactivity is probably negligible.

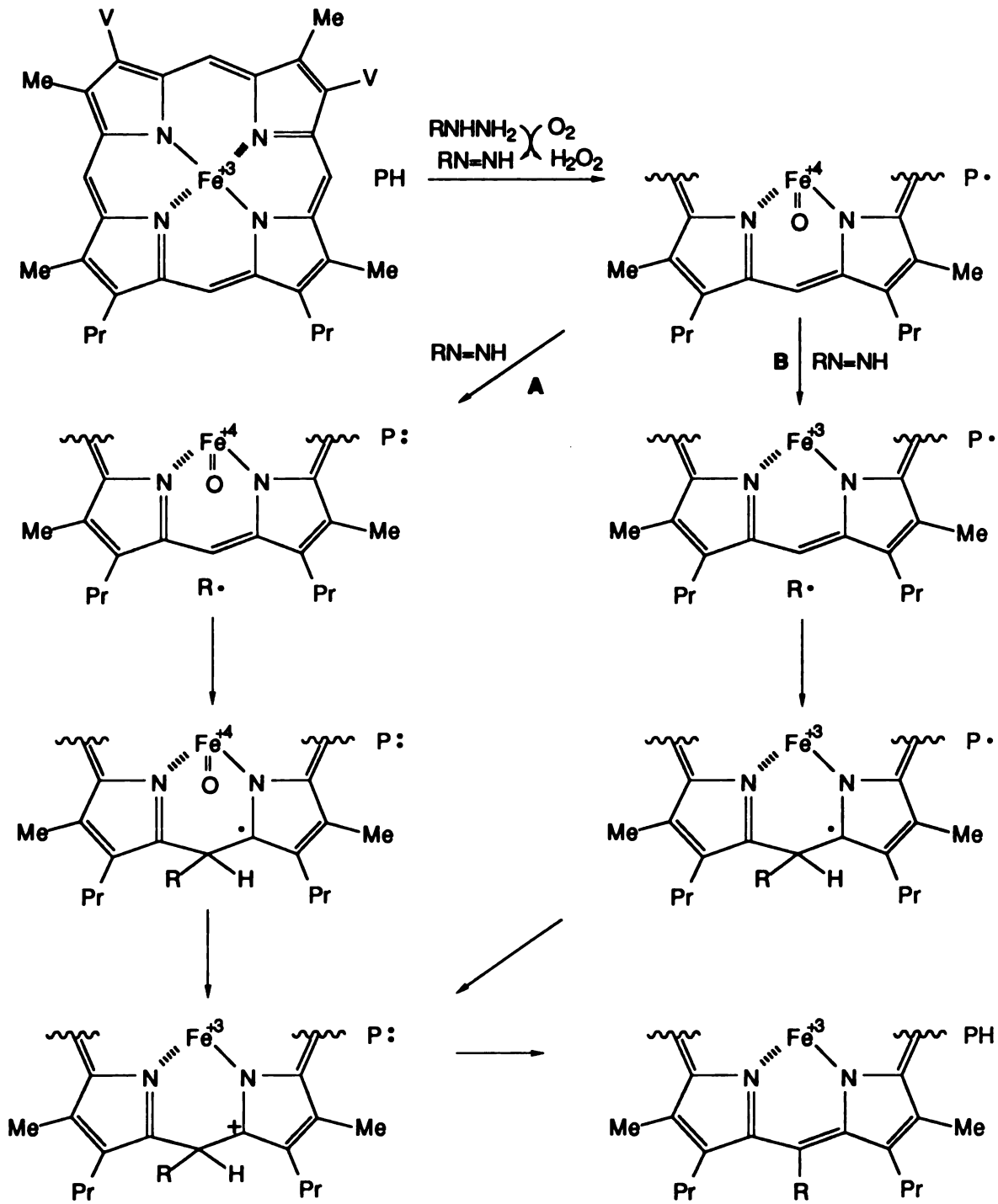

Scheme 4.3 Proposed mechanism for formation of the γ-*meso*-alkyl adducts. The radical R· is formally obtained by H· abstraction from the alkyldiazene (RN=NH). Me stands for methyl, V for vinyl, Pr for propyl in the heme prosthetic group and PH for the protein.

The oxidation state of the heme group when carbon radicals are generated is similar between the two reactions. The reaction of bromotrichloromethane with ferrous myoglobin produces the trichloromethyl radical and ferric heme. Similarly, the reaction of alkylhydrazine (or alkyldiazene) with the two-electron oxidized myoglobin (the ferryl oxygen species/protein radical) forms the alkyl radical and the ferric heme (mechanism B, Scheme 4.3). The water molecule should be able to escape when it is generated from the ferryl oxygen in the electron transfer step that produces the alkyl radical, so there should be no steric interference by the ferryl oxygen. If the protein radical takes the electron in the step that generates the alkyl radical, the reaction would yield the alkyl radical and the ferryl species analogous to that in the δ-*meso* addition of horseradish peroxidase (mechanism A, Scheme 4.3). However, this is not consistent with the finding that the phenyl radical adds to the iron to give an iron-phenyl complex in high yield (Augusto et al., 1982b; Kunze & Ortiz de Montellano, 1983; Ringe et al., 1984). Since the sixth heme coordination site is occupied in the ferryl species, it is unlikely that the hemoprotein is in the ferryl state after the phenyl radical is released. In agreement with this, the phenyl radical released from phenylhydrazine reacts with the iron atom of ferric myoglobin (Ringe et al., 1984).

The different regiochemistries may be controlled by the lipophilic properties of the substrates. The trichloromethyl radical, which originates from a lipophilic hydrocarbon, may be generated deep within the heme crevice, whereas the alkyl radicals, which arise from relatively hydrophilic alkylhydrazines, may be generated at the interface between the active site and the aqueous medium. This is consistent with the crystal structures of the myoglobins (Takano, 1977a; Evans & Brayer, 1988), which show that the γ-*meso* carbon faces the entry from the aqueous medium into the heme crevice (Fig. 4.21). Since methyl radicals are highly reactive, they may react at the site where they are generated, whereas the trichloromethyl radical, which is relatively stable due to the electron conjugating effect of the chlorines (Chu, 1980), may have a chance to move to the back of the heme pocket. The stabilities of the radicals, based on their bond dissociation energies, are methyl radical (104

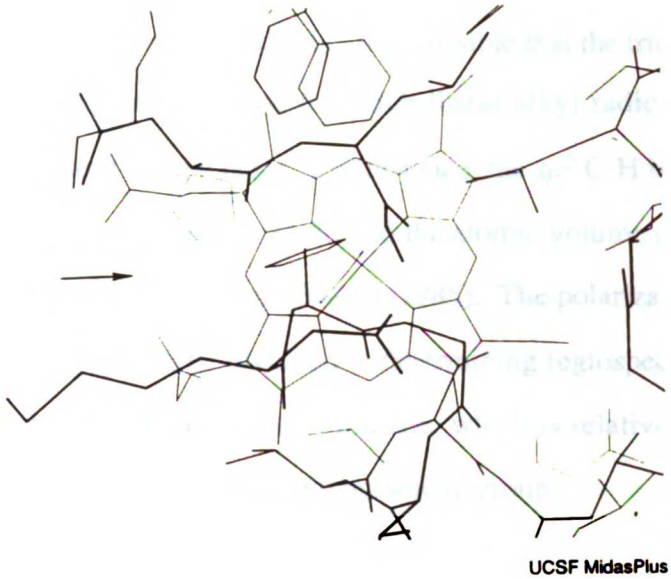

Fig. 4.21 Protein residues in the vicinity of the entry channel and heme crevice are shown from the crystal structure of horse heart myoglobin obtained with 2.8Å resolution (Evans & Brayer, 1988). An arrow indicates the γ-*meso* position between the two propionic acid substituents of the heme group.

kcal/mol), trichloromethyl radical (96 kcal/mol) and phenyl radical (110 kcal/mol) (Nonhebel et al., 1979; March, 1985). However, it has been suggested in the reduction of arenediazonium cations by ferrous hemoglobin that aryl radicals diffuse into the heme crevice to form iron-phenyl complexes after electron transfer from the ferrous iron to the diazonium group at the interface between the protein and the aqueous medium (Doyle et al., 1987). Therefore, alkyl radicals should also be able to move freely to the back of the heme pocket. For the same reason, the trichloromethyl radical should be able to react with the γ-*meso* carbon. However, even if alkyl radicals reach the back, they may react with the protein radical rather than with the heme vinyl group because diradical coupling reactions are very rapid. The modified protein has not been investigated in our studies. The alkyl radicals may react with a pyrrole nitrogen of the myoglobin prosthetic group in very low yield, in contrast to formation of the N-phenyl adducts in high yield from the reaction of

myoglobin with phenyl radicals. This difference may be explained by the reactivity, steric bulkiness and lipophilicity of carbon radicals. It is possible that the trichloromethyl radical does not react with the γ-*meso* position to which linear alkyl radicals add because the former is sterically bulkier than the latter. For instance, the sp^2 C-H bond length (1.10 Å) is shorter than the C-Cl bond length (1.73 Å) and the atomic volume of H (14.4 cm^3/mol) is smaller than that of Cl (22.7 cm^3/mol) (March, 1985). The polarizable properties of the trichloromethyl radical may also be involved in determining regiospecificity. The radical generated from the one electron oxidation of nitrite, which is relatively polarizable, also adds to the heme 2-vinyl group of myoglobin prosthetic group.

The difference in the intrinsic reactivities of carbon radicals seems to be the most important factor in determining the regiochemistry. However, the alkyl and trichloromethyl radicals are not easily generated under reductive and oxidative conditions, respectively, which makes a direct comparison of their regiospecificities under the same conditions difficult.

CHAPTER 5

Conclusions

Hemoproteins have received much attention due to their functions in biological systems. Since myoglobin is a small protein whose crystal structure is available and crystal structures of products derived from myoglobin are obtainable, they are frequently used for *in vitro* model studies of other hemoproteins. Myoglobin normally functions as an oxygen reservoir in muscle and hemoglobin as an oxygen carrier in blood. When the globins serve as oxygen transporters, their iron atoms are in the ferrous state. However, the globins may catalyze redox reactions *in situ* when they are autooxidized to the ferric state because the ferric globins catalyze such reactions *in vitro*. In addition, the reaction of metmyoglobin with H_2O_2 is of interest because it is relevant to pathological process such as reperfusion injury.

The reactions of the globins with H_2O_2 produces a ferryl oxygen species and a protein radical. The nature of the protein radical has been extensively studied since Gibson and coworkers first reported its formation in the reaction of sperm whale myoglobin with H_2O_2 (pH 8.0) in 1958 (Gibson et al., 1958). Further studies by King and coworkers suggested that the free radical resides first at a phenylalanine or histidine residue and is then transferred to a tyrosine residue to form the more stable tyrosine radical (King et al., 1964; King et al., 1967).

The evidence obtained to date suggests that Tyr 103 is, indeed, the site of the protein radical generated in the reaction of metmyoglobin with H_2O_2. This protein radical is involved in various reactions. Our investigations of the basic properties of the protein radical suggest that it decays by four reactions: (1) epoxidation of olefins, (2) crosslinking of the heme group to the protein, (3) protein-protein crosslinking, and (4) the abstraction of an electron from the substrates or the prosthetic group to facilitate the return of the enzyme

to the resting state. Reaction (3) only occurs in sperm whale myoglobin while the other reactions probably occur in all myoglobins.

The epoxidation of olefins is one of the reactions that is typically catalyzed by cytochrome P-450. A ferryl oxygen transfer mechanism has been proposed for the cytochrome P-450-catalyzed epoxidation of styrene derives from evidence that styrene has access to the activated oxygen. Accessibility of substrates to the activated oxygen of P-450 is also supported by the fact that the internal carbon of unconjugated terminal olefins is covalently bound to the activated oxygen in the resulting heme adducts (Ortiz de Montellano & Reich, 1986). Classical peroxidases, however, do not epoxidize olefins, in agreement with the proposal that substrates cannot approach the ferryl oxygen due to steric hindrance by the protein matrix. The results are consistent with those obtained from the reactions of these hemoproteins with phenylhydrazine because phenyl radicals add to the iron atom to give an iron-phenyl complex in cytochrome P-450 (Augusto et al., 1982b; Kunze & Ortiz de Montellano, 1983; Ringe et al., 1984), but attack the δ-*meso* heme edge in horseradish peroxidase (Ator & Ortiz de Montellano, 1987). Therefore, the origin of the epoxide oxygen and the stereochemistry of the olefin can be used as a probe of the mechanisms and active site structures of hemoproteins. Chloroperoxidase, a peroxidase that has a cysteine rather than histidine heme ligand, has been found to catalyze the H_2O_2-dependent oxidation of styrene to styrene oxide and phenylacetaldehyde. The epoxide oxygen derives quantitatively from the peroxide and the olefin stereochemistry is completely retained (Ortiz de Montellano et al., 1987). Hence, the epoxidation of styrene by chloroperoxidase is indistinguishable from that of cytochrome P-450 and is presumably mediated by a ferryl oxygen that is accessible to the substrate. The high molar ratio of phenylacetaldehyde to styrene oxide in the chloroperoxidase versus P-450 reactions suggests that chloroperoxidase has a more polar active site environment than does cytochrome P-450. Except for this, the active site structure of chloroperoxidase appears to resemble that of

cytochrome P-450 more than that of horseradish peroxidase (Ortiz de Montellano et al., 1987).

The globins catalyze the H_2O_2-dependent oxidation of styrene to styrene oxide and benzaldehyde (Ortiz de Montellano & Catalano, 1985). Thirty five percent of the epoxide oxygen derives from the peroxide in the reaction of equine myoglobin with styrene, indicating that part of the epoxidation proceeds by a mechanism similar to that of cytochrome P-450 (Ortiz de Montellano & Catalano, 1985). The rest of the epoxidation has been proposed to proceed by a cooxidative mechanism in which the peroxyl radical generated from reaction of the protein radical with molecular oxygen epoxidizes the styrene. This heterogeneity in the epoxidation mechanism rationalizes the partial loss of stereochemistry observed in the epoxidation of styrene (Ortiz de Montellano & Catalano, 1985). The protein radical abstracts an electron from the iron atom to facilitate return of the enzyme to the ferric state in the former mechanism whereas the protein radical participates more directly in the epoxidation in the latter. The involvement of the protein radical in the epoxidation in both mechanisms was confirmed by the demonstration that myoglobin does not oxidize styrene under conditions that produce the ferryl species but not the protein radical. Participation of hydroxyl radicals in the oxidation of styrene by myoglobin is ruled out because a comparable amount of styrene oxide and benzaldehyde is produced even after time is allowed for decay of the hydroxyl radical. The protein radical is thus required for the epoxidation of olefins.

The protein-mediated cooxidation reaction should result in modification of the protein at the site to which oxygen binds. Digestion of the apoprotein of peroxide-treated myoglobin with *Staphylococcal* V8 protease showed that a peptide containing Tyr 103 is modified in the presence of styrene and peroxide. The modification does not involve binding of styrene oxide to the protein because the modification is not observed when styrene oxide is incubated with myoglobin. The modified peptide, however, has not been characterized.

The protein radical becomes covalently bound to the heme group when horse myoglobin is treated with H_2O_2 (Catalano et al., 1989). The protein site of the covalently bound product has been identified as Tyr 103. The site of attachment of the heme group to the protein, however, had not been identified. The crystal structure of horse heart myoglobin shows that Tyr 103 is close to the heme 4-vinyl group and is not too distant from the β-*meso* carbon of the prosthetic heme group. The 4-vinyl group is not involved in the crosslinking reaction, however, because crosslinking occurs normally when apomyoglobin reconstituted with mesoheme, which has ethyl instead of vinyl substituents, is incubated with H_2O_2. The β-*meso* carbon is therefore proposed as the site of attachment to the protein (Catalano et al., 1989).

The reaction of sperm whale myoglobin with H_2O_2 results in the formation of dimers (Rice et al., 1983). The sites of protein-protein crosslink have been identified as Tyr 103 of one myoglobin and Tyr 151 of the other (Tew & Ortiz de Montellano, 1988). This result led us to study the roles of tyrosine residues in myoglobin. The fact that dimers are formed from the reactions of H_2O_2 with recombinant sperm whale myoglobin and the Tyr146Phe mutant, but not from that with the Tyr151Phe mutant, indicates that Tyr 151 is required for dimerization.

The protein radical participates in the reaction by abstracting an electron from the substrate, the iron atom or the porphyrin ring of the prosthetic group. When nitrite reacts with horse myoglobin in the presence of H_2O_2, an electron is transferred from the nitrite anion to the protein radical and the resulting nitrite radical adds to the 2-vinyl group of the prosthetic group (Bondoc & Timkovich, 1989). A part of the epoxidation of olefins catalyzed by the globins proceeds by a ferryl oxygen transfer mechanism in which the protein radical abstracts an electron from the iron atom and returns the enzyme to the resting state (Ortiz de Montellano & Catalano, 1985; Catalano & Ortiz de Montellano, 1987). When horse myoglobin is incubated with small, linear alkylhydrazines, alkyl groups add to the γ-*meso* carbon of the prosthetic group (Choe & Ortiz de Montellano, 1991).

Metmyoglobin is oxidized to the ferryl species by H_2O_2 generated from oxygen *in situ* with concomitant oxidation of alkylhydrazines to alkyldiazenes. Alkyldiazenes fragment to molecular nitrogen and alkyl radicals with reduction of the ferryl to the ferric species. After alkyl radicals add to the γ-*meso* carbon of the prosthetic group, an electron from the porphyrin ring is transferred to the protein radical in order to re-aromatize the porphyrin ring (Choe & Ortiz de Montellano, 1991).

The protein radical involved in the reactions is Tyr 103, the primary site of radical formation in the reaction of myoglobin with H_2O_2. Studies of the protein radical may contribute to a better understanding of the globins and other enzymes that generate protein radicals.

CHAPTER 6

Experimental

Materials. Chloroperoxidase (from *Caldariomyces fumago*), horse metmyoglobin (skeletal muscle, type I), human hemoglobin, bovine liver catalase (16,000 units/mg protein, thymol-free), 11-microperoxidase (from equine heart cytochrome c), NADPH, *Staphylococcus aureus* (Strain V8, type XVII) protease, trypsin (bovine, TPCK-treated, type XIII), elastase (from porcine pancreas, type IV), bovine hematin (type I), protoheme (equine hemin, type III), mesoporphyrin IX dihydrochloride, d_1-ethanol and 30% hydrogen peroxide were purchased from Sigma. Styrene, styrene oxide, benzaldehyde, 2-undecanone, 1,2-epoxy-3,3,3-trichloropropane, phenylacetylene, *n*-butyllithium, *tert*-butylhydrazine·HCl, 2,2,2-trifluoroethylhydrazine (70% w/w in water), POBN (a-(4-pyridyl-1-oxide)-N-*tert*-butylnitrone), KCN and 2-butanone (spectroscopic grade) were purchased from Aldrich. Mesoheme was obtained from Porphyrin Products (Logan, Utah). Methylhydrazine sulfate was purchased from American Tokyo Kasei, ethylhydrazine oxalate, *n*-propylhydrazine oxalate and *n*-butylhydrazine oxalate from Fluka, and 2-phenylethylhydrazine·HCl from K & K Laboratories. Solvents used for HPLC were HPLC grade. Buffers were prepared with deionized and double distilled water, and were passed through a Chelex column or stirred overnight with a Chelex resin (Bio-Rad).

Unit definition. Chloroperoxidase: one unit will catalyze the conversion of 1 mmol of monochlorodimedon to dichlorodimedon per min at pH 2.75 at 25°C in the presence of potassium chloride and H_2O_2. *Staphylococcus aureus* (Strain V8, type XVII) protease: one unit will hydrolyze 1 mmol of N-t-BOC-L-glutamic acid α-phenyl ester per min at pH 7.8 at 37°C. Catalase (bovine liver, thymol free): one unit will decompose 1 mmol of

H_2O_2 per min at pH 7 at 25°C while the H_2O_2 concentration falls from 10.3 to 9.2 mM. The rate of disappearance of H_2O_2 is monitored at 240 nm.

Instruments. Gas liquid chromatography was obtained using a Hewlett Packard Model 5890A instrument fitted with 30-meter DB-5 (1 μ thick) capillary column (DB-1 for the experiments described in 6.1.9) and flame ionization detector. Peaks were integrated with a Hewlett-Packard model 3390A integrator. Gas chromatography-mass spectrometry was performed on an AEI Kratos MS-25 coupled to a Varian 3700 gas chromatograph fitted with a 30 meter capillary column. Mass spectra were obtained by direct chemical ionization on a VG 70 SE mass spectrometer or electron impact (70 eV) on a Kratos MS 25 instrument. Liquid secondary ion mass spectra were performed on a Kratos MS 50 mass spectrometer using 1% trifluoroacetic acid/tetraglyme matrix. Absorption spectra were recorded on a Hewlett Packard Model 8450A fitted with diode array detector. For the spectra above 800 nm, an Aminco DW-2000 UV-VIS instrument was used. High performance liquid chromatography was carried out on a Hewlett-Packard 1090A system or a system composed of two Beckman 110A pumps, a Beckman model 420 controller, and a Hewlett-Packard 1040A diode array detecter. Analytical HPLC was done using a 250 x 4.6 mm column packed with Alltech Partisil ODS-3 (5 μ) and preparative HPLC was performed on a 250 x 9.4 mm Whatman Partisil 10 ODS-3 column, unless otherwise mentioned. Low pressure chromatography was obtained on an FMI Model RP1G150 lab metering pump connected to a Hitachi model 100 variable wavelength detector and a Lichroprep Si 60 size B silica gel column. ^1H NMR spectra were measured on a Varian FT-80 or a General Electric GN 500 MHz instrument. The signals of spin trapped radicals were monitored on a Varian E-104 EPR spectrometer.

6.1 The epoxidation of styrene

6.1.1 Oxidation of styrene by chloroperoxidase

The incubation was initiated by adding chloroperoxidase (20 units) to 1 ml of a solution of styrene (5 mM) and H_2O_2 (10 mM) in 0.1 M potassium phosphate buffer (pH 6, chelex-treated). The solution was incubated at room temperature for 5 min with occasional agitation. After 2-undecanone (5 μg/ml) was added as an internal standard, the incubation solution was extracted twice with 1 ml of diethyl ether. The combined extracts were washed with saturated NaCl solution, and the organic layer was dried over anhydrous K_2CO_3 and then concentrated before being analyzed by gas-liquid chromatography with the column programmed to rise from 80°C to 210°C at 5°C/min. Control incubations were carried out in the absence of H_2O_2 or chloroperoxidase. A standard curve was made to quantitate the products: known amounts (10, 20, 40 and 80 μg) of styrene oxide were added to incubation solutions in the absence of styrene and the solutions were worked up as above. After analyses by gas chromatography, the ratio of peak areas of styrene oxide to 2-undecanone was obtained. A plot was made of this ratio versus the amount of styrene oxide used.

Various styrene concentration (1, 2, 5, 10, 20 and 50 mM) were used to find the optimal conditions. The hydrogen peroxide concentration (1, 2, 5, 10, 20, 40 and 80 mM) and incubation time (0.5, 1, 2, 5, 10, 15, 30 and 60 min) were also varied independently. The conditions given above resulted from this optimization procedure.

In experiments to determine the origin of phenylacetaldehyde, instead of using styrene a comparable amount of styrene oxide obtained in the standard incubation was added to 1 ml of a solution of H_2O_2 (10 mM) in 0.1 M potassium phosphate buffer (pH 6.0). Chloroperoxidase (20 units) was added to start the incubation. After 5 min of incubation at room temperature, the mixture was worked up by the normal procedure. The

amounts of phenylacetaldehyde formed from this procedure and from a standard incubation were compared.

In order to see if the enzyme is inactivated by H_2O_2, chloroperoxidase was preincubated with H_2O_2 for 5 min at room temperature before styrene (5 mM) was added. The resulting mixture was incubated for another 5 min at room temperature and then worked up as above.

6.1.2 Synthesis of trans-[1-^{2}H]styrene

Trans-[1-^{2}H]styrene was prepared by the known procedure (Baldwin & Carter, 1983). Phenylacetylene was purified by distillation at 62°C (45 torr). All glassware was dried in the oven overnight and flushed with nitrogen gas. Triphenyltin hydride (53.26 g, 151.7 mmol) was transferred to a 250 ml round bottomed flask in the glove bag under a nitrogen atmosphere. Freshly distilled phenylacetylene (17.5 ml, 159.3 mmol) was slowly added to the triphenyltin hydride via a cannula under a nitrogen atmosphere. The mixture was stirred at room temperature and the color turned yellow 5 to 10 minutes into the reaction. The reaction was highly exothermic and a white cake which precluded further stirring was formed 20 minutes after the reaction started. The cake that formed was allowed to stand for an additional 40 minutes before it was taken up in cold pentane. The solid styryltriphenyltin (60.5 g, 133.5 mmol, 88% yield) was collected by vacuum filtration: m.p. 116-120°C (literature 119-120°C, Baldwin et al.); ^{1}H NMR (80 MHz) 7.53 (m, 5H, Ph-), 7.28 (m, 15H, $(Ph)_3$-) and 7.08 ppm (s, 2H, -HC=CH-).

Freshly distilled tetrahydrofuran (300 ml) was added to a 500 ml three necked round flask fitted with a 100 ml dropping funnel that was dried in the oven and flushed with nitrogen gas. The styryltriphenyltin (60.5 g, 133.5 mmol) was transferred to the flask via a cannula and the mixture stirred continuously under an atmosphere of nitrogen. *n*-Butyllithium in hexane (61.2 ml, 2.4 M, 146.85 mmol) was also transferred to the dropping funnel via a cannula and the reaction solution cooled to -78°C to allow dropwise

addition of the *n*-butyllithium solution. As the reaction progressed, the color turned from yellow to purple. After addition of *n*-butyllithium was complete, the mixture was allowed to warm to 0°C over 2 hours and then again cooled to -78°C to allow the dropwise addition of d_1-ethanol (16 ml, 267 mmol). The color changed from purple to yellow. Cold pentane (300 ml) was added after stirring an additional 30 minutes and the butyltriphenyltin removed by filtration through a celite (acid washed) pad. Butylated hydroxytoluene (50 mg) was added to the filtrate as an antioxidant. The filtrate was concentrated to 100 ml on a rotary evaporator, a second 100 ml of cold pentane was added to the residue, and the mixture was filtered and concentrated to 70 ml. The resulting solution was distilled in a kugelrohr distillation apparatus (50°C, less than 1 torr). The collection bulbs of the appropriate fractions were kept at -78°C and combined. Residual traces of pentane were removed by swirling at 0.5 torr after butylated hydroxytoluene (1 mg) was added to the solution. Product (3.967 g, 37.8 mmol) was obtained in 28% yield. ^{1}H NMR by 80 MHz (Fig. 6.1): 7.3 (m, 5H, Ph-), 6.67 (d of t, 1H, J_1 = 1.5 Hz, J_2 = 17.5 Hz, Ph-HC=C-) and 5.69 ppm (d, 1H, J = 17.5 Hz, *cis*-Ph-C=CH-). Less than 2% residual *trans*-proton signal was seen at 5.2 ppm. EIMS: m/z 105 (M^+), 77 (Ph^+).

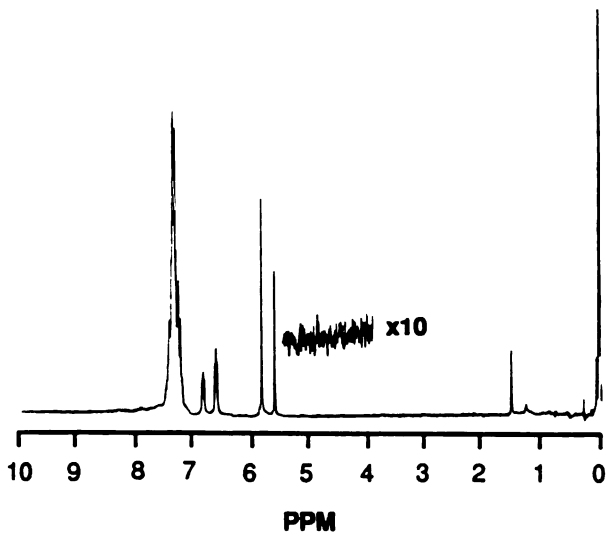

Fig. 6.1 NMR spectrum of *trans*-[1-^{2}H]styrene. No signal is found in the region of the proton *trans* to the phenyl ring (5.2 ppm; inset)..

6.1.3 Origin of the oxygen in styrene oxide

$H_2{}^{18}O_2$ was prepared from $^{18}O_2$ (Sawaki & Foote, 1979) by Dr. Carlos Catalano and the peroxide concentration was measured iodometrically (Pesez & Bartos, 1974). The $H_2{}^{18}O_2$ (10 µl) was added to the solution containing 4 ml H_2O, 1 ml 10% KI and 0.2 ml 1N HCl. The mixture was incubated in the dark for 15 min, and the electronic absorption spectrum taken at 353 nm (ε=25.5 $mM^{-1}cm^{-1}$) after adding 5 ml of H_2O. In separate sets of experiments, known amounts of H_2O_2 (0, 25, 50, 100 µM) were used. The concentration of $H_2{}^{18}O_2$ (52 mM) was then obtained from the standard plot that was constructed from the absorbances versus the known concentrations of H_2O_2. The $^{18}O_2$ content of the peroxide was determined by mass spectrometric analysis of the menadione epoxide produced by reaction of the peroxide with menadione under basic conditions (Ortiz de Montellano & Catalano, 1985). The $^{18}O_2$ content of the H_2O_2 was determined to be 75%.

A 2-ml standard incubation was carried out using $H_2{}^{18}O_2$ (400 µl, 10 mM). Since $H_2{}^{18}O_2$ was stored in 1N HCl containing 1 mM EDTA, the solution was adjusted to pH 6 with saturated KOH solution (18 µl). No internal standard was added prior to work-up. The diethyl ether extract was analyzed by gas chromatography-mass spectrometry using a 30-m SE-52 column programmed to rise from 50 to 150°C at 5°C/min. The control incubation was carried out similarly using H_2O_2, and the ether extract was also analyzed by GC-MS.

6.1.4 Stereochemistry of the epoxidation of styrene by chloroperoxidase

Styrene oxide was isolated by the standard procedure from large scale (25 ml) incubations in which *trans*-[1-^{2}H]styrene was substituted for styrene. No internal standard was added, however, and the ether extract of the incubation mixture was reduced to a volume of 0.5 ml. It was then fractionated by low pressure chromatography on a Lichroprep Si-60 size B silica gel column with 15% ether/pentane (v/v) as the elution

solvent. The eluent at a flow rate of 5 ml/min was monitored at 265 nm. The styrene oxide fraction was collected and carefully concentrated by evaporation to avoid loss of styrene oxide. The concentrated sample was transferred to an NMR tube with deuterochloroform, and again concentrated by nitrogen gas. This procedure was repeated several times before the styrene oxide was analyzed on a GE 500 MHz NMR spectrometer. If the ether-pentane mixture is evaporated to dryness before the deuterochloroform is added, it is difficult to avoid losing the styrene oxide.

6.1.5 Epoxidation of styrene by purified cytochrome P-450IIB1 (P-450$_b$)

Cytochrome P-450$_b$ and cytochrome P-450 reductase were purified from the livers of male Sprague Dawley rats (Komives & Ortiz de Montellano, 1987). The frozen preparations of P-450 and P-450 reductase were thawed on ice. The concentrations of P-450 and P-450 reductase were adjusted to make the final concentrations 1 and 2 nmol/ml, respectively, in the final mixture. A suspension of dilauroylphosphatidylcholine in H_2O (2 mg/ml) was prepared by sonicating for 10 min with a Branson Sonicator equipped with a microprobe tip. The two proteins and 20 µl of dilauroylphosphatidylcholine were allowed to stand together for 10 min at room temperature before adding a solution of styrene (10 mM) in 0.75 ml of 0.1 M potassium phosphate buffer (pH 7.4, chelex-treated) containing 20% glycerol and 1 mM DETAPAC. This mixture was preincubated at 37°C for 2 min before NADPH (0.5 mM) was added to initiate the reaction. The final mixture (1 ml) was incubated at 37°C for 5 min and worked up, and the extract was analyzed by GLC as already described.

6.1.6 Stereochemistry of the epoxidation of styrene by rat liver microsomes

Microsomes were prepared from the livers of male Sprague Dawley rats injected intraperitoneally for 4 days with a daily 80 mg/kg dose of phenobarbital (Komives & Ortiz de Montellano, 1987). A 200-ml volume of liver microsomes (3 nmol of P-450), 1,2-epoxy-3,3,3,-trichloropropane (10 mM), and *trans*-[1-^{2}H]styrene (9 mM) in 0.1 M

potassium phosphate buffer (pH 7.4) was preincubated for 2 min at 37°C. NADPH (0.5 mM) was added to initiate the reaction. After the mixture was incubated for 10 min at 37°C, it was then cooled and extracted with 150 ml of diethyl ether. The organic fraction was washed with saturated NaCl solution and was dried over anhydrous K_2CO_3. The organic layer was concentrated to a volume of 0.5 ml, and the styrene oxide was isolated, purified, and analyzed as described for the material obtained with chloroperoxidase.

6.1.7 Oxidation of olefins by 11-microperoxidase

The incubation was initiated by adding 11-microperoxidase (0.2 mg, 107 μM) to 1 ml of a solution of styrene (5 mM) and hydrogen peroxide (10 mM) in 0.1 M potassium phosphate buffer (pH 7). After incubation at room temperature with occasional agitation for 5 min, the mixture was worked up as mentioned above. The hydrogen peroxide concentration (5, 10, 20, 30, 40 and 80 mM), microperoxidase concentration (0.2, 0.5, 0.7, 1 and 1.5 mg), and incubation time (2, 5, 10 and 15 min) were varied independently to optimize the conditions.

Since *cis*-stilbene contains 2 to 3% *trans*-stilbene, it was purified by low pressure chromatography with 10% ether/hexane. The column was eluted at a flow rate of 4 ml/min, and the eluent was monitored at 265 nm. *cis*-Stilbene was eluted with a retention time of 12 min and *trans*-stilbene of 16 min. The purified *cis*-stilbene contained less than 0.2% *trans*-stilbene. The incubation was carried out by adding 11-microperoxidase (0.2 mg, 107 μM) to 1 ml of a solution of purified *cis*-stilbene (50 μM) and hydrogen peroxide (10 mM) in 0.1 M potassium phosphate buffer (pH 7). After the mixture was incubated for 10 min at 0°C, it was worked up and the extract analyzed by GLC on a 30 meter DB-5 capillary column run isothermally at 180°C. The retention time of *cis*-stilbene was 9.7 min and *trans*-stilbene 16 min.

In experiments to monitor Soret loss as a function of time in the oxidation of *cis*-stilbene (50 μM) by 11-microperoxidase (107 μM) and H_2O_2 (10 mM), an aliquot (10 μl)

was taken from 1 ml of a reaction mixture and its absorption spectrum (400 nm) was measured after 1, 5, 11, 17, 26 and 90 min.

6.1.8 Low temperature EPR studies

The EPR Dewar jar was connected to a coil of copper tubing which was also connected to a nitrogen gas cylinder. The EPR Dewar jar was placed into the microwave cavity and the copper coil was then immersed in liquid nitrogen (-196°C) to lower the temperature of the microwave cavity. The microwave cavity was cooled with a stream of cold nitrogen gas during the entire experiment. The Dewar jar was filled with liquid nitrogen and capped with a piece of aluminium foil. The myoglobin (300 μM) was incubated with 1.5 equivalents of H_2O_2 at 0°C, and aliquots were removed from the mixture and immediately frozen 0, 0.5, 1, 2, 5, 10, 20 and 30 min after the incubation started. In another set of experiments, 1.5 equivalents of H_2O_2 (450 μM) were added to a mixture of myoglobin (300 μM) and styrene (10 mM), and aliquots were removed from the mixture at the specified time as described above. EPR spectra were recorded on an IBM PC/XT computer and a Techmar Labmaster analog to digital (12 bit resolution) converter with signal averaging performed in real time. Signals were monitored with the following parameters: g value, 2 (6); field center, 3269 G (1090 G); modulation frequency, 100 kHz (100 kHz); modulation amplitude, 8 G (20 G); microwave power, 2 mW (10 mW); microwave frequency, 9.085 GHz (9.085 GHz); scan time, 8 min (4 min); scan range 500 G (1000 G); time constant, 1 sec (0.5 sec); receiver gain, 8 x 10^3 (1.25 x 10^3). The numbers in the parentheses represent the parameters used to monitor high spin ferric myoglobin whereas those out of the parentheses were used for the protein radical.

6.1.9 The reaction of the myoglobin [Fe(IV)=O] species with styrene

The ferryl species was prepared by the method of Aviram et al. with some modification (Aviram et al., 1978). Horse myoglobin (30.6 mg, 300 μM) was dissolved

in 6 ml of potassium phosphate buffer (0.2 M, pH 7.4, chelexed). The solution was prepared in a 25-ml three necked round bottomed flask fitted to a 3-ml UV cuvette and a vacuum/argon gas line. The solution was deoxygenated and saturated with argon gas several times by freeze-thaw cycles. Meanwhile, sodium dithionite (470 mg, 2.7 mmol) was dissolved in 5 ml of NaOH solution (1 mM) prepared as above, and deoxygenated again. H_2O_2 (612 µl, 5.4 mmol) was diluted in 5 ml of potassium phosphate buffer (0.2 M, pH 7.4) and prepared as above. Oxygen-free sodium dithionite solution (0.94 mg, 0.9 mM, 10 µl of stock solution) was transferred to the myoglobin solution by a syringe flushed several times with argon gas. The color of the solution changed from brown to pink. The addition of H_2O_2 (3.6 mM, 20 µl of stock solution) to the ferrous myoglobin changed its color to red. The resulting protein solution was loaded onto a G-25 column which was soaked in and pre-equilibrated with argon-bubbled buffer to remove excess sodium dithionite and H_2O_2. The purified myoglobin [Fe(IV)=O] complex (6 ml) was collected in a graduated cylinder. One third of the protein solution (2 ml) was taken for the electronic absorption spectrum and aerobic reaction with styrene (10 mM, 20 µl of 1 M stock solution in acetonitrile). Another one third was kept under argon gas for the reaction with styrene (10 mM). The last part was deoxygenated and saturated with argon gas three times, and then incubated with styrene (10 mM) under argon gas. After incubation at 0°C for 90 min, 2-undecanone (8.25 µg) was added to each reaction mixture as an internal standard. The reaction mixture was extracted with diethyl ether (2 x 4 ml) and the organic layer was washed with brine, and then dried over anhydrous potassium carbonate. The ether fraction was then concentrated to 0.3 ml on a rotary evaporator without using a water bath before being analyzed by GLC on a DB-1 capillary column (0.25 mm/i.d., 0.25 µ thick, 30-m long). The temperature was programmed to rise from 80 to 210°C at 5°C/min.

In a set of eight incubations, a 1 ml-incubation solution of myoglobin (5.1 mg, 300 µM) and 1.5 equivalents of H_2O_2 (10 µl of 45 mM stock solution in buffer) was allowed to stand for a specified time to let the protein radical decay. After standing at 0°C for 0, 0.5,

1, 2, 5, 10, 20 and 30 min, each incubation was initiated by adding styrene (10 mM, 10 μl of 1 M stock solution in acetonitrile). The mixture was then incubated at 0°C for 90 min. 2-Undecanone (4.125 μg) was added to each mixture before the metabolites were extracted with ether (2 x 2 ml). The ether fraction was washed with brine, dried over anhydrous potassium carbonate, concentrated to 0.2 ml on a rotary evaporator and analyzed by GLC.

6.1.10 Construction of a standard curve

Myoglobin (5.1 mg, 300 μM) was dissolved in 0.98 ml of phosphate buffer (0.2 M, pH 7.4). Styrene oxide (1, 2, 5, 10 and 20 μg in acetonitrile) instead of styrene was added to the protein solution and each reaction mixture contains 10 μl of acetonitrile. The 1 ml-incubation solution was incubated at 0°C for 90 min after addition of 1.5 equivalents of H_2O_2 (10 μl of 45 mM stock solution). At the end of the incubation, the mixture was worked up as described previously in the presence of 2-undecanone (4.125 μg). A plot was constructed between the amount of styrene oxide added and the ratio of peak area of styrene oxide to that of 2-undecanone detected by GLC.

Benzaldehyde (0.5, 1, 2.5 and 5 μg) was added instead of styrene to quantitate the amount of benzaldehyde produced in the oxidation of styrene by myoglobin and H_2O_2. A standard curve was constructed in the same way as above.

6.2 H_2O_2-induced damage to myoglobin

6.2.1 The site of attachment of the heme group to the protein: via the heme vinyl groups?

6.2.1.1 Preparation of apomyoglobin (Teale, 1959)

Horse metmyoglobin (30 mg/ml in glass distilled water) was cooled to 0°C and acidified to pH 2 with concentrated HCl. The mixture was then quickly extracted with an equal volume of cold 2-butanone in a separatory funnel. The mixture was allowed to stand for at least one hour at 4°C. The lower aqueous layer containing the apoprotein was

extracted with cold 2-butanone twice and dialyzed against glass distilled water for 48 hours before it was lyophilized. The dried apoprotein, obtained in 77% yield was stored at -20°C until used. The Soret absorption of a solution of the apoprotein indicated retention of a trace (2.0-3.0%) of the heme moiety.

6.2.1.2 Preparation of mesoheme (Morell et al., 1961)

Mesoporphyrin IX dihydrochloride (10 mg, 15.6 μM) was dissolved in 1 ml of pyridine and 50 ml of glacial acetic acid. A saturated aqueous solution of $FeSO_4$ (1 ml) was added, and the mixture was kept at 80°C for 10 min under a stream of N_2 and then for another 10 min in air to allow autooxidation to the ferric state. The mixture was saturated with NaCl and then extracted with diethyl ether. The organic layer was washed with 25% HCl to remove the unreacted porphyrin and was then rinsed with water and dried over Na_2CO_3 before the solvent was removed on a rotary evaporator. The electronic absorption spectrum of the product obtained in 19% yield (2.2 mg) is nearly identical to the spectrum of mesohemin in ether (Fuhrhop & Smith, 1975): 371 (S'), 397 (S), 506 (IV), 530 (III), 580 (II) and 630 nm (I), S/S' (0.84); lit. 370 (S'), 397 (S), 506-508 (IV), 534 (III), 585 (II) and 632-634 nm (I), S/S' (0.84).

6.2.1.3 Reconstitution of apomyoglobin with exogenous heme

The apomyoglobin (200 mg, 12.2 μmol) was dissolved in 25 ml of 0.01 M borate buffer (pH 9.2), and the mixture was cooled to 0°C. The mesoheme (9 mg, 14 μmol, prepared as in 6.2.1.2 or obtained commercially) in 5 ml of 0.01 N NaOH was added dropwise at 0°C with gentle stirring to the apomyoglobin solution. The mixture was stirred for a further 5 min at 0°C and was then centrifuged on a table top centrifuge. The supernatant was loaded onto a Sephadex G-25 (2.5x35 cm) column pre-equilibrated and eluted with 0.01 M potassium phosphate buffer (pH 6.3). The brown-color-band was collected and loaded onto a CMC-52 column (2.5x25 cm) which had been washed with 0.2 N HCl and then with water, 0.2 N NaOH, and water again before equilibration with 0.01

M phosphate buffer (pH 6.3). The column was washed with 300-400 ml of the same buffer before the reconstituted enzyme was eluted as a tight, red-brown band by changing to 0.03 M phosphate buffer (pH 7). The eluted hemoprotein was dialyzed against 0.2 M chelex-treated buffer (potassium phosphate buffer, pH 7.4 or potassium acetate buffer, pH 4.5). The final volume was 21 ml. The control reaction was carried out simultaneously using protoheme (9 mg, 14 μmol). The hemoprotein concentration was determined from the electronic absorption spectrum and by measurements of the prosthetic group concentration by the pyridine hemochromogen assay, and the protein concentration by both Lowry and Biorad assays.

6.2.1.4 Hemoprotein assays

Electronic absorption hemoprotein assay

The reconstituted myoglobin in phosphate buffer was diluted with water to take electronic absorption spectra. The concentration of hemoprotein was determined from the absorbances and the extinction coefficients given in table 6.1 (Smith & Gibson, 1959).

Table 6.1

Horse metmyoglobin extinction coefficients ($mM^{-1}cm^{-1}$)

Protein	280 (ε)	Soret (ε)	α-band (ε)	β-band (ε)
proto	280 (28.9)	408 (153)	500 (9.5)	630 (3.9)
meso	-	394 (102)	492 (-)	

Pyridine hemochromogen assay (Riggs, 1981)

The hemoprotein in a total volume of 250 μl phosphate buffer (pH 7.4) was added to 750 μl of alkaline pyridine solution (10 ml pyridine, 3 ml 1N NaOH and 17 ml H_2O) and the solution was mixed thoroughly. After 3 min, excess sodium dithionite was added to

the sample. The color changed to red. The absorbance at 557 nm for protoheme ($\varepsilon = 34.4$ mM^{-1}), or 546 nm for mesoheme ($\varepsilon = 33.2$ mM^{-1}), was measured (Fuhrhop & Smith, 1975).

Lowry protein assay (Lowry et al., 1951)

To the reconstituted protein in a total volume of 100 µl phosphate buffer, 1 ml of solution A was added and mixed thoroughly. After the mixture was vortexed and allowed to stand at room temperature for 10 min, 3 ml of solution B was added with agitation. The mixture was heated to 50°C for a further 10 min. The resulting solution was cooled on ice and the absorbance at 660 nm was measured immediately. The concentration of protein was determined from the standard curve that was obtained by plotting the known amounts of horse myoglobin (0, 41.2, 206, 329.6 and 412 µg) versus the absorbances obtained from this assay. Solution A contained 1 ml of 1% $CuSO_4.5H_2O$, 1 ml of 2% potassium tartrate and 20 ml of 10% Na_2CO_3 in 0.5 M NaOH and solution B contained 1:10 solution A:2 N phenol reagent.

Biorad assay (Bradford, 1976)

This assay depends on the fact that the binding of Coomassie Brilliant Blue G-250 to protein causes a shift in the absorption maximum of the dye from 465 to 595 nm. The assay was performed as described on the Biorad concentrated protein assay reagent bottle. The concentrated reagent was diluted with 4 volumes of glass distilled water and filtered. The protein solution was added to 5 ml of diluted reagent and mixed thoroughly. The absorbance at 595 nm was monitored. The protein concentration was determined from the standard curve that was constructed from known amounts of horse myoglobin (0, 41.2, 206, 329.6 and 412 µg) and the corresponding absorbances obtained from this assay.

6.2.1.5 Oxidation of reconstituted myoglobins

Solutions of myoglobin reconstituted with protoheme or mesoheme were concentrated to final volumes of 2 ml by a Centricon cx-10 concentrator. Each of the two

hemoprotein solutions was divided into two 1-ml (2 μmol) aliquots. The four aliquots were cooled to 0°C, and chilled H_2O_2 (10 μmol) was added to one of the two aliquots from each of the reconstituted proteins, causing the color to turn red. An equal volume of buffer was added to the second aliquot of each solution. After incubation at 0°C for 30 min, KCN (250 mM final) was added to the four aliquots and the solutions were dialyzed against glass distilled water for 48 hours. The heme groups were removed with acidic 2-butanone and the apoprotein solutions were dialyzed as described above. The absorption spectra of the resulting apoproteins were recorded and compared.

6.2.2 Attempts to isolate the heme-peptide

6.2.2.1 Preparation of apomyoglobin at pH 4.5

Chilled H_2O_2 (5.75 μl, 50 μmol) was added to the myoglobin (169 mg, 10 μmol) in 24 ml potassium acetate buffer (0.2 M, pH 4.5, chelexed). The color of the protein solution changed from brown to red. After incubation for 30 min at 0°C, KCN (1.25 mmol) was added to stop the incubation. A control incubation to which no H_2O_2 was added was carried out simultaneously. The solutions were then dialyzed against glass distilled water for 48 hours before the heme was removed with acidic 2-butanone. The resulting apoprotein was dialyzed against water for 48 hours, lyophilized, and stored at -20°C. The colorless apoprotein (100 mg), which retains 2-5% residual heme, was obtained in 61% yield from a control reaction whereas brown apoprotein (140 mg) with 20% of the heme chromophore was obtained from a complete reaction.

6.2.2.2 Digestion of apomyoglobin containing 20% heme with protease

Apomyoglobin (10 mg) was dissolved in 1 ml of NH_4HCO_3 buffer (0.05 M, pH 8.5) and digested with TPCK-treated trypsin at 37°C for 6 hours. The ratio (w/w) of the protein to trypsin was 83:1. In another set of experiments, the protein dissolved in 1 ml of NH_4HCO_3 buffer (0.01 M, pH 8) containing 2 M urea was digested with elastase (50:1) at

37°C overnight. At the end of the incubation, the mixture was lyophilized and analyzed by HPLC using a step gradient of 0-35% solvent B over 30 min, 35-40% B over 20 min, 40-70% B over 30 min and 70-100% B over 5 min. The tryptic heme-peptide was rechromatographed by HPLC using a step gradient of 35-39% solvent B over 30 min, 39-50% B over 10 min and 50-70% B over 20 min. The flow rate was 1 ml/min. Solvent A was 0.1% TFA in water and solvent B was 0.1% TFA in acetonitrile. The peptides were monitored at 220, 280 and 400 nm simultaneously.

6.2.2.3 Attempts to isolate the heme-bound protein

Several approaches were attempted to isolate heme-bound protein (20%) in apoprotein of H_2O_2-treated myoglobin prepared as described in 6.2.2.1.

SDS-PAGE: Apoproteins of H_2O_2-treated and untreated myoglobin were analyzed by SDS-PAGE (20% acrylamide).

IEF: Apoprotein of H_2O_2-treated myoglobin was loaded on IEF gel using IEF mix 3-9.

HPLC: Apoprotein of H_2O_2-treated myoglobin was dissolved in 40% solvent B and analyzed by reverse phase HPLC using a gradient of 40-50% solvent B over 60 min. Solvent A was 0.1% TFA in water and solvent B was 0.1% TFA in acetonitrile. The flow rate was 1 ml/min.

FPLC: Apoprotein of H_2O_2-treated myoglobin (2.5 mg) was dissolved in 1 ml of NH_4HCO_3 buffer (10 mM, pH 8.5) and analyzed by FPLC fitted to an anionic exchange column (mono Q) monitored at 280 nm at a flow rate of 1 ml/min. The column was eluted for 20 min using 0 to 20% solvent D followed by for 30 min using 20 to 100% solvent D. Solvent C was 10 mM NH_4HCO_3 (pH 8.5) and solvent D was 700 mM NH_4HCO_3 (pH 8.5). The fractions of interest were analyzed by SDS-PAGE (20% acrylamide).

Biogel column: After dialysis, the apoprotein solution in the bag was concentrated using PEG powder (polyethylene glycol, 8000) and centrifuged on a Sorvall for 30 min. The supernatant was loaded onto the gel filtration column (Biogel P-100; 50-100 mesh;

exclusion limit 100,000 daltons; 2.5 x 75 cm) pre-equilibrated with water. The supernatant from the complete reaction was loaded first, followed by that from the control reaction because the former was brown so it was easily monitored by its color. The eluent was combined every 5 min, and its absorbance was measured at both 280 and 408 nm. Some fractions were concentrated by Milipore cx-10 ultrafiltration unit and analyzed by SDS-PAGE (15%). Fractions containing the heme chromophore, 12-30 and 33-47 were digested independently with elastase for 18 hours at 37°C. The resulting digests were analyzed by reverse phase HPLC with a gradient program of 0 to 60% solvent B over 60 min. Solvent A was 0.1% TFA in water and solvent B was 0.1% TFA in acetonitrile.

6.2.3 Styrene dependent protein modification

6.2.3.1 Preparation of apomyoglobin in the presence of styrene

Horse metmyoglobin (338 mg, 20 μmol) and styrene (57 μl, 0.5 mmol) were dissolved in 50 ml potassium phosphate buffer (0.2 M, pH 7.4) containing 0.5 mM desferral. Chilled H_2O_2 (11.5 μl, 0.1 mmol) was added and the mixture was incubated at 0°C for 30 min. A control incubation was also carried out with addition of the same volume of buffer in place of H_2O_2. Styrene oxide (0.5 μl in a total 2 μl of acetonitrile, 4 μmol) was added to the control solution 15 min into the incubation. At the end of the incubation, KCN (0.1 mmol) was added to the mixtures to stop the incubation. The color of the mixtures turned red. Both mixtures were treated as described below.

Method A: The solutions were dialyzed against glass distilled water for 48 hours. The proteins were then concentrated to a volume of 30 ml with an Amicon cx-10 ultraconcentration unit and dialyzed again against water. The heme groups were removed by extracting with an equal volume of cold 2-butanone three times after the proteins were acidified to pH 2 with concentrated HCl. The apoproteins were then dialyzed against water for 48 hours. Some proteins precipitated 24 hours into the dialysis. The dialyzed apoproteins were lyophilized and stored at -20°C until used.

Method B: The solutions were treated as described in Method A except that the apoproteins were centrifuged after dialysis. The soluble apoproteins and the precipitates were lyophilized, respectively.

Method C: The solutions were treated as described in Method A. The length of dialysis, however, was reduced to half of the time described in Method A but the frequency of change of water remained the same. A little protein was precipitated at the end of the final dialysis. The resulting apoproteins were lyophilized.

The apoprotein (200 mg) obtained from the control reaction retained 2-4% of the heme whereas the apoprotein (250 mg) from the complete reaction contained 9-12% of the heme chromophore.

6.2.3.2 Digestion of apomyoglobin with *Staphylococcal* V8 protease

Apomyoglobins (10 mg) obtained from 6.2.3.1 were dissolved in 1 ml of NH_4HCO_3 buffer (0.1 M, pH 8) containing 4 M urea. A little amount of peroxide-untreated apomyoglobin remained undissolved. The mixtures were preincubated at 37°C for 5 min before protease solutions (30 µl, 2500 units/ml water) were added. The resulting solutions were incubated at 37°C for 6 hours with additions of 20-µl aliquots of V8 protease being added after 2 and 4 hours of incubation. The solutions were then lyophilized, redissolved in 1 ml of 0.1% aqueous trifluoroacetic acid, filtered through a 5 µ filter needle, and analyzed by reverse phase HPLC on a column packed with Partisil 5 C_8 (5 µ). The column was eluted at a flow rate of 1 ml/min using a step gradient of 0-40% solvent B over 90 min, 40-70% B over 30 min and 70-100% B over 5 min. Solvent A was 0.1% TFA/water and solvent B was 0.1% TFA/acetonitrile. The peptides were monitored at 220, 280 and 400 nm. Preparative experiments were similarly performed using 60 mg of the apomyoglobin. The sample was prepared as above and analyzed by a preparative HPLC system using a gradient program of 15-40% B over 50 min, 40-70% B over 30 min and 70-100% B over

5 min. The flow rate was 3 ml/min. Appropriate fractions were rechromatographed in the analytical HPLC system.

6.2.4 The roles of the tyrosine residues in peroxide treated myoglobin

The gene for sperm whale myoglobin was synthesized and expressed in *E. coli*. Site specific mutagenesis was performed to replace each of Tyr 146 and Tyr 151 by a phenylalanine. Gene synthesis and mutagenesis were accomplished by Dr. Angela Wilks. Since recombinant sperm whale myoglobin has an extra methionine at the N terminal end, its molecular weight (17,946) reflects addition of a methionine to native sperm whale myoglobin.

Proteins were oxidized with potassium ferricyanide (5 µl of stock solution, 20.3 µM) and purified by a G-25 column equilibrated with phosphate buffer (50 mM, pH 7.0). Recombinant sperm whale myoglobin (wild type, 145.57 µg, final: 40.5 µM) was diluted to 200 µl with chelex-treated potassium phosphate buffer (50 mM, pH 7.0). The Tyr151Phe was diluted to the same concentration (final: 40.5 µM) as the wild type and the Tyr146Phe (40.5 µM) was used without further dilution. The wild type and mutant enzymes were incubated independently with H_2O_2 (607.5 µM) at 0°C for 1 hour. Parallel incubations, in which buffer was added in place of H_2O_2 were also carried out using the wild type and the mutants. At the end of the incubation period, an aliquot (15 µl) was taken from each reaction mixture and half (hemoprotein: 5.20 µg) was loaded on SDS-PAGE (15%).

6.3 γ-*Meso* substitution of the myoglobin prosthetic heme group by alkylhydrazines

6.3.1 Reactions of horse metmyoglobin with alkylhydrazines

A solution of horse myoglobin (10 mg, 0.59 µmol) in 500 µl of potassium phosphate buffer (0.1 N, pH 7.4) containing 1 mM EDTA was preincubated at 37°C in the dark for 2 min. After an 80-fold excess (47.2 µmol) of the appropriate alkylhydrazine in 500 µl of

phosphate buffer was added, the mixtures were incubated for 30 min at 37°C. The incubations were quenched by adding glacial acetic acid (330 μl) and the resulting mixtures were allowed to stand several hours at 4°C before being extracted twice with 2 ml portions of diethyl ether. A table top centrifuge was used to break up emulsions. The ether extracts were combined, rinsed with water, and concentrated on a rotary evaporator. The residue was redissolved in 25% solvent F and 75% solvent E and analyzed by reverse phase HPLC. The column was eluted at a flow rate of 1 ml/min with 25% solvent F over 40 min followed by 50% F over 20 min. Solvent E was 5:5:1 methanol:water:glacial acetic acid and solvent F was 10:1 methanol:glacial acetic acid. The column effluent was monitored at 400 nm. Heme (λ_{max}=397 nm) eluted at 16.7 min and the *meso*-alkyl hemes (λ_{max}=405 nm) at 18.78 (methyl), 20.98 (ethyl), 25.47 (*n*-propyl) and 34.18 min (*n*-butyl). Adduct yields were decreased when the incubations were carried out at 25 or 0°C rather than 37°C.

In experiments to show the formation of H_2O_2 *in situ*, catalase (0.25 mg, 4 μM, final) was added in 250 μl of buffer prior to adding ethyl or *n*-butylhydrazine oxalate (47.2 mM) in 250 μl buffer. The incubations were carried out as described above and the mixtures were worked up, and analyzed by HPLC.

For anaerobic experiments, the flask containing the myoglobin solution was evacuated and filled with argon gas three times. The solution was then warmed to 37°C and oxygen-free ethylhydrazine oxalate prepared as above was introduced by a syringe. The incubation and work-up procedure were identical to those used for the standard incubation.

In one set of experiments, H_2O_2 (1 equivalent, 0.59 μmol) was added under aerobic and anaerobic conditions 30 seconds prior to adding the ethylhydrazine oxalate. The incubation conditions were as described above.

In experiments intended to detect isoporphyrin formation, standard incubations with ethyl or *n*-butylhydrazine oxalate were carried out to detect isoporphyrin formation.

Aliquots were removed after 0.5, 2, 10, 20 and 30 min and their spectra were recorded from 300 to 1000 nm on an Aminco DW 2000 instrument.

In order to quantitate the heme bound to the protein during the reaction, the standard incubation with *n*-butylhydrazine oxalate was carried out. After the incubation period, the mixtures were acidified to pH 2 with concentrated HCl and extracted with an equal volume of cold 2-butanone three times. After 2-butanone was removed by rotary evaporator, the ratio of $\lambda_{408}/\lambda_{280}$ of the sample was compared to that of myoglobin.

6.3.2 Quantitation of *n*-butyl adduct formation

The standard incubation was carried out using *n*-butylhydrazine. After the incubation, mesoheme (0.1922 mg, 0.31 μmol) was added as an internal standard and the mixture was worked up. In order to completely separate heme and mesoheme, HPLC was performed with a step gradient program: 25% solvent H over 50 min (0.8 ml/min), 25% H over 20 min (1 ml/min) and 60% H over 20 min (1 ml/min). Solvent G was composed of 3:7:1 acetonitrile:water:glacial acetic acid and solvent H was 10:1 acetonitrile:glacial acetic acid. The retention times of heme, mesoheme, and the γ-*meso* butyl heme in this system were, respectively, 31.26, 41.25, and 61.11 min.

6.3.3 EPR studies

POBN (0.6 mM) was added at room temperature immediately after ethylhydrazine oxalate (47.2 mM) was added to the myoglobin solution (590 μM). An aliquot was transferred to a melting point capillary tube which was placed into an EPR tube. In some of these EPR experiments, either catalase (4 μM) or H_2O_2 (1 equiv) was added, or either myoglobin or ethylhydrazine was omitted. The signals of spin trapped radicals were monitored with the following parameters: microwave power, 20 mW; modulation amplitude, 2.0 G; time constant, 0.25 second; scan time, 4 min; scan range, 100 G; receiver gain, 2×10^4.

6.3.4 Isolation of the *n*-butylhydrazine heme adduct

A 40-fold excess of *n*-butylhydrazine oxalate (252 mg, 1.416 mmol) was added at 37°C to a solution of myoglobin (600 mg, 35.4 mmol) in 60 ml of potassium phosphate buffer (0.1 N, pH 7.4) containing 1 mM EDTA. After incubating for 40 min, a further 252 mg of *n*-butylhydrazine oxalate was added and the incubation continued for an additional 1 hour. The reaction was carried out in the dark. The final reaction mixture was acidified with glacial acetic acid, and the mixture was allowed to stand at 4°C overnight. The mixture was then extracted with two portions of diethyl ether (180 ml total). A table top centrifuge was used to break up the emulsions that formed during the extraction procedure. The combined ether extracts were rinsed with water and taken to dryness on a rotary evaporator. The residue was chromatographed on a preparative HPLC column that was eluted isocratically for 50 min at a flow rate of 3.5 ml/min using 80% solvent E (5:5:1 methanol:water:glacial acetic acid) and 20% F (10:1 methanol:glacial acetic acid). The fractions having λ_{max}= 405 nm were pooled and rechromatographed in the same HPLC system.

The purified heme adduct thus obtained was esterified by allowing it to stand overnight at 4°C in 200 ml of 5% H_2SO_4 (v/v) in methanol. The adduct was then extracted into 200 ml CH_2Cl_2 after an equal volume of water was added. The organic fraction was rinsed with water and was concentrated to dryness on a rotary evaporator. The esterified residue was then demetallated (Morell et al., 1961; Fuhrhop & Smith, 1975) by dissolving it in a few drops of dry pyridine and combining the solution with 14 ml of glacial acetic acid. All glassware was dried by flushing with argon gas before use. The resulting dark red solution was stirred under a stream of argon gas for 10 min before adding 0.5 ml of a saturated solution of ferrous sulfate in hydrochloric acid. The mixture, whose color turned pink, was stirred for 5 min at room temperature under a stream of argon gas before it was poured into a mixture of 15 ml of saturated aqueous sodium acetate and 15 ml of diethyl

ether. The ether layer was rinsed with water and the solvent was removed at a rotary evaporator.

The zinc complex of the porphyrin adduct was prepared by adding a small amount of zinc acetate in methanol to the esterified porphyrin adduct in chloroform. The completion of chelation was confirmed by monitoring at 422 nm, 552 and 586 nm. The resulting zinc complex was purified immediately by preparative HPLC. The column was eluted with 90% methanol and 10% water for 35 min at a flow rate of 3.5 ml/min. The zinc complex fractions were pooled and evaporated to dryness.

6.3.5 Isolation of the ethylhydrazine heme adduct

Ethylhydrazine oxalate (708 mg, 4.72 mmol) was dissolved in 10 ml of phosphate buffer (0.1 N, pH 7.4). Half of this solution was added to a solution of myoglobin (1 g, 59 μmol) in 90 ml of the same buffer containing 1 mM EDTA and the remaining half added after incubation for 40 min at 37°C. After an additional hour at 37°C, glacial acetic acid (34 ml) was added and the mixture was extracted with diethyl ether. The ethyl heme adduct was isolated by preparative HPLC. The column was eluted with 85% solvent E and 15% F for 40 min at a flow rate of 3 ml/min. The purified heme adduct was rechromatographed in the same system. Esterification and demetallation were carried out as described for the *n*-butyl adduct.

6.3.6 NMR of *n*-butyl and ethyl heme adducts

^{1}H NMR spectra were measured in deuterated chloroform (sample concentration: 0.3-0.4 mg/350 μl) at 18°C on a General Electric GN 500 MHz FT NMR instrument. Spectra were obtained with a sweep width of 3300 Hz in a 16K block with a 1 Hz line-broadening. The $CHCl_3$ peak at 7.24 ppm was used as an internal reference. One-dimensional ^{1}H NOE experiments were carried out using a 65-68 dB decoupler pulse (4 sec) and a delay time of 1 sec. Typically, 128 scans were taken for each of the two NOE spectra in interweaving 8 scan blocks. NOE difference spectra were provided by subtracting the off-resonance (9.1

ppm) spectrum from the on-resonance spectrum. Decoupling experiments were performed with the decoupler set at 75 dB and a delay time of 1 msec. ^{1}H NOESY data were obtained using a delay time of 3 sec and a mixing time of 200 msec, and processed on a Sun/AT&T System 4 computer. The NOESY spectra were obtained with 2K data points in the t_2 dimension and 400 data points of 16 free induction decays each in the t_1 dimension. The free induction decays were zero-filled once and apodized with a 7 Hz Gaussian window function in both dimensions. ^{1}H NOESY spectra were taken only for the *n*-butyl heme adduct.

6.3.7 Reaction of human hemoglobin with ethylhydrazine

To a slightly turbid solution of hemoglobin (10 mg, 0.6 μmol based on heme) in 500 μl phosphate buffer (0.1 N, pH 7.4) containing 1 mM EDTA was added a 20 (1.77 mg)-, 40 (3.54 mg)-, or 80 (7.1 mg)-fold excess of ethylhydrazine oxalate in 500 μl of phosphate buffer. The resulting solutions were incubated in one set of experiments at 25°C and in another at 37°C for 30 min before they were worked up as described for the myoglobin incubations.

REFERENCES

Ames, B. N., Cathcart, R., Schwers, E. and Hochstein, P. (1981) *Proc. Natl. Acad. Sci. USA* **78**, 6858-6862.

Ashley, G. W. and Stubbe, J. (1985) *Pharmac. Ther.* **30**, 301-329.

Ator, M. A., David, S. K. and Ortiz de Montellano, P. R. (1987) *J. Biol. Chem.* **262**, 14954-14960.

Ator, M. A., David, S. K. and Ortiz de Montellano, P. R. (1989) *J. Biol. Chem.* **264**, 9250-9257.

Ator, M. A. and Ortiz de Montellano, P. R. (1987) *J. Biol. Chem.* **262**, 1542-1551.

Augusto, O., Beilan, H. S. and Ortiz de Montellano, P. R. (1982a) *J. Biol. Chem.* **257**, 11288-11295.

Augusto, O., Kunze, K. L. and Ortiz de Montellano, P. R. (1982b) *J. Biol. Chem.* **257**, 6231-6241.

Aviram, I., Wittenberg, B. A. and Wittenberg, J. B. (1978) *J. Biol. Chem.* **253**, 5685-5689.

Baldwin, J. E. and Carter, C. G. (1983) *J. Org. Chem.* **48**, 3912-3917.

Bangcharoenpaurpong, O., Champion, P. M., Hall, K. S. and Hager, L. P. (1986) *Biochemistry* **25**, 2374-2378.

Barry, B. A. and Babcock, G. T. (1987) *Proc. Natl. Acad. Sci. USA* **84**, 7099-7103.

Bartlett, P. (1957) *Rec. Chem. Proc.* **18**, 111.

Bartnicki, E. W., Belser, N. O. and Castro, C. E. (1978) *Biochemistry* **17**, 5582-5586.

Battioni, P., Mahy, J. P., Gillet, G. and Mansuy, D. (1983) *J. Am. Chem. Soc.* **105**, 1399-1401.

Beaven, G. H. and White, J. C. (1954) *Nature* **173**, 389-391.

Beckwith, J. R., Clark, R. and Hager, L. P. (1963) *J. Biol. Chem.* **238**, 3086-3090.

Berti, G. (1973) *Top. Stereochem.* **7**, 95-251.

Beutler, E. (1969) *Pharmacol. Rev.* **21**, 73-103.

Bielski, B. H. J. and Richter, H. W. (1977) *J. Am. Chem. Soc.* **99**, 3019-3023.

Black, S. D. and Coon, M. J. (1982) *J. Biol. Chem.* **257**, 5929-5938.

Blanke, S. R. and Hager, L. P. (1988) *J. Biol. Chem.* **263**, 18739-18743.

Blanke, S. R. and Hager, L. P. (1990) *J. Biol. Chem.* **265**, 12454-12461.

Blanke, S. R., Yi, S. and Hager, L. P. (1989) *Biotech. Lett.* **11**, 769-774.

Bondoc, L. L. and Timkovich, R. (1989) *J. Biol. Chem.* **264**, 6134-6145.

Bornheim, M. A., Underwood, M. C., Caldera, P., Rettie, A., Trager, W., Wrighton, S. and Correia, M. A. (1987) *Molec. Pharmacol.* **32**, 299-308.

Bradford, M. M. (1976) *Anal. Biochem.* **72**, 248-254.

Brown, C. A. and Black, S. D. (1989) *J. Biol. Chem.* **264**, 4442-4449.

Campbell, C. D. and Rees, C. W. (1969) *J. Chem. Soc., Chem. Commun.* 752-756.

Case, G. D. and Leigh, J. S., Jr. (1976) *Biochem. J.* **160**, 769-783.

Castellino, A. J. and Bruice, T. C. (1988) *J. Am. Chem. Soc.* **110**, 158-162.

Castro, C. E. and Bartnicki, E. W. (1975) *Biochemistry* **14**, 498-503.

Catalano, C. E. (1987) Ph. D., University of California, San Francisco.

Catalano, C. E., Choe, Y. S. and Ortiz de Montellano, P. R. (1989) *J. Biol. Chem.* **264**, 10534-10541.

Catalano, C. E. and Ortiz de Montellano, P. R. (1987) *Biochemistry* **26**, 8373-8380.

Champion, P. M., Chiang, R., Munck, E., Debrunner, P. G. and Hager, L. P. (1975) *Biochemistry* **14**, 4159-4166.

Chance, M., Powers, L., Kumar, C. and Chance, B. (1986) *Biochemistry* **25**, 1259-1265.

Choe, Y. S. and Ortiz de Montellano, P. R. (1991) *J. Biol. Chem.* **266**, 8523-8530.

Chou, P. and Fasman, G. C. (1978) *Adv. Enzymol. Relat. Areas Mol. Biol.* **47**, 45-148.

Chu, K. C. (1980) in *Burger's Medicinal Chemistry* Part 1 (Wolff, M. E., ed), Wiley & Sons, New York, Part 1, pp. 401.

Clutterbuck, P. W., Mukhopadhyay, S. L., Oxford, A. E. and Raistrick, H. (1940) *Biochem. J.* **34**, 664-677.

Cohen, G. and Hochstein, P. (1964) *Biochemistry* **3**, 895-900.

Collman, J. P., Kodadek, T. and Brauman, J. I. (1986) *J. Am. Chem. Soc.* **108**, 2588-2594.

Corbett, M. D., Baden, D. G. and Chipko, B. R. (1979) *Bioorg. Chem.* **8**, 91-95.

Courtin, F., Deme, D., Virion, A., Michot, J. L., Pommier, J. and Nunez, J. (1982) *Eur. J. Biochem.* **124**, 603-609.

Courtin, F., Michot, J.-L., Virion, A., Pommier, J. and Deme, D. (1984) *Biochem. Biophys. Res. Commun.* **121**, 463-470.

Cramer, S. P., Dawson, J. H., Hager, L. P. and Hodgson, K. O. (1978) *J. Am. Chem. Soc.* **100**, 7282-7290.

Davies, H. W., Britt, S. G. and Pohl, L. R. (1986a) *Chem.-Biol. Interact.* **58**, 345-352.

Davies, H. W., Britt, S. G. and Pohl, L. R. (1986b) *Arch. Biochem. Biophys.* **244**, 387-392.

Davies, H. W., Satoh, H., Schulick, R. D. and Pohl, L. R. (1985) *Biochem. Pharmacol.* **34**, 3203-3206.

Davies, M. J. (1990) *Free Rad. Res. Comms.* **10**, 361-370.

Davies, M. J. (1991) *Biochim. Biophys. Acta* **1077**, 86-90.

Dawson, J. H. (1988) *Science* **240**, 433-439.

Dawson, J. H., Holm, R. H., Trudell, J. R., Barth, G., Linder, R. E., Bunnenberg, E., Djerassi, C. and Tang, S. C. (1976) *J. Am. Chem. Soc.* **98**, 3707-3709.

Dawson, J. H., Kau, L.-S., Penner-Hahn, J. E., Sono, M., Eble, K. S., Bruce, G. S., Hager, L. P. and Hodgson, K. O. (1986) *J. Am. Chem. Soc.* **108**, 8114-8116.

Dawson, J. H. and Sono, M. (1987) *Chem. Rev.* **87**, 1255-1276.

Dawson, J. H., Trudell, J. R., Barth, G., Linder, R. E., Bunnenberg, E., Djerassi, C., Chiang, R. and Hager, L. P. (1976) *J. Am. Chem. Soc.* **98**, 3709-3710.

De Matteis, F., Gibbs, A. H. and Tephly, T. R. (1980) *Biochem. J.* **189**, 645-648.

Delaforge, M., Battioni, P., Mahy, J. P. and Mansuy, D. (1986) *Chem.-Biol. Interact.* **60**, 101-114.

Depillis, G. D. and Ortiz de Montellano, P. R. (1989) *Biochemistry* **28**, 7947-7952.

Derome, A. E. (1987) *Modern NMR Techniques for Chemistry Research* (Baldwin, J. E., ed), Pergamon Press, Oxford, pp. 97-120 and 239-244.

Dickerson, R. E. and Geis, I. (1983) *Hemoglobin: Structure, Function, Evolution, and Pathology*, The Benjamin/Cummings Publishing Co. Inc., Menlo Park, pp. 1-176.

Doyle, M. P., Mahapatro, S. N., Guy, J. K., Hester, M. R., Van Zyl, C. M. and Boundy, K. L. (1987) *Inorg. Chem.* **26**, 3387-3392.

Dunford, H. B. and Stillman, J. S. (1976) *Coord. Chem. Rev.* **19**, 187-251.

Dus, K., Katagiri, M., Yu, C. A., Erbes, D. L. and Gunsalus, I. C. (1970) *Biochem. Biophys. Res. Commun.* **40**, 1423-1430.

Edwards, S. L., Xuong, N. H., Hamlin, R. C. and Kraut, J. (1987) *Biochemistry* **26**, 1503-1511.

Ehrenberg, A. and Reichard, P. (1972) *J. Biol. Chem.* **247**, 3485-3488.

Elfarra, A. A., Duescher, R. J. and Pasch, C. M. (1991) *Arch. Biochem. Biophys.* **286**, 244-251.

Evans, S. V. and Brayer, G. D. (1988) *J. Biol. Chem.* **263**, 4263-4268.

Fang, G.-H., Kenigsberg, P., Axley, M. J. and Hager, L. P. (1986) *Nucleic Acids Res.* **14**, 8061-8071.

Fenical, W. (1982) *Science* **215**, 923-928.

Fox, J. B., Jr., Nicholas, R. A., Ackerman, S. A. and Swift, C. E. (1974) *Biochemstry* **13**, 5178-5186.

Fuhrhop, J.-H. and Smith, K. M. (1975) *Porphyrins and Metalloporphyrins*, 2nd ed. (Smith, K. M., ed) Elsevier Scientific Publishing Co., New York, pp. 1-869.

Galaris, D., Cadenas, E. and Hochstein, P. (1989) *Arch. Biochem. Biophys.* **273**, 497-504.

Galaris, D., Mira, D., Sevanian, A., Cadenas, E. and Hochstein, P. (1988) *Arch. Biochem. Biophys.* **262**, 221-231.

Galaris, D., Sevanian, A., Cadenas, E. and Hochstein, P. (1990) *Arch. Biochem. Biophys.* **281**, 163-169.

Geigert, J., Dalietos, D. J., Neidleman, S. L., Lee, T. D. and Wadsworth, J. (1983a) *Biochem. Biophys. Res. Comm.* **114**, 1104-1108.

Geigert, J., Dewitt, S. K., Neidleman, S. L., Lee, G., Dalietos, D. J. and Moreland, M. (1983b) *Biochem. Biophys. Res. Comm.* **116**, 82-85.

Geigert, J., Lee, T. D., Dalietos, D. J., Hirano, D. S. and Neidleman, S. L. (1986) *Biochem. Biophys. Res. Commun.* **136**, 778-782.

Gelb, M. H., Heimbrook, D. C., Malkonen, P. and Sligar, S. G. (1982) *Biochemistry* **21**, 370-377.

George, P. and Irvine, D. H. (1952) *Biochem. J.* **52**, 511-517.

George, P. and Irvine, D. H. (1954) *Biochem. J.* **58**, 188-195.

George, P. and Irvine, D. H. (1956) *J. Colloid Sci.* **11**, 327-339.

Gerald, P. S. and Effron, M. L. (1961) *Proc. Natl. Acad. Sci., USA* **47**, 1758-1767.

Gibson, J. F. and Ingram, D. J. E. (1956) *Nature* **178**, 871-872.

Gibson, J. F., Ingram, D. J. E. and Nicholls, P. (1958) *Nature* **181**, 1398-1399.

Goldberg, B. and Stern, A. (1977) *Mol. Pharmacol.* **13**, 832-839.

Goldberg, B., Stern, A., Peisach, J. and Blumberg, W. E. (1979) *Experientia* **35**, 488-489.

Golly, I. and Hlavica, P. (1983) *Biochim. Biophys. Acta* **760**, 69-76.

Goodin, D. B., Mauk, A. G. and Smith, M. (1987) *J. Biol. Chem.* **262**, 7719-7724.

Griller, D. and Wayner, D. D. M. (1989) *Pure Appl. Chem.* **61**, 717-724.

Groves, J. T. (1980) in *Metal Ion Activation of Dioxygen* (Spiro, T. G., ed) Wiley & Sons, New York, pp. 125-162.

Groves, J. T., Avaria-Neisser, G. E., Fish, K. M., Imachi, M. and Kuczkowski, R. L. (1986) *J. Am. Chem. Soc.* **108**, 3837-3838.

Groves, J. T., McClusky, G. A., White, R. E. and Coon, M. J. (1978) *Biochem. Biophys. Res. Commun.* **81**, 154-160.

Groves, J. T. and Myers, T. S. (1983) *J. Am. Chem. Soc.* **105**, 5791-5796.

Groves, J. T. and Stern, M. K. (1987) *J. Am. Chem. Soc.* **109**, 3812-3814.

Groves, J. T. and Subramanian, D. V. (1984) *J. Am. Chem. Soc.* **106**, 2177-2181.

Groves, J. T. and Watanabe, Y. (1986) *J. Am. Chem. Soc.* **108**, 507-508.

Guengerich, F. P. (1978) *Biochemistry* **17**, 3633-3639.

Gutteridge, J. M. C. (1986) *FEBS Lett.* **201**, 291-295.

Hager, L. P., Doubek, D. L., Silverstein, R. M., Hargis, J. H. and Martin, J. C. (1972) *J. Am. Chem. Soc.* **94**, 4364-4366.

Halpert, J. (1981) *Biochem. Pharmacol.* **30**, 875-881.

Halpert, J. (1982) *Mol. Pharmacol.* **21**, 166-172.

Halpert, J., Naslund, B. and Betnér, I. (1983) *Mol. Pharmacol.* **23**, 445-452.

Halpert, J. and Neal, R. A. (1980) *Mol. Pharmacol.* **17**, 427-431.

Harbury, H. A. and Loach, P. A. (1959) *Proc. Natl. Acad. Sci. USA* **45**, 1344-1359.

Harel, S. and Kanner, J. (1985) *J. Agric. Food Chem.* **33**, 1188-1192.

Harel, S., Salan, M. A. and Kanner, J. (1988) *Free Radicals Res. Com.* **5**, 11-19.

Harrison, J. E. and Schultz, J. E. (1976) *J. Biol. Chem.* **251**, 1371-1374.

Haugen, D. A. (1989) *Chem. Res. Toxicol.* **2**, 379-385.

Hebbel, R. P. and Eaton, J. W. (1989) *Sem. Hematol.* **26**, 136-149.

Heimbrook, D. C., Mulholland, R. L., Jr. and Hecht, S. M. (1986) *J. Am. Chem. Soc.* **108**, 7839-7840.

Henschler, D., Hoos, W. R., Fetz, H., Dallmeier, E. and Metzler, M. (1979) *Biochem. Pharmacol.* **28**, 543-548.

Hill, H. A. O. and Thornalley, P. J. (1981) *FEBS Lett.* **125**, 235-238.

Hollenberg, P. F. and Hager, L. P. (1978) in *Methods in Enzymology*, vol. 52 (Fleischer, S., and Packer, L., eds), Academic Press, New York, pp. 521-529.

Hollenberg, P. F., Rand-Meir, T. and Hager, L. P. (1974) *J. Biol. Chem.* **249**, 5816-5825.

Huang, P. C. and Kosower, E. M. (1968) *J. Am. Chem. Soc.* **90**, 2367-2376.

Itano, H. A., Hirota, K. and Vedvick, T. S. (1977) *Proc. Natl. Acad. Sci. USA* **74**, 2556-2560.

Itano, H. A. and Matteson, J. L. (1982) *Biochemistry* **21**, 2421-2426.

Kagen, L. J. (1973) *Myoglobin: Biochemical, Physiological, and Clinical Aspects*, Columbia University Press, New York, pp. 1-151.

Kanner, J. and Harel, S. (1985a) *Arch. Biochem. Biophys.* **237**, 314-321.

Kanner, J. and Harel, S. (1985b) *Lipids* **20**, 625-628.

Kedderis, G. L., Koop, D. R. and Hollenberg, P. F. (1980) *J. Biol. Chem.* **255**, 10174-10182.

Kedderis, G. L., Rickert, D. E., Pandey, R. N. and Hollenberg, P. F. (1986) *J. Biol. Chem.* **261**, 15910-15914.

Keilin, D. and Hartree, E. F. (1935) *Proc. Roy. Soc. London, Ser. B* **117**, 1-15.

Kendrew, J. C. (1961) *Sci. Am.* **205**, 96-110.

Kendrew, J. C., Dickerson, R. E., Strandberg, B. E., Hart, R. G., Davies, D. R., Phillips, D. C. and Shore, V. C. (1960) *Nature* **185**, 422-427.

Kenigsberg, P., Fang, G.-H. and Hager, L. P. (1987) *Arch. Biochem. Biophys.* **254**, 409-415.

King, N. K., Looney, F. D. and Winfield, M. E. (1964) *Biochim. Biophys. Acta* **88**, 235-236.

King, N. K., Looney, F. D. and Winfield, M. E. (1967) *Biochim. Biophys. Acta* **133**, 65-82.

King, N. K. and Winfield, M. E. (1963) *J. Biol. Chem.* **238**, 1520-1528.

King, N. K. and Winfield, M. E. (1966) *Aust. J. Biol. Sci.* **19**, 211-217.

Knappe, J., Neugebauer, F., Blaschkowski, H. P. and Ganzler, M. (1984) *Proc. Natl. Acad. Sci. USA* **81**, 1332-1335.

Kobayashi, S., Nakano, M., Goto, T., Kimura, T. and Schaap, A. P. (1986) *Biochem. Biophys. Res. Commun.* **135**, 166-171.

Kobayashi, S., Nakano, M., Kimura, T. and Schaap, A. P. (1987) *Biochemistry* **26**, 5019-5022.

Komives, E. A. and Ortiz de Montellano, P. R. (1987) *J. Biol. Chem.* **262**, 9793-9802.

Koppenol, W. H. (1976) *Nature* **262**, 420-421.

Kosower, E. M. (1971) *Accts. Chem. Res.* **4**, 193-198.

Krejcarek, G. E., Bryant, R. G., Smith, R. J. and Hager, L. P. (1976) *Biochemistry* **15**, 2508-2511.

Kremer, M. L. (1981) *Israel J. Chem.* **21**, 72-75.

Krueger, P. J. (1975) in *The Chemistry of the Hydrazo, Azo and Azoxy Groups*, Part 2 (Patai, S., ed), Wiley & Sons, New York, pp. 160-162.

Kubic, V. L. and Anders, M. W. (1981) *Chem.-Biol. Interact.* **34**, 201-207.

Kulmacz, R. J., Tsai, A.-L. and Palmer, G. (1987) *J. Biol. Chem.* **262**, 10524-10531.

Kunze, K. L., Mangold, B. L. K., Wheeler, C., Beilan, H. S. and Ortiz de Montellano, P. R. (1983) *J. Biol. Chem.* **258**, 4202-4207.

Kunze, K. L. and Ortiz de Montellano, P. R. (1983) *J. Am. Chem. Soc.* **105**, 1380-1381.

Labeque, R. and Marnett, L. J. (1987) *J. Am. Chem. Soc.* **109**, 2828-2829.

Libby, R. D. and Rotberg, N. S. (1990) *J. Biol. Chem.* **265**, 14808-14811.

Libby, R. D., Thomas, J. A., Kaiser, L. W. and Hager, L. P. (1982) *J. Biol. Chem.* **257**, 5030-5037.

Liebler, D. C. and Guengerich, F. P. (1983) *Biochemistry* **22**, 5482-5489.

Lowry, O. H., Rosebrough, N. J., Farr, A. L. and Randall, R. J. (1951) *J. Biol. Chem.* **193**, 265-275.

Lunetta, J. M., Sugiyama, K. and Correia, M. A. (1989) *Mol. Pharmacol.* **35**, 10-17.

Maeda, Y., Morita, Y. and Yoshida, C. (1973) *J. Biochem. Tokyo* **70**, 509-514.

Makino, R., Chiang, R. and Hager, L. P. (1976) *Biochemistry* **15**, 4748-4754.

Mansuy, D., Battioni, P., Mahy, J.-P. and Gillet, G. (1982) *Biochem. Biophys. Res. Commun.* **106**, 30-36.

Mansuy, D., Leclaire, J., Fontecave, M. and Momenteau, M. (1984) *Biochem. Biophys. Res. Commun.* **119**, 319-325.

March, J. (1985) *Advanced Organic Chemistry: Reactions, Mechanisms, and Structure*, 3rd ed., Wiley & Sons, New York, pp. 1-1120.

Mashino, T., Nakamura, S. and Hirobe, M. (1990) *Tetrahedron Lett* **31**, 3163-3166.

McCarthy, M.-B. and White, R. E. (1983) *J. Biol. Chem.* **258**, 9153-9158.

Mieyal, J. J., Ackerman, R. S., Blumer, J. L. and Freeman, L. S. (1976) *J. Biol. Chem.* **251**, 3436-3441.

Miki, H., Harada, K., Yamazaki, I., Tamura, M. and Watanabe, H. (1989) *Arch. Biochem. Biophys.* **275**, 354-362.

Miller, R. E. and Guengerich, F. P. (1982) *Biochemistry* **21**, 1090-1097.

Millikan, G. A. (1939) *Physiol. Rev.* **19**, 503-554.

Mimoun, H. (1981) *Pure Appl. Chem.* **53**, 2389-2399.

Morell, D. B., Barrett, J. and Clezy, P. S. (1961) *Biochem. J.* **78**, 793-797.

Morris, D. R. and Hager, L. P. (1966) *J. Biol. Chem.* **241**, 1763-1768.

Moss, T. H., Ehrenberg, A. and Bearden, A. J. (1969) *Biochemistry* **8**, 4159-4162.

Murthy, M. R. N., Reid, T. J., III, Sicignano, A., Tanaka, N. and Rossmann, M. G. (1981) *J. Mol. Biol.* **152**, 465-499.

Nelson, D. R. and Strobel, H. W. (1988) *J. Biol. Chem.* **263**, 6038-6050.

Nieder, M. and Hager, L. P. (1984) *Fed. Proc.* **43**, 2008.

Noguchi, T., Fong, K., Lai, E. K., Alexander, S. S., King, M. M., Olson, L., Poyer, J. L. and McCay, P. B. (1982) *Biochem. Pharmacol.* **31**, 615-624.

Nonhebel, D. C., Tedder, J. M. and Walton, J. C. (1979) *Radicals*, Cambridge University Press, London, pp. 1-200.

Ortiz de Montellano, P. R. (1985) in *Bioactivation of Foreign Compounds* (Anders, M. W., ed) Academic Press, Orlando, pp. 121-155.

Ortiz de Montellano, P. R. (1986) in *Cytochrome P-450: Structure, Mechanism, and Biochemistry* (Ortiz de Montellano, P. R., ed) Plenum Press, New York, pp. 217-271.

Ortiz de Montellano, P. R. (1987) *Acc. Chem. Res.* **20**, 289-294.

Ortiz de Montellano, P. R. (1990) *Pharmac. Ther.* **48**, 95-120.

Ortiz de Montellano, P. R. and Catalano, C. E. (1985) *J. Biol. Chem.* **260**, 9265-9271.

Ortiz de Montellano, P. R., Choe, Y. S., Depillis, G. and Catalano, C. E. (1987) *J. Biol. Chem.* **262**, 11641-11646.

Ortiz de Montellano, P. R. and Correia, M. A. (1983) *Ann. Rev. Pharmacol. Toxicol.* **23**, 481-503.

Ortiz de Montellano, P. R., David, S. K., Ator, M. A. and Tew, D. (1988) *Biochemistry* **27**, 5470-5476.

Ortiz de Montellano, P. R. and Grab, L. A. (1986) *Mol. Pharmacol.* **30**, 666-669.

Ortiz de Montellano, P. R. and Grab, L. A. (1987) *Biochemistry* **26**, 5310-5314.

Ortiz de Montellano, P. R. and Kerr, D. E. (1983) *J. Biol. Chem.* **258**, 10558-10563.

Ortiz de Montellano, P. R. and Kerr, D. E. (1985) *Biochemistry* **24**, 1147-1152.

Ortiz de Montellano, P. R. and Kunze, K. L. (1981) *J. Am. Chem. Soc.* **103**, 6534-6536.

Ortiz de Montellano, P. R., Kunze, K. L. and Augusto, O. (1982) *J. Am. Chem. Soc.* **104**, 3545-3546.

Ortiz de Montellano, P. R., Kunze, K. L. and Beilan, H. S. (1983a) *J. Biol. Chem.* **258**, 45-47.

Ortiz de Montellano, P. R., Kunze, K. L., Cole, S. P. C. and Marks, G. S. (1980) *Biochem. Biophys. Res. Commun.* **97**, 1436-1442.

Ortiz de Montellano, P. R., Mangold, B. L. K., Wheeler, C., Kunze, K. L. and Reich, N. O. (1983b) *J. Biol. Chem.* **258**, 4208-4213.

Ortiz de Montellano, P. R. and Mathews, J. M. (1981) *Biochem. J.* **195**, 761-764.

Ortiz de Montellano, P. R., Mathews, J. M. and Langry, K. C. (1984) *Tetrahedron* **40**, 511-519.

Ortiz de Montellano, P. R. and Reich, N. O. (1986) in *Cytochrome P-450: Structure, Mechanism, and Biochemistry* (Ortiz de Montellano, P. R., ed) Plenum Press, New York, pp. 273-314.

Osawa, Y., Highet, R. J., Bax, A. and Pohl, L. R. (1991) *J. Biol. Chem.* **266**, 3208-3214.

Osawa, Y., Highet, R. J., Murphy, C. M., Cotter, R. J. and Pohl, L. R. (1989) *J. Am. Chem. Soc.* **111**, 4462-4467.

Osawa, Y., Martin, B. M., Griffin, P. R., Yates, J. R., III, Shabanowitz, J., Hunt, D. F., Murphy, A. C., Chen, L., Cotter, R. J. and Pohl, L. R. (1990) *J. Biol. Chem.* **265**, 10340-10346.

Osawa, Y. and Pohl, L. R. (1989) *Chem. Res. Toxicol.* **2**, 131-141.

Ostovic, D. and Bruice, T. C. (1989) *J. Am. Chem. Soc.* **111**, 6511-6517.

Paleus, S., Ehrenberg, A. and Tuppy, A. (1955) *Acta Chem. Scand.* **9**, 365-374.

Penner-Hahn, J. E., Eble, K. S., McMurry, T. J., Renner, M., Balch, A. L., Groves, J. T., Dawson, J. H. and Hodgson, K. O. (1986) *J. Am. Chem. Soc.* **108**, 7819-7825.

Pesez, M. and Bartos, J. (1974) *Colorimetric and Fluorimetric Analysis of Organic Compounds and Drugs* (Schwarz, M. K., ed), Marcel Dekker, Inc., New York, pp. 329-337.

Porter, D. J. T. and Bright, H. J. (1983) *J. Biol. Chem.* **258**, 9913-9924.

Poulos, T. L. (1988) in *Advances in Inorganic Biochemistry* vol. 7, (Eichhorn, G. L. and Marzilli, L. G., eds), Elsevier Science Publishing Co., Inc., New York, pp. 1-36.

Poulos, T. L., Finzel, B. C., Gunsalus, I. C., Wagner, G. C. and Kraut, J. (1985) *J. Biol. Chem.* **260**, 16122-16130.

Poulos, T. L., Finzel, B. C. and Howard, A. J. (1986) *Biochemistry* **25**, 5314-5322.

Poulos, T. L., Finzel, B. C. and Howard, A. J. (1987) *J. Mol. Biol.* **195**, 687-700.

Poyer, J. L., Floyd, R. A., McCay, P. B., Janzen, E. G. and Davis, E. R. (1978) *Biochem. Biophys. Acta* **539**, 402-409.

Pryor, W. A. (1986) *Ann. Rev. Physiol.* **48**, 657-667.

Raag, R., Swanson, B. A., Poulos, T. L. and Ortiz de Montellano, P. R. (1990) *Biochemistry* **29**, 8119-8126.

Reichard, P. and Ehrenberg, A. (1983) *Science* **221**, 514-519.

Rice, R. H., Lee, Y. M. and Brown, W. D. (1983) *Arch. Biochem. Biophys.* **221**, 417-427.

Riggs, A. (1981) in *Methods in Enzymology* vol. 76 (Antonini, E., Rossi- Bernadi, L., and Chianocone, E., eds), Academic Press, New York, pp. 20-21.

Ringe, D., Petsko, G. A., Kerr, D. E. and Ortiz de Montellano, P. R. (1984) *Biochemistry* **23**, 2-4.

Ringe, D., Turesky, R. J., Skipper, P. L. and Tannenbaum, S. R. (1988) *Chem. Res. Toxicol.* **1**, 22-24.

Roberts, J. E., Hoffman, B. M., Rutter, R. and Hager, L. P. (1981) *J. Biol. Chem.* **256**, 2118-2121.

Rostorfer, H. H. and Totter, J. R. (1956) *J. Biol. Chem.* **221**, 1047-1055.

Rutter, R. and Hager, L. P. (1982) *J. Biol. Chem.* **257**, 7958-7961.

Saito, S. and Itano, H. A. (1981) *Proc. Natl. Acad. Sci. U.S.A.* **78**, 5508-5512.

Salemme, F. R. (1977) *Ann. Rev. Biochem.* **46**, 299-329.

Sangster, D. F. (1971) *Free Radical and Electrophilic Hydroxylation* (Patai, S., ed), Interscience Publishers, London, pp. 133-191.

Saunders, B. C., Holmes-Siedel, A. G. and Stark, B. P. (1964) in *Peroxidase* Butterworths Inc., London, pp.10-25.

Sawaki, Y. and Foote, C. (1979) *J. Am. Chem. Soc.* **101**, 6292-6296.

Sawyer, D. T. and Nanni, E. J. (1981) in *Oxygen and Oxy-Radicals in Chemistry and Biology* Academic Press, New York, pp. 15-41.

Schaefer, W. H., Harris, T. M. and Guengerich, F. P. (1987) *Arch. Biochem. Biophys.* **257**, 186-193.

Schulz, C. E., Devaney, P. W., Winkler, H., Debrunner, P. G., Doan, N., Chiang, R., Rutter, R. and Hager, L. P. (1979) *FEBS Lett.* **103**, 102-105.

Schulz, C. E., Rutter, R., Sage, J. T., Debrunner, P. G. and Hager, L. P. (1984) *Biochemistry* **23**, 4743-4754.

Shahangian, S. and Hager, L. P. (1981) *J. Biol. Chem.* **256**, 6034-6040.

Sharpless, K. B., Teranishi, A. Y. and Backvall, J. E. (1977) *J. Am. Chem. Soc.* **99**, 3120-3128.

Shaw, P. D., Beckwith, J. R. and Hager, L. P. (1959) *J. Biol. Chem.* **234**, 2560-2564.

Shaw, P. D. and Hager, L. P. (1959) *J. Am. Chem. Soc.* **81**, 1011-1012.

Shaw, P. D. and Hager, L. P. (1961) *J. Biol. Chem.* **236**, 1626-1630.

Shiga, T. and Imaizumi, K. (1975) *Arch. Biochem. Biophys.* **167**, 469-479.

Sitter, A. J., Reczek, C. M. and Terner, J. (1985) *Biochim. Biophys. Acta* **828**, 229-235.

Smith, K. M. and Gibson, Q. H. (1959) *Biochem. J.* **73**, 101-106.

Smith, P. and Maples, K. R. (1985) *J. Magn. Reson.* **65**, 491-496.

Sono, M., Andersson, L. A. and Dawson, J. H. (1982) *J. Biol. Chem.* **257**, 8308-8320.

Sono, M., Dawson, J. H., Hall, K. and Hager, L. P. (1986) *Biochemistry* **25**, 347-356.

Springer, B. A., Egeberg, K. D., Sligar, S. G., Rohlfs, R. J., Mathews, A. J. and Olson, J. S. (1989) *J. Biol. Chem.* **264**, 3057-3060.

Starke, D. W., Blisard, K. S. and Mieyal, J. J. (1984) *Mol. Pharmacol.* **25**, 467-475.

Starke, D. W. and Mieyal, J. J. (1989) *Biochem. Pharmacol.* **38**, 201-204.

Stryer, L. (1981) *Biochemistry*, 2nd ed., W. H. Freeman and Co., San Francisco, pp. 1-949.

Tajima, G. and Shikama, K. (1987) *J. Biol. Chem.* **262**, 12603-12605.

Takano, T. (1977a) *J. Mol. Biol.* **110**, 537-568.

Takano, T. (1977b) *J. Mol. Biol.* **110**, 569-584.

Taniguchi, H., Imai, Y. and Sato, R. (1984) *Biochem. Biophys. Res. Commun.* **118**, 916-922.

Teale, F. W. J. (1959) *Biochem. Biophys. Acta* **35**, 543.

Tephly, T. R., Gibbs, A. H. and De Matteis, F. (1979) *Biochem. J.* **180**, 241-244.

Tew, D. and Ortiz de Montellano, P. R. (1988) *J. Biol. Chem.* **263**, 17880-17886.

Thomas, J. A. and Hager, L. P. (1968) *Biochem. Biophys. Res. Comm.* **32**, 770-775.

Thomas, J. A., Morris, D. R. and Hager, L. P. (1970) *J. Biol. Chem.* **245**, 3129-3134.

Tomoda, A., Sugimoto, K., Suhara, M., Takeshita, M. and Yoneyama, Y. (1978) *Biochem. J.* **171**, 329-335.

Tu, A. T., Reinosa, J. A. and Hsiao, Y. Y. (1968) *Experientia* **24**, 219-221.

Uyeda, M. and Peisach, J. (1981) *Biochemistry* **20**, 2028-2035.

Varadarajan, R., Lambright, D. and Boxer, S. (1989) *Biochemistry* **28**, 3771-3781.

Wallace, W. J., Houtchens, R. A., Maxwell, J. C. and Caughey, W. S. (1982) *J. Biol. Chem.* **257**, 4966-4977.

Webster, S. H. (1949) *Blood* **4**, 479-497.

Wilbur, D. J. and Allerhand, A. (1976) *J. Biol. Chem.* **251**, 5187-5194.

Wiseman, J. S., Nichols, J. S. and Kolpak, M. X. (1982) *J. Biol. Chem.* **257**, 6328-6332.

Wittenberg, J. B. (1970) *Physiol. Rev.* **50**, 559-636.

Yonetani, T. (1976) in *The enzymes* 13C, 3rd ed. (Boyer, P. D., ed), Academic Press, New York, pp. 345-361.

Yonetani, T. and Schleyer, H. (1967) *J. Biol. Chem.* **242**, 1974-1979.

CAT. NO. 23 012

PRINTED IN U.S.A.